

https://dspace.org/

Comparison of the HIV-1 VPU interaction with CD4 and CD74

Le Noury, Denise Anne

2016-10-24
http://hdl.handle.net/10539/21252

Downloaded from a DSpace repository. https://dspace.org/

COMPARISON OF THE HIV-1 VPU INTERACTION WITH CD4 AND CD74

Denise Anne Le Noury

A thesis submitted to the Faculty of Health Sciences,

University of the Witwatersrand,

In fulfilment of the requirements for the degree of

Doctor of Philosophy

Johannesburg, February 2016

The more that you read, the more things you will know.

The more that you learn, the more places you'll go.

- Dr Seuss

DECLARATION

I declare that this Thesis is my own, unaided work. It is being submitted for the Degree of Doctor of Philosophy at the University of the Witwatersrand, Johannesburg. It has not been submitted before for any degree or examination at any other University.

_____

Denise Anne Le Noury

_____ day of _____ 20_____.

Publications & Presentations Arising from this Study

The following scientific outputs have been derived from this thesis:

Publications

1. **Le Noury DA**, Mosebi S, Papathanasopoulos MA and Hewer R. "Functional roles of HIV-1 Vpu and CD74: details and implications of the Vpu-CD74 interaction." *Cellular Immunology*, 2015, 298: 25-32.

Manuscripts in Preparation

1. **Le Noury DA**, Mosebi S, Papathanasopoulos MA and Hewer R. "Expression and Purification of Vphu::GFP fusion protein from mammalian cells."
2. **Le Noury DA**, Mosebi S, Papathanasopoulos MA and Hewer R. "Human CD74 is downregulated by HIV-1 Vpu in U937 cells."

Conference Contributions

1. **Le Noury D**, Mosebi S, Papathanasopoulos M and Hewer R, "CD74 is downregulated by HIV-1 Vpu in U937 cells", MBRT, University of the Witwatersrand, South Africa, 3 December 2015. Oral presentation.
2. **Le Noury D**, Mosebi S, Papathanasopoulos M, Kleynhans R and Hewer R, "CD74 is targeted for proteasomal degradation by HIV-1 Vpu", MAM-14, Emperor's Palace, South Africa, 23-27 November 2014. Oral Presentation.
3. **Le Noury D**, Mosebi S, Papathanasopoulos M, Kleynhans R and Hewer R, "Human immunodeficiency virus type-1 Vpu targets CD74 for proteasomal degradation", SASBMB, Cape Town, South Africa, 6-9 July 2014. Poster presentation.
4. **Downer D**, Mosebi S, Byth-Illing HA and Hewer R, "Exploring the Interaction between HIV-1 Vpu and CD74 of the MHCII", SASBMB/FASBMB, Drakensberg, South Africa, 29 January - 01 February 2012. Oral Presentation.

ABSTRACT

Viral protein U (Vpu) is a versatile accessory protein of human immunodeficiency virus type 1 (HIV-1) and some simian immunodeficiency virus isolates. Amongst other functions, Vpu targets human CD4 for ubiquitination and proteasomal degradation. This process requires the presence of phospho-serine residues within the Vpu cytoplasmic domain in order to allow for the recruitment of beta-transducin repeat-containing protein (β-TrCP) and ultimately the E3 ligase complex. Similarly, it has been shown that the Vpu cytoplasmic domain also interacts with the human CD74 cytoplasmic region. CD74, the invariant chain of major histocompatibility complex class II (MHCII), is involved in the presentation of foreign antigens to CD4+ T cells. The Vpu/CD74 interaction may prevent the maturation of the MCHII complex resulting in the downmodulation of cell surface levels of MHCII. There are several structural similarities between the human CD4 and CD74 host proteins. Consequently, we hypothesised that HIV-1 Vpu targets human CD74 for proteasomal degradation through the binding of β-TrCP similar to that of Vpu-mediated CD4 proteasomal degradation. In view of this, this study aimed to delineate the binding interaction between HIV-1 Vpu and CD74 and to determine whether Vpu also targets CD74 for proteasomal degradation. An *in silico* homology study determined that the α-helices found within the cytoplasmic domains of CD4 and CD74 were similar with an RMSD of 1.437 Å. Recombinant Vpu::GFP fusion proteins were expressed in HEK 293T cells and purified in sufficient quantities and purity for use in subsequent *in vitro* assays. Using ELISAs, it was found that CD74 effectively prevented the binding of an anti-Vpu antibody, but not an anti-GFP antibody, to the Vpu::GFP fusion protein with an IC_{50} of 888.67 ± 130.08 nM. Further to this, using CD74 overlapping peptides of increasing lengths in combination with a Vpu overlapping peptide set, it was determined that the sequences “RIRERAEDSGNESEG” and “EDQKP” in the Vpu and CD74 cytoplasmic regions, respectively, contain the binding sites for this interaction. While the CD4 and CD74 cytoplasmic peptides yielded different responses after binding Vpu peptides, these two host proteins were shown to compete for binding to the Vpu protein. This provides evidence that steric hindrance has an effect on binding. Finally, total CD74 levels including cell membrane and intracellular fractions were significantly downregulated by Vpu at

24 and 48 hours (p = 0.0270 and 0.0062, respectively) as indicated by immunoprecipitation and flow cytometry in Vpu-transfected U937 cells. Notably, Vpu phosphorylation mutants (S52A and S52/56A) were unable to reduce CD74 levels within U937 cells, indicating that CD74 is not targeted for proteasomal degradation. In conclusion, this study has defined the specific Vpu/CD74 binding site and provides novel evidence that CD74 is downregulated in the presence of Vpu. Moreover, CD74 is not targeted for proteasomal degradation through the binding of β-TrCP and the recruitment of the E3 ligase complex. These findings have future relevance for HIV-1 treatment and management as CD74 downregulation is yet another mechanism by which HIV-1 impairs the host immune response.

ACKNOWLEDGEMENTS

I would like to acknowledge the Department of Molecular Medicine and Haematology at the University of the Witwatersrand Medical School, the National Research Foundation, the Centre for Metal-based Drug Discovery and Mintek for the financial support throughout my studies. I would like to acknowledge my supervisors, Prof Maria Papathanasopoulos, Dr Salerwe Mosebi and Dr Raymond Hewer for the scientific knowledge they have provided throughout this research and for being such an inspiration to me.

To Maria, thank you for never failing to step in when I needed your help and for setting a brilliant example of an excellent researcher for me to look up to.

To Sal, thank you for all of your wonderful support and advice. You were an amazing wealth of information and ideas whenever I was stuck and I appreciate the meticulous care you took in every aspect of my work. Thank you so much for the time and effort you put in for me.

To Ray, where do I even start? Thank you for your patience, understanding, enthusiasm, your unswerving willingness to help and for all those behind-the-scenes miracles you worked for me on a daily basis. Your guidance, support and friendship have been invaluable over these few years. You convinced me to start my PhD in the first place; I am so grateful that you never gave up on me and cheered me on the whole way until the end.

Thanks to all my colleges at CMDD for their support and encouragement. Thanks in particular to Angela Harrison and Shaakira Abrahams for the laughs, the chats and helping me through the stressful moments.

I would like to thank Novartis for hosting me for 3 months during my PhD and extend a special note of gratitude to my “NGS family”. You guys were and are still awesome!

Thanks to Martine Whitehead for all of the diagrams in this work and for putting up with my constant requests for fixing the figures.

I would like to thank my all my family and friends, whose love and support have seen me through. Without you to cheer me on, this task would have been impossible. Finally, to my mom – there aren't enough words to completely describe my appreciation, so thank you for everything.

TABLE OF CONTENTS

Page

Declaration..... i

Publications and Presentations Arising from this Study..... ii

Abstract..... iii

Acknowledgements..... v

Table of Contents..... vii

List of Figures..... ix

List of Tables..... xii

List of Abbreviations..... xiii

Chapter One: Literature Review..... 1

1.1) General introduction to HIV-1 accessory proteins..... 1

1.2) HIV-1 Vpu..... 2

1.2.1) Introduction to Vpu..... 2

1.2.2) The structure of Vpu..... 3

1.2.3) The primary functions of Vpu..... 5

1.2.4) Additional functions of Vpu..... 6

1.2.4.1) Vpu in apoptosis..... 7

1.2.4.2) Downregulation of MHCI..... 8

1.2.4.3) Inhibition of Tetherin..... 8

1.2.4.4) Regulation of Env/CD4 complexes..... 9

1.2.4.5) Vpu protects infected cells from lysis..... 9

1.2.4.6) Vpu inhibits NF-κB pathways..... 10

1.3) CD4 degradation through binding Vpu..... 11

1.3.1) Introduction to CD4..... 11

1.3.2) Multiple HIV-1 proteins target CD4..... 11

1.3.3) CD4 degradation..... 12

1.3.4) Vpu/CD4 specific interactions for degradation..... 13

1.4) Major Histocompatibility Complex Class II..... 18

1.5) CD74/Invariant chain..... 22

1.6) Similarities between CD4 and CD74..... 29

1.7) Project hypothesis and objectives..... 29

Chapter Two: Materials and Methods..... 31

2.1) CD4/CD74 homology study..... 31

2.2) National Institutes of Health Reagents……..... 32
2.3) Culture of U937 and HEK 293T cell lines……..... 33
2.4) Construction of Vpu::GFP and Vpu phosphorylation mutants..... 33
2.5) Expression and purification of Vpu::GFP……..... 35
2.6) *In vitro* assays for protein-protein interactions……..... 37
2.7) Immunoprecipitations……..... 40
2.8) Flow cytometry……..... 42
2.9) Statistical analyses……..... 43

Chapter Three: Results……..... 44
3.1) Peptide characterization……..... 44
3.1.1) Predicted structure and peptide properties……..... 44
3.1.2) Sequence and structural alignment of CD4 and CD74……..... 47
3.2) Sequencing and expression of Vpu::GFP in HEK 293T cells…..... 49
3.3) Binding interaction of Vpu with CD4 and CD74……..... 53
3.3.1) Confirmation of Vpu binding CD4 and CD74……..... 53
3.3.2) CD74 binds to an immunodominant domain on Vpu……..... 55
3.3.3) CD4 and CD74 compete for binding to Vpu……..... 57
3.3.4) Binding site delineation……..... 57
3.3.5) Peptide size plays a role in antibody inhibition……..... 63
3.4) CD4, CD74 and MHCII are downregulated in the presence of Vpu... 64

Chapter Four: Discussion……..... 74
4.1) CD4 and CD74 are structurally similar……..... 74
4.2) CD4 and CD74 bind to different sequences within a closely related region……..... 76
4.3) Vpu mediates CD74 downregulation……..... 79
4.4) Further considerations……..... 84
4.5) Concluding remarks……..... 86

References……..... 88

Appendices.....…….. 103

LIST OF FIGURES

Page

Figure 1.1: Schematic representation of Vpu based on nuclear magnetic resonance (NMR) structural elucidation. Pg 3

Figure 1.2: Schematic representation of CD4 degradation through binding human immunodeficiency virus type-1 (HIV-1) viral protein "u" (Vpu). Pg 17

Figure 1.3: Schematic representation of the structure of a major histocompatibility complex class I (MHCI) molecule. Pg 19

Figure 1.4: Schematic representation of the structure of a major histocompatibility complex class II (MHCII) molecule. Pg 20

Figure 1.5: Schematic representation of CD74. Pg 24

Figure 1.6: Schematic representation of the signal cascade induced by the CD74 cytoplasmic domain fragment (CD74-ICD) for cell survival. Pg 27/28

Figure 3.1: Predicted secondary structure of the T-cell surface glycoprotein CD4. Pg 45

Figure 3.2: The predicted secondary structure of the CD74 cytoplasmic domain. Pg 46

Figure 3.3: Hydrophobicity plots calculated for each of the peptides. Pg 47

Figure 3.4: Amino acid sequence alignment of the cytoplasmic domains of CD4 and CD74. Pg 48

Figure 3.5: Homology model of the CD74 cytoplasmic domain against the CD4 cytoplasmic domain. Pg 49

Figure 3.6: Nucleotide sequence analysis of the constructed Vpu::GFP plasmid. Pg 50/51

Figure 3.7: Micrographs taken of control and transfected HEK 293T and U937 cells at 48 hours post-transfection. Pg 52

Figure 3.8: Analysis and Western blot showing expression of the Vpu::GFP fusion protein in HEK 293T cells at approximately 36 kDa. Pg 52

Figure 3.9: The absorbance spectrum of the Vpu::GFP fusion protein. Pg 53

Figure 3.10: Interactions between full length recombinant Vpu::GFP and CD74 or CD4 peptides with anti-CD4 antibody. Pg 54

Figure 3.11: Interactions between full length recombinant Vpu::GFP and CD74 or CD4 peptides with anti-CD74 antibody. Pg 55

Figure 3.12: Interactions between Vpu::GFP and CD74 or CLIP peptides. Pg 56

Figure 3.13: Fitted dose response curve for the Vpu/CD74 interaction. Pg 56

Figure 3.14: Competitive binding study between CD4 and CD74 peptides to Vpu::GFP. Pg 57

Figure 3.15: Testing of Vpu overlapping peptides (NIH) with A) a subtype B anti-Vpu antiserum (NIH cat #969) and B) a subtype C anti-Vpu antiserum (NIH cat #11942). Pg 58

Figure 3.16: Interaction of coated Vpu overlapping peptides 10 and 13 with CD74 overlapping peptides. Pg 59

Figure 3.17: Interaction of coated Vpu overlapping peptides 18 and 19 with CD74 overlapping peptides. Pg 60

Figure 3.18: Interaction of coated Vpu overlapping peptides 18 and 19 with CD4 cytoplasmic peptide. Pg 61

Figure 3.19: CD74 reduces antibody binding to Vpu peptides while CD4 enhances antibody binding. Pg 62

Figure 3.20: CD4 binds to the Vpu responsive peptides. Pg 63

Figure 3.21: Individual peptides are unable to prevent antibody binding. Pg 63

Figure 3.22: Total CD74 levels are downregulated by Vpu::GFP. Pg 64

Figure 3.23: CD4 is downregulated by Vpu in U937 cells at 24 hours post-transfection. Pg 65

Figure 3.24: Effect of Vpu on MHCII levels in A) control, B) PMA-treated and C) IFN-γ-treated U937 cells at 24 hours but not 48 hours. Pg 67/68

Figure 3.25: Effect of Vpu on CD74 levels in A) control, B) PMA-treated and C) IFN-γ-treated U937 cells. Pg 69/70

Figure 3.26: CD74 is downregulated by A) Vpu-SM in U937 cells at 24 hours and is downregulated by B) Vpu-DM at both 24 and 48 hours. Pg 72

LIST OF TABLES

Page

Table 2.1: **Reagents from the NIH AIDS Research and Reference Reagent Program used within this study.** **Pg 33**

Table 2.2: **Amino acid sequences of the HIV-1 Consensus Vpu Peptides, obtained from the NIH AIDS Research and Reference Reagent Program.** **Pg 39**

Table 2.3: **Amino acid sequences of the nine CD74 10-mer and 15-mer overlapping peptides that were produced and used in the ELISA studies.** **Pg 40**

Table 3.1: Average fluorescence counts (± SD) for total CD4 levels in U937 cells that were either mock-transfected or Vpu-transfected. **Pg 66**

Table 3.2: Average fluorescence counts (± SD) are indicated for total MHCII levels in U937 cells that were either mock-transfected or Vpu-transfected. **Pg 68**

Table 3.3: Average fluorescence counts (± SD) are indicated for total CD74 levels in U937 cells that were either mock-transfected or Vpu-transfected. **Pg 70**

Table 3.4: Average fluorescence counts (± SD) are indicated for total CD74 levels in U937 cells that were either mock-transfected or Vpu-transfected with the Vpu single (SM) and double (DM) phosphorylation mutants. **Pg 73**

Table A.1: Absorbance (A_{650}) values for all ELISA data recorded in the Results chapter, indicating which peptides were coated/plated and which were incubated with the plated peptides. **Pg 104**

LIST OF ABBREVIATIONS

AGTR1	angiotensin II type 1 receptor
AIDS	acquired immune deficiency syndrome
AngII	angiotensin II
APC	antigen presenting cell
APOBEC3G	apolipoprotein B mRNA-editing enzyme, catalytic polypeptide-like 3G
ARF6	ADP ribosylation factor 6
BAFF	B cell activating factor
BLR	baseline response
BSA	bovine serum albumin
BST-2	bone marrow stromal cell antigen 2
β-TrCP	beta transducin repeat-containing protein
CB	coating buffer
CCL5	chemokine (C-C motif) ligand 5
CD74-ICD	CD74 intracellular domain fragment
CIITA	class II transactivator
CLIP	class-II-associated Ii-chain peptide
CSP	chemical shift perturbation
CTL	cytotoxic T lymphocyte
DMEM	Dulbecco's modified Eagle's medium
DSSP	dictionary of protein secondary structure
DOPE	discrete optimized protein energy

DPC	dodecylphosphocholine
EDTA	ethylenediaminetetraacetic acid
ELISA	enzyme-linked immunosorbent assay
Env	envelope glycoprotein
ER	endoplasmic reticulum
ERAD	ER-associated protein degradation
ERK-1/2	p44/p42 extracellular-signal-regulated kinase family
FACS	fluorescence activated cell sorting
FCS	foetal calf serum
FITC	fluorescein isothiocyanate
FRET	Försters resonance energy transfer
GBMV	generalized born with molecular volume
GPI	glycosyl phosphatidylinositol
HAART	highly active antiretroviral therapy
HEK 293T	human embryonic kidney 293T
HEPES	(4-(2-hydroxyethyl)-1-piperazineethanesulfonic acid
HIV-1	human immunodeficiency virus type 1
HLA-DM	human leukocyte antigen-DM
HLA-DR	human leukocyte antigen-DR
HRP	horseradish peroxidase
IC_{50}	half maximal inhibitory concentration
ICD	intracellular cytoplasmic domain
I-CLiPs	intramembrane cleaving proteases

IFN-α	interferon-α
IFN-γ	interferon-γ
kDa	kilo Dalton
LB	Luria-Bertani broth
MAPKs	mitogen-activated protein kinases
MCP-1	monocyte chemoattractant protein-1
MHCI	major histocompatibility complex class I
MHCII	major histocompatibility complex class II
MIF	macrophage inhibitory factor
Nef	negative factor
NF-κB	nuclear factor κB
NK	natural killer
NKT	natural killer T
NMR	nuclear magnetic resonance
NOE	nuclear overhauser effect
NTB-A	NK-T and B cell antigen
PACS-1	phosphofurin acidic cluster sorting protein-1
PBS	phosphate buffered saline
PDB	protein data bank
PDF	probability density function
PE	phycoerythrin
PI3K	phosphatidylinositol 3'-kinase
PMA	phorbol 12-myristate 13-acetate

PVDF	polyvinylidene difluoride
RIP	regulated intramembrane proteolysis
RMSD	root mean square deviation
RPMI	Roswell park memorial institute
SISA	simple interactive statistical analysis
SIV	simian immunodeficiency virus
SDS	sodium dodecyl sulphate
SDS-PAGE	sodium dodecyl sulphate polyacrylamide gel electrophoresis
$TAF_{II}105$	TBP-associated factor $_{II}105$
TBP	TATA box binding protein
TBS	tris buffered saline
TBST	tris buffered saline with Tween 20
TFIID	transcription factor IID
TMB	3,3',5,5'-tetramethylbenzidine liquid
Vif	virion infectivity factor
Vpr	viral protein R
Vpu	viral protein U

CHAPTER ONE: LITERATURE REVIEW

1.1 General introduction to HIV-1 accessory proteins

Human immunodeficiency virus type 1 (HIV-1) is a retrovirus that causes Acquired Immune Deficiency Syndrome (AIDS). This creates a life-long infection through the presence of latent, perpetual HIV-1 reservoirs within CD4+ T cells that persist even throughout treatment with highly active antiretroviral therapy (HAART) (reviewed in Chun and Fauci, 1999). This disease impairs the immune system through the infection of cells that are vital for generating an immune response (reviewed in Peters and Sperber, 1999) and is characterized by a considerable decrease in CD4+ T cells and a grossly weakened immune system which then becomes incapable of dealing with other opportunistic infections (Komoto *et al.*, 2003). HIV-1 has an integrated genome of approximately 9.8 kilobases and encodes proteins that are needed for cell entry, replication and budding. It also contains several genes, such as *vif*, *vpr*, *nef* and *vpu*, which encode accessory regulatory proteins with apparent importance, that were once deemed "non-essential" (reviewed in Strebel, 1996; Marassi *et al.*, 1999). However, it is now recognized that HIV-1 accessory proteins are indeed needed for replication as they are designed to be multifunctional, and counteract the antiviral activity of host restriction factors (reviewed in Dubé *et al.*, 2010a).

HIV-1 accessory proteins are versatile adaptor molecules that are able to connect viral and cellular proteins to cellular pathways, as well as regulate these pathways through protein-protein interactions in order to promote viral replication (Hussain *et al.*, 2007). These proteins are actively involved in the establishment of infective persistence within the host. Decreased levels of these accessory proteins may lead to a significant loss in the severity of disease, as these accessory proteins have important functions for the disruption of host mechanisms that are in place to restrict the spread of HIV-1 infection (Nomaguchi *et al.*, 2008). Virion infectivity factor (Vif) targets the antiviral factor apolipoprotein B mRNA-editing enzyme, catalytic polypeptide-like 3G (APOBEC3G) for proteasomal degradation, as in the absence of Vif this antiviral factor is incorporated into new viruses and causes an inhibition of viral DNA synthesis

(reviewed in Kirchhoff, 2010). Viral protein R (Vpr) is involved in numerous activities including the induction of cell death and activation of proviral transcription (reviewed in Kirchhoff, 2010). Negative factor (Nef) is reportedly the most functionally diverse of the accessory proteins as it functions to alter cell signalling pathways, and affect antigen presentation as well as gene expression and receptor surface expression (reviewed in Kirchhoff, 2010). Finally, viral protein "u" (Vpu) has also been shown to have multiple functions within the host cell, the most well-known being the degradation of the HIV-1 receptor, CD4, as well as efficient virion release (reviewed in Kirchhoff, 2010).

1.2 HIV-1 Vpu

1.2.1 Introduction to Vpu

Many aspects of HIV-1 infection involve the host cell membranes and as such many membrane proteins like Vpu, are intimately involved in the spread of HIV-1 (Marassi *et al.*, 1999). Vpu is an important accessory protein that is found only in HIV-1 and a few simian immunodeficiency virus (SIV) isolates such as SIVcpz (chimpanzee), SIVmon (mona monkey), SIVgsn (greater spot-nosed monkey), SIVmus (mustached monkey) and SIVden (Dent's mona monkey), but is not found within HIV-2 (reviewed in Dubé *et al.*, 2010a). Related isolates that do not express a functional Vpu protein have far less severity in terms of disease outcome (reviewed in Leligdowicz and Rowland-Jones, 2008). Vpu is a conserved protein that contains a 12 residue sequence (ERAEDSGNESEG) that is constant through all HIV isolates that express Vpu (Myers *et al.*, 1992; Chen *at al.*, 1993). Vpu and the envelope (Env) glycoprotein are cotranslationally expressed from the same bicistronic mRNA that is dependent on the HIV-1 Rev protein, resulting in approximately equal amounts of both Vpu and Env (reviewed in Strebel, 1996; reviewed in Dubé *et al.*, 2010a). Vpu is expressed in the later stages of infection and the cellular location of Vpu appears to depend on the subtype of the virus (reviewed in Dubé *et al.*, 2010a). It is thought that Vpu contains two trafficking signals in the hinge region that lies between the transmembrane domain and the cytoplasmic domain as well as within the second or C-terminal α-helix (reviewed in Dubé *et al.*, 2010a). It has been suggested that there are deviations in the primary sequences of these trafficking signals between HIV-1 subtypes which would explain why Vpu expressed from different subtypes is not localized within the same cellular compartments. This difference is demonstrated between subtype B and subtype C, where subtype B Vpu localizes

mainly within intracellular membranes such as the endoplasmic reticulum (ER), Golgi and endosomes, while subtype C Vpu is reportedly found mostly at the plasma membrane (reviewed in Dubé *et al.*, 2010a).

1.2.2 The structure of Vpu

Vpu consists of 81 residues with a size of 9 kilo Daltons (kDa) and is a type I integral membrane protein with two distinct domains: the N-terminal transmembrane hydrophobic helix (residues 1-27) and two amphipathic α helices (residues 35-50 and 58-70 respectively) that form part of the cytoplasmic domain and are separated by a linker region (residues 47-58), as shown in Figure 1.1. The linker region contains two highly conserved serine residues, namely Ser52 and Ser56, which are phosphorylated by casein kinase II (reviewed in Andrew and Strebel, 2010). It has been suggested that Vpu is not constitutively phosphorylated, but rather that two forms of Vpu exist within the cell, both unphosphorylated and phosphorylated (Belaïdouni *et al.*, 2007) as demonstrated by the schematics in Figure 1.1 A and B, respectively.

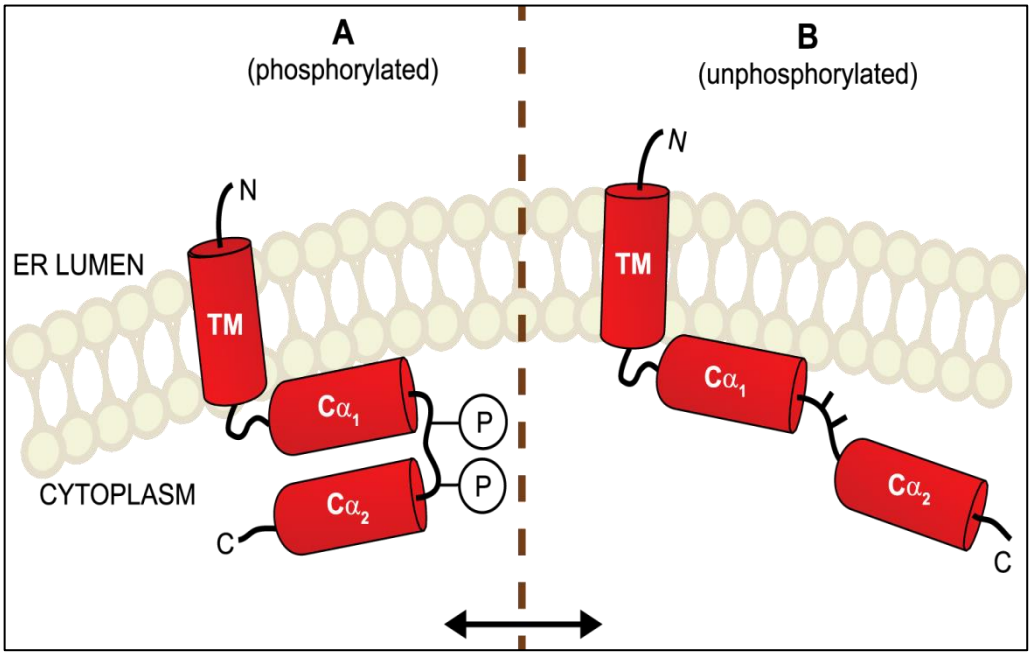


Figure 1.1: Schematic representation of Vpu based on nuclear magnetic resonance (NMR) structural elucidation. This schematic shows the N-terminal region, followed by a relatively short transmembrane domain and the two α-helices that reside in the cytoplasm. The two conserved phosphorylated serine residues that are required for CD4 degradation lie in the linker region between the two cytoplasmic helices (adapted from Andrew and Strebel, 2010; Dubé *et al.*, 2010a).

The transmembrane and cytoplasmic domains have been shown to fold independently of each other (Ma *et al.*, 2002; Hussain *et al.*, 2007; Nomaguchi *et al.*, 2008). Nuclear magnetic resonance (NMR) studies have shown that the transmembrane domain lies vertically within the lipid bilayer while the two cytoplasmic helices lie parallel to the lipid bilayer (Marassi *et al.*, 1999). More recent evidence has indicated that the transmembrane domain tilts at an angle of approximately 6-15 degrees (Kukol and Arkin, 1999; Park *et al.*, 2003) and that the linker region between the two cytoplasmic helices is largely flexible, allowing for the second cytoplasmic helix to move and possibly lie parallel to the first cytoplasmic helix (reviewed in Andrew and Strebel, 2010). The first cytoplasmic helix is considered to lie parallel to and be partly buried in the membrane to shield the hydrophobic residues, leaving the charged residues exposed. However, the exact conformation of Vpu may be dependent on oligomerization or the interaction with other host proteins (Kukol and Arkin, 1999; Lemaitre *et al.*, 2006; Wittlich *et al.*, 2009; reviewed in Andrew and Strebel, 2010). Using molecular simulation structures, it was shown that there are slight structural differences in the cytoplasmic domain between the phosphorylated and unphosphorylated forms of Vpu, with the phosphorylated protein adopting a more compact structure in comparison to the unphosphorylated protein (Lemaitre *et al.*, 2006), as depicted in Figure 1.1 A and B. This may be because in the absence of phosphorylation, the C-terminal helix of the cytoplasmic domain would seem to lie in the aqueous phase and the phosphorylation of the conserved serine residues in the linker region is thought to have an effect on the secondary structure, resulting in the shift of the C-terminal helix to a position that is parallel to the first cytoplasmic helix (Lemaitre *et al.*, 2006). Nuclear overhauser effect (NOE) spectra have suggested that the two cytoplasmic helices lie in an antiparallel formation and that there is likely to be spatial proximity between the C-terminal region and the linker region containing the phosphorylated serines. The side chains of the serine residues are thought to be exposed to the buffer or solvent, making these residues accessible to casein kinase II for phosphorylation (Wittlich *et al.*, 2009). Vpu is mostly found to be in the ER and Golgi apparatus but may also be found to some extent at the plasma membrane (Pacyniak *et al.*, 2005; Hussain *et al.*, 2007); however Vpu is not found in culture fluid or supernatant, suggesting that the protein is not associated with virions (Ma *et al.*, 2002). Vpu is able to form oligomeric complexes with itself through the action of the

transmembrane domain even in the absence of a membrane environment and it has been shown *in silico* as well as *in vitro* to form pentamers (Maldarelli *et al.*, 1993; Kukol and Arkin, 1999; Hussain *et al.*, 2007).

1.2.3 The primary functions of Vpu

The two primary functions of Vpu are the release of new virus particles from infected cells and the degradation of CD4, the primary receptor protein for HIV-1. The second function occurs through the binding of beta-transducin repeat-containing protein (β-TrCP), which requires the cytoplasmic domain of Vpu with the two phosphorylated serine residues. These two functions occur within separate cellular compartments; therefore Vpu operates at different locations within the cell (Schubert and Strebel, 1994). These functions have been shown to rely on the two distinct domains of Vpu. A Vpu mutant that only contains the transmembrane domain was unable to target CD4 for degradation but was partially able to enhance virus release in comparison to wild-type Vpu (Schubert *et al.*, 1996). To add to this, a Vpu mutant with a randomized transmembrane domain was able to induce CD4 degradation, while the release of virus in the presence of this mutant were completely abrogated and levels of virus released were comparable to those in the absence of Vpu. This indicates that an intact cytoplasmic domain is required for CD4 degradation with the transmembrane domain only functioning as a membrane anchor for this particular function, while an intact transmembrane domain is needed for the efficient release of newly assembled virus particles from the membrane (Schubert *et al.*, 1996). However, it has been shown that mutations within different regions of the transmembrane domain may play different roles in terms of CD4 degradation (Tiganos *et al.*, 1998). In this regard, it was found that mutations within the N-terminal or middle portions of the transmembrane domain have no effect on the ability of Vpu to bind to and degrade CD4, while a mutation within the C-terminal portion of the transmembrane domain resulted in the total loss of binding between Vpu and CD4. This particular transmembrane mutant had the conserved tryptophan residue (Trp22) moved to a position that is two residues C-terminal to its original position, which may affect the overall conformation of the protein within this domain and thus possibly influence the ability of Vpu to bind to CD4. Simultaneously, these mutants had a reduced efficiency with regard to virus particle release (Tiganos *et al.*, 1998), which rather suggests that the overall

structure of the whole Vpu protein contributes to both of these functions. The two main functions of Vpu contribute together to an increase in the production of new viruses (Ma *et al.*, 2002) and without an active Vpu protein, new virions collect within the cell and lead to cytotoxicity (Marassi *et al.*, 1999).

Initially it was thought that Vpu is able to promote the release of new viruses through the formation of Vpu oligomeric complexes in the transmembrane domain, as these have an ion channel activity within cell membranes (Willey *et al.*, 1992a; Chen *et al.* 1993; Strebel, 1996; Schubert *et al.*, 1998; Hussain *et al.*, 2007). However, more recent studies have shown that Vpu functions to promote virus release through the mechanism of antagonising the host restriction factor, tetherin, otherwise known as bone marrow stromal cell antigen (BST-2) (Neil *et al.*, 2008; Van Damme *et al.*, 2008; Skasko *et al.*, 2011). This leaves the purpose of the ion channel activity of Vpu unclear, as mutational studies indicated that Vpu defective in the ability to form ion channels was still able to co-localize with and effectively inhibit tetherin (Skasko *et al.*, 2011). However it has been suggested that the ion channel activity influences the levels of intracellular calcium (Willey *et al.*, 1992a; Willey *et al.*, 1992b) and that this leads to a decrease of calcium within the lumen of the ER. This ultimately expedites the degradation of proteins retained within the ER, as depleted levels of calcium in the ER stimulate an increase in the rate of proteolysis within this compartment (Wileman *et al.*, 1991).

1.2.4 Additional functions of Vpu

There are other important functions of Vpu including the induction of apoptosis in infected cells, the modulation of major histocompatibility complex class I (MHCI), the counteraction of the host restriction factor tetherin which functions to inhibit the release of new virus particles from the cell, the regulation of gp160 processing into gp120 and gp41 for virus assembly, as well as the finding that Vpu affects the down regulation of the major histocompatibility complex class II (MHCII) by binding the invariant chain (CD74) via interactions between their cytoplasmic domains (Willey *et al.*, 1992b; Kerkau, 1995; Strebel, 1996; Marassi *et al.*, 1999; Hussain *et al.*, 2008; Nomaguchi *et al.*, 2008).

1.2.4.1 Vpu in apoptosis

Vpu has been shown to induce apoptosis in HIV-1-infected T cells (Akari *et al.*, 2001). Nuclear factor κB (NF-κB) is found in an inactive form bound to its inhibitor, IκB, within the cytoplasm. Upon degradation of IκB and the stimulation of cells with cytokines or chemokines, NF-κB becomes activated and moves to the nucleus where it activates gene expression of factors, for example B cell activating factor (BAFF) and chemokine (C-C motif) ligand 5 (CCL5), that are implicated in the activation and development of B and T cells (Bour *et al.*, 2001). Vpu that contains the two phosphorylated serine residues is able to bind to β-TrCP thereby inhibiting the degradation of IκB, which finally prevents the activation of NF-κB. The decrease in active NF-κB ultimately leads to a decrease in the expression of antiapoptotic proteins, such as Bcl-2 (section 1.5). In conjunction with increased caspase-3 levels, this caused apoptosis within HIV-1 infected T cells (Akari *et al.*, 2001) although it has been suggested that this finding may differ depending on which HIV-1 isolate is investigated as well as the type of cell that is infected (Komoto *et al.*, 2003). This was demonstrated through the use of primary CD4+ T cells and human MT-4 cells as these cells responded differently to apoptosis induction by HIV-1 isolates with different Vpu mutations (Komoto *et al.*, 2003). It is likely that the phosphorylation of serine residues are important for a protein to be recognized and bound by β-TrCP as other targets for β-TrCP degradation have also been found to contain phosphorylated serine residues. Although there are both phosphorylated and unphosphorylated forms of Vpu within a cell, HIV-1 Vpu is for the most part found to be phosphorylated, indicating that Vpu and β-TrCP may form highly stable complexes. As Vpu accumulates within the cell over time, this prolonged interaction between Vpu and β-TrCP results in a continued inhibition of other β-TrCP functions. It was previously thought that Vpu itself is not degraded as a consequence of its interaction with β-TrCP (Bour *et al.*, 2001). However, Belaïdouni *et al.* (2007) have shown ubiquitination and 26S proteasomal degradation of wild-type Vpu within HeLa cells, but not of a Vpu phosphorylation mutant with substitutions at residues 52 and 56, indicating that Vpu is degraded through interaction with β-TrCP and the conserved phosphorylated serine residues are required for this. Further to this, Vpu has another serine residue at position 61 which facilitated the degradation of Vpu when this residue is phosphorylated (Estrabaud *et al.*, 2007). Therefore the differential phosphorylation of Vpu determines which protein will be

ubiquitinated and degraded – either the target host protein or Vpu itself. The mutation of this serine residue (position 61) with an alanine has been shown to stabilize the protein (Hill *et al.*, 2010).

1.2.4.2 Downregulation of MHCI

Another function of Vpu is the modulation of MHCI molecules. Although Nef is considered to be the major viral protein involved in MHCI downregulation (Specht *et al.*, 2010), Vpu is also involved in this function, though through a different mechanism. This reportedly occurs through the interference of the biosynthetic pathway of MHCI molecules by Vpu within the ER. It is possible that this is achieved by the ability of Vpu to induce the degradation of MHCI molecules before they can reach the cell surface, similar to that of CD4 (Kerkau *et al.*, 1997). However, the specific degradation of MHCI molecules through interaction with Vpu has not yet been expressly indicated.

1.2.4.3 Inhibition of Tetherin

Yet another protein that is inhibited or antagonized by Vpu is the host restriction factor tetherin. Tetherin is a membrane protein that is induced by interferon-α (IFN-α) and is expressed on the cell surface of differentiated B cells and bone marrow stromal cells (Neil *et al.*, 2008). Tetherin is a 30-36 kDa type II transmembrane protein that consists of an N-terminal cytoplasmic domain, a transmembrane domain, a coiled-coil extracellular domain as well as a C-terminal glycosyl phosphatidylinositol (GPI) membrane anchor (Skasko *et al.*, 2011). It is believed that the GPI anchor is essential for the inhibition of viral release from the cell as removal of this domain completely suppresses the function of tetherin (Neil *et al.*, 2008). It has been shown that tetherin functions to harness newly assembled virions to each other as well as to the cell membrane. Vpu has been found to co-localize with tetherin and these two proteins interact specifically through the binding of their transmembrane domains. Not all cell types require Vpu for virion release. However, those cell types that are dependent on Vpu for this function, but that are deficient in Vpu, show the accumulation of mature and assembled virions at the surface which later are internalized to the endosomes (Neil *et al.*, 2008). The ability of Vpu to inhibit tetherin at the surface of the cell relies on both the transmembrane domain of Vpu as well as the conserved serine residues in the cytoplasmic linker region. This would suggest that Vpu targets tetherin for proteasomal degradation. However it was found that inhibition of the

proteasome had little effect on the ability of Vpu to antagonize tetherin (Van Damme *et al.*, 2008). Previous studies reported the possibility that Vpu downregulates tetherin by trapping it within the Golgi network (Dubé *et al.*, 2010b) and an ER-associated protein degradation (ERAD) type of degradation (Mangeat *et al.*, 2009). More recently it was shown that Vpu rather targeted cell surface tetherin and removed it directly from the plasma membrane (Skasko *et al.*, 2011) thus greatly enhancing virion release.

1.2.4.4 Regulation of Env/CD4 complexes

Vpu regulates the formation of Env/CD4 complexes within the ER in HeLa cells (Willey *et al.*, 1992b). This allows for the processing of Env to form gp120 and gp41 as Vpu appears to disrupt the Env/CD4 complexes by targeting CD4 for proteasomal degradation. Gp120 and gp41 are required for the assembly of new viruses; therefore Vpu indirectly plays a role in particle assembly. This function is described in more detail in section 1.3.2 (Marassi *et al.*, 1999; Nomaguchi *et al.*, 2008).

1.2.4.5 Vpu protects infected cells from lysis

Natural killer (NK) cells play a vital role in the immune system as they are able to lyse specific targeted cells and are thus important as a line of defence against viral infections. These cells need to be regulated either by activation or inactivation by a variety of receptors in order to carry out their immune functions. The NK-T and B cell antigen (NTB-A) is one such receptor that functions as a coactivator to instigate the degranulation of NK cells in which lytic granules are produced and released in order to facilitate lysis of the target cell (Richard and Cohen, 2010). Vpu binds to NTB-A, an interaction that is reliant on the Vpu transmembrane domain, and in so doing mediates the downregulation of NTB-A on the cell surface which restricts the degranulation of NK cells. This in turn protects the infected cells from lysis (Shah *et al.*, 2010).

Similar to the downregulation of NTB-A, Vpu also downregulates CD1d at the cell surface. This protein is expressed on antigen presenting cells (APCs) including monocytes, dendritic cells as well as macrophages, and is involved in the presentation of lipid antigens to natural killer T (NKT) cells. Vpu binds to CD1d thereby causing a downregulation of this protein on APCs (reviewed in Dubé *et al.*, 2010). Vpu co-localizes with CD1d within intracellular compartments,

indicating that there is an interaction between these two proteins which allows Vpu to interfere with the recycling of CD1d from intracellular compartments to the cell surface. A reduction in the surface expression of CD1d leads to a decrease in the activation of NKT cells; therefore this is yet another way in which Vpu functions to protect infected cells from lysis and ultimately impair the development of immune responses. It is interesting to note that CD1d, like many other host factors, is targeted by both Vpu as well as Nef (Moll *et al.*, 2010).

1.2.4.6 Vpu inhibits NF-κB pathways

Another way in which Vpu may undermine the immune system is by possibly preventing the translocation of the CD74 intracellular cytoplasmic domain fragment (CD74-ICD) to the nucleus. This would prevent the initiation of the NF-κB signal cascade that affects B cell maturation, proliferation and survival, as explained in detail in section 1.5. There may be many additional consequences to the effect of Vpu on the NF-kB pathways, however there are multiple other HIV-1 proteins that are involved in the decrease of antiapoptotic proteins or the induction of apoptosis, such as Nef, Tat, Vpr and Env (Komoto *et al.*, 2003; Nomaguchi *et al.*, 2008). For example, Nef also affects antigen presentation by MHCII molecules as it upregulates the expression of CD74 at the cell surface (reviewed in Kirchhoff, 2010), thereby preventing it from complexing with immature MHCII in the ER, as well as contributing to the modulation of NF-κB pathways by preventing the release of CD74-ICD from the plasma membrane. This indicates that Vpu does not positively influence viral persistence alone, but rather contributes to this along with other HIV-1 proteins. Nef and Vpu in particular seem to work in conjunction for a greater overall effect on the immune system.

In summary, Vpu has many crucial functions by which it contributes to the impairment of the immune system and disease outcome. It plays an important role in multiple key aspects of the immune system, including antigen presentation, induction of apoptosis, prevention of the lysis of infected cells and interference with the expression of survival proteins within immune cells to name a few.

1.3 CD4 degradation through binding Vpu

1.3.1 Introduction to CD4

As previously mentioned in sections 1.2.3 and 1.2.4, Vpu has a variety of approaches by which it undermines the immune system. One of the most documented approaches would be the targeting of CD4 for degradation (Willey *et al.*, 1992a; Chen *et al.*, 1993; Schubert *et al.*, 1998). As CD4 is an important protein in the immune response, Vpu significantly debilitates the immune system by targeting this protein for degradation. CD4 is a 55 kDa class I membrane glycoprotein that consists of a lumenal domain, a transmembrane domain and a 38 residue cytoplasmic domain (Willey *et al.*, 1992a). NMR structural analyses indicate that the transmembrane α-helix spans residues 372-395 and the amphipathic cytoplasmic α-helix comprises of residues 403-413 and is positioned closely to the membrane, while the C-terminus remains unstructured (Wittlich *et al.*, 2010). This protein is synthesized within the ER and is transported to the cell surface through the Golgi network (Willey *et al.*, 1992a) and is expressed on a set of T lymphocytes which are able to recognize antigen presenting MHCII molecules (Schubert *et al.*, 1998; Wittlich *et al.*, 2010).

CD4 is a highly important component for the proper functioning of the immune system as it assists with the protection against both intracellular and extracellular parasites, bacteria and viruses. It is involved in many different roles including the production of cytokines, recruitment of neutrophils, basophils and eosinophils, as well as assisting B cells with the production of antibodies (Killar *et al.*, 1987; Mosman and Coffman, 1989; Paul and Seder, 1994; Weaver *et al.*, 2006; reviewed in Zhu and Paul, 2008) and it also serves as the primary receptor for HIV-1 in order for HIV-1 to gain entry to the cell (Schubert *et al.*, 1998). Additionally, downregulation and degradation of CD4 modulates the activation of T lymphocytes and also prevents the superinfection of the host (Magadan *et al.*, 2010).

1.3.2 Multiple HIV-1 proteins target CD4

CD4 is targeted by three separate viral proteins, namely Nef, Env and Vpu. Nef binds to the cytoplasmic domain of CD4 thereby reducing the surface expression of CD4 in particular by targeting CD4 for internalization or endocytosis via a clathrin-dependent process, leading to subsequent lysosomal degradation. The Env precursor, gp160, binds to CD4 within the ER and acts as a trap by

preventing newly synthesized CD4 from moving to the cell surface (Nomaguchi *et al.*, 2008; Wittlich *et al.*, 2010; reviewed in Andrew and Strebel, 2010). CD4 has been shown to be degraded in the ER after co-expression with Vpu in HeLa cells (Willey *et al.*, 1992a; Bour *et al.*, 1995), which not only affects the recognition of MHCII presenting molecules, but also frees the Env precursor thereby allowing for both the maturation and trafficking of Env (Nomaguchi *et al.*, 2008). The formation of Env/CD4 complexes is of some importance in Vpu-mediated degradation of CD4, although Env itself is not able to induce CD4 degradation. This is because even in the absence of Env, Vpu is still able to degrade CD4 as long as CD4 is unable to move out of the ER, further indicating that Env functions only as a trap (Willey *et al.*, 1992a). This is further supported by data indicating that not only Env, but interactions between the transmembrane domains of Vpu and CD4, as well as the polyubiquitination of the CD4 cytoplasmic region, also serve to trap CD4 within the ER (Magadan *et al.*, 2010). Similarly, in the absence of CD4, Vpu is not involved in the processing of Env (Willey *et al.*, 1992b). However, if CD4 remains bound to Env in the ER, the processing of Env is inhibited resulting in downstream consequences for new virus formation (Marassi *et al.*, 1999). Using fluorescence activated cell sorting (FACS)-based Försters resonance energy transfer (FRET), it was shown that Nef and Vpu were found in their expected locations within the cell, i.e. Nef at the plasma membrane and Vpu at the ER, Golgi and plasma membrane (Banning *et al.*, 2010). The binding of Nef and Vpu to CD4 within their respective cellular compartments was also corroborated using this approach (Banning *et al.*, 2010). These two viral proteins work together to target CD4 as Vpu cannot bind to CD4 at the cell surface and Nef cannot prevent the movement of CD4 from the ER to the cell surface (reviewed in Andrew and Strebel, 2010). The combined effect of both Nef and Vpu on the downregulation of CD4 leads to a continuous downregulation of this protein, as Nef is expressed early in infection and targets pre-existing CD4, while Vpu is expressed at a later stage and targets newly synthesized CD4 (Magadan *et al.*, 2010). Therefore, the downregulation of CD4 appears to be of significance to HIV-1 as it dedicates two accessory proteins to this function.

1.3.3 CD4 degradation

There have been conflicting reports regarding the involvement of the ERAD pathway in Vpu-mediated CD4 degradation. This arises from the fact that there

are multiple ERAD pathways with varying mechanisms of targeting proteins that have imperfections in one or more of their domains. However it has been found that the Vpu-mediated degradation of CD4 relies on the VCP-UFD1L-NPL4 complex to disassociate CD4 from the ER membrane. This complex is a vital element of the ERAD mechanism, thus indicating that the degradation of CD4 is in part reliant on this pathway (Magadan *et al.*, 2010). To add to this, it was found that Vpu-mediated degradation of CD4 is unable to occur in the absence of the AAA ATPase Cdc48/p97, which is required to extract ERAD proteins from the ER membrane in order for these proteins to be degraded by the 26S proteasome (Binette *et al.*, 2007). The ability of Vpu to induce degradation of CD4 was blocked by the use of proteasome inhibitors and required cytosolic protein polyubiquitination machinery that targets ubiquitination sites in the CD4 cytoplasmic domain (Fujita *et al.*, 1997; Schubert *et al.*, 1998). The use of proteasome inhibitors did not hinder the binding between Vpu and CD4. It was also found that the ubiquitin-activating enzyme E_1, which is required to attach ubiquitin to proteins, is involved in Vpu-mediated CD4 degradation (Schubert *et al.*, 1998). It should be noted that protease inhibitors which do not affect the proteasome were not able to prevent the Vpu-mediated degradation of CD4 (Fujita *et al.*, 1997). Also, the degradation of CD4 by Vpu is not affected by the inhibition of the lysosomal protein degradation machinery. This degradation process is membrane-dependent and requires the expression of both CD4 and Vpu within the same membrane compartment. Additionally, Vpu is able to target both glycosylated and unglycosylated forms of CD4 (Chen *et al.*, 1993; Schubert *et al.*, 1998).

1.3.4 Vpu/CD4 specific interactions for degradation

The cytoplasmic tail of CD4 is necessary for sensitivity to Vpu as this region contains the binding site for Vpu as well as sequences that are significant for degradation (Willey *et al.*, 1994; Bour *et al.*, 1995). Removal of 13 residues from the cytoplasmic tail of CD4 did not affect the ability of Vpu to cause the degradation of CD4, yet the removal of 32 residues from the CD4 cytoplasmic tail was reported to prevent Vpu-mediated degradation of CD4 (Chen *et al.*, 1993). This indicates that a region of approximately 19 residues (from 402 to 420) within the CD4 cytoplasmic domain is needed for Vpu-mediated degradation (Chen *et al.*, 1993). This Vpu-responsive region lies close to the membrane and contains

two phosphorylated serine residues, which are not involved in Vpu-mediated degradation (Willey *et al.*, 1994). This same region on CD4 was found to be important in the binding of Vpu, and not only important for degradation. CD4 mutants that lacked this binding site were not sensitive to Vpu-mediated degradation providing evidence that the binding interaction between CD4 and Vpu is necessary for degradation (Bour *et al.*, 1995). In addition to this, a mutant $CD4_{KRcyto}$ having lysine substituted with arginine at positions 411, 417, 418 and 428 within the cytoplasmic domain of CD4, was found to be stable in the presence of Vpu. Despite this, the $CD4_{KRcyto}$ mutant was still able to bind to Vpu, thus suggesting that the ubiquitination of the lysine residues may be required for Vpu-mediated CD4 degradation (Schubert *et al.*, 1998). More specifically, Bour *et al.* (1995) described two discrete amino acid sequences in the cytoplasmic tail of CD4, namely EKKTCQCP and LSEKKT, the removal of which resulted in a decrease in the ability of Vpu to induce CD4 degradation. More recent studies have indicated that it is not only the lysine residues in the cytoplasmic domain of CD4 that are ubiquitinated. The same $CD4_{KRcyto}$ mutant was found to be ubiquitinated and degraded in the presence of Vpu within human embryonic kidney (HEK) 293T cells, although significantly less than the wild-type protein. This indicates that the lysine residues do play an important role in the ubiquitination of CD4, but they are not solely responsible for this process (Binette *et al.*, 2007). Furthermore, it was demonstrated that the removal of serine and threonine residues in addition to lysine residues completely abolished the ubiquitination and degradation of CD4 in the presence of Vpu. This indicates that there are multiple ubiquitin target sites within the CD4 cytoplasmic domain (Magadan *et al.*, 2010). It is not only specific amino acid sequences that are required for binding of CD4 to Vpu. It has been shown that the presence of a membrane proximal α-helix within the CD4 cytoplasmic domain is needed in order to bind to Vpu as it may provide an interface for this protein interaction, and the disruption of this α-helix abrogates the degradation of CD4 through interaction with Vpu. However, CD4 mutants that have an altered primary sequence, but that are still able to form an α-helix, are also still capable of binding Vpu (Tiganos *et al.*, 1997), indicating that structural determinants may be of a greater significance for binding than sequence alone.

Sequences in the cytoplasmic domain of Vpu are also needed to induce the degradation of CD4 (Chen *et al.*, 1993; Bour *et al.*, 2001). The CD4 binding site on Vpu overlaps with the immunodominant domain, as CD4 prevents the binding of antibodies directed against the Vpu cytoplasmic domain (Schneider *et al.*, 1990; Bour *et al.*, 1995). In a similar study, it was also shown that an antibody directed against a Vpu cytoplasmic peptide with the sequence HAPWDVDDL was masked through the binding of CD4 to Vpu (Tiganos *et al.*, 1997), suggesting that this sequence is part of the binding region for CD4. It has been shown that the cytoplasmic region of Vpu contains an invariant sequence of 10 residues and that a deletion of only a portion of this sequence or a deletion of only 6 C-terminal residues severely limits Vpu-mediated CD4 degradation (Chen *et al.*, 1993). As such, it has been suggested that this region is an active site on Vpu as it is found on the same side of the membrane and possibly lines up with the Vpu-responsive region on CD4 which indicates the possibility that these are the interacting regions on the two proteins (Willey *et al.*, 1994). Additional studies have also shown that the membrane proximal α-helix in the Vpu cytoplasmic domain is required for CD4 binding. Specifically, mutational studies indicated that residues 28-47 and 76-81 in the cytoplasmic domain of Vpu are needed in order to bind CD4 (Margottin *et al.*, 1996). Further to this, it has been shown that the overall secondary structure of the Vpu cytoplasmic domain is necessary in order to mediate the degradation of CD4, as mutants containing disruption in either of the Vpu cytoplasmic α-helices were unable to target CD4 for degradation, even though these mutations did not affect the phosphorylated serine residues in the linker region (Tiganos *et al.*, 1997). Alanine-scanning mutagenesis was used to identify specific residues within the second cytoplasmic helix of Vpu that may be involved in CD4 downregulation. This approach allowed for the identification of a highly conserved leucine at position 63 that is essential for CD4 downregulation, as well as valine at position 68 that is also important for this particular function of Vpu (Hill *et al.*, 2010). Chemical shift perturbation (CSP) analysis likewise showed that both cytoplasmic α-helices of Vpu are involved in binding CD4, though the C-terminal α-helix demonstrated the most substantial chemical shift changes which suggests that this helix has a more pronounced role in binding CD4 compared to the membrane-proximal helix (Singh *et al.*, 2012). As previous studies indicated that while both α-helices are necessary for degradation and only the first α-helix is needed for binding (Tiganos *et al.*1997), it is possible that

the binding of CD4 induces a conformational change in Vpu that is more suitable for the downstream events leading to CD4 degradation.

Although binding of Vpu to CD4 is necessary for CD4 degradation, this step alone is not enough to induce degradation. Two Vpu mutants, a deletion mutant and a phosphorylation mutant, were both able to bind to CD4 but were unable to induce degradation (Bour *et al.*, 1995), indicating that phosphorylation is not required for Vpu binding to CD4. However, this does indicate that phosphorylation of the serine residues in Vpu (Ser52 and Ser56) is required for CD4 degradation (Bour *et al.*, 1995). Vpu acts as a molecular adaptor by recruiting the E3 ubiquitin ligase complex to CD4 in the ER for degradation by proteasomes (Nomaguchi *et al.*, 2008; reviewed in Andrew and Strebel, 2010). Vpu has been found to interact with human β-TrCP and the phosphorylation of two serine residues in the Vpu cytoplasmic domain at positions 52 and 56 is necessary for this binding. The most well-known consensus sequence for β-TrCP binding is $DS^{P}G\Phi XS^{P}$ where S^{P} is a phosphorylated serine, Φ is a hydrophobic residue and X is any other residue (Nomaguchi *et al.*, 2008). It must be noted that there are other sequences that β-TrCP recognizes for binding (Belaïdouni *et al.*, 2007). β-TrCP contains seven WD repeats that are involved in mediating the interaction with Vpu in a phosphoserine-dependent manner. It also contains an F-box domain that targets the substrate protein for degradation by allowing the interaction of β-TrCP with Skp1p, a factor that provides a link to the ubiquitin proteolysis machinery. This shows that the binding sites on Vpu for CD4 and β-TrCP are separate and independent of each other (Margottin *et al.*, 1998; reviewed in Andrew and Strebel, 2010). In this way, CD4 becomes polyubiquitinated along its cytoplasmic domain and is therefore targeted for proteasomal degradation through the binding of Vpu (Hussain *et al.*, 2008).

It has been proposed by Margottin and co-workers (1998), that the degradation of CD4 may be summarized as follows: infection of cells with HIV-1 leads to the formation of CD4-Env complexes in the ER, trapping CD4. The cytoplasmic domain of Vpu binds to the cytoplasmic domain of CD4 and β-TrCP is then recruited to the Vpu/CD4 complex. The ternary complex consisting of Vpu/CD4/β-TrCP then recruits Skp1p and ultimately the E3 ligase complex, leading to the ubiquitination and degradation of CD4. CD4 is unable to bind to β-TrCP in the

absence of Vpu, indicating that Vpu is a linker protein between CD4 and β-TrCP (Margottin *et al*, 1998). This is represented schematically in Figure 1.2. Vpu itself is not degraded in the process (Nomaguchi *et al.*, 2008). As previously highlighted in section 1.3.2, retention of CD4 in the ER is a requirement for degradation, as Vpu is unable to degrade any CD4 molecule that has already exited the ER. The degradation of CD4 within the ER ultimately results in decreased cell surface levels of CD4, thereby impairing the immune system (Strebel, 1996). However, even though the degradation of CD4 is sufficient for effective immune impairment (Wonderlich *et al.*, 2011), Vpu has many other functions, including the targeting of antigen presentation through downmodulation of the MHCII.

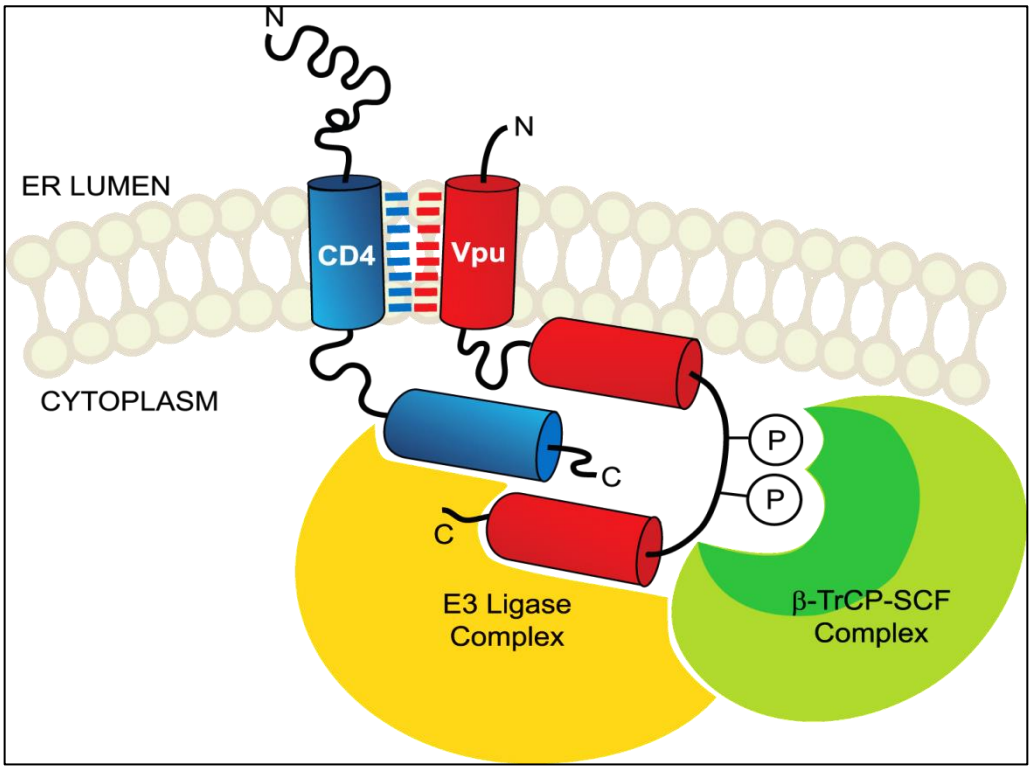


Figure 1.2: Schematic representation of CD4 degradation through binding human immunodeficiency virus type-1 (HIV-1) viral protein "u" (Vpu). Vpu binds CD4 in the endoplasmic reticulum (ER) and targets CD4 for proteasomal degradation through the recruitment of the E3 ligase complex. CD4 becomes ubiquitinated and is degraded by the action of the 26S proteasome. This not only impairs the immune system to a large extent, but it also results in the release of the HIV-1 envelope (Env) protein for further processing and new virion assembly (adapted from Nomaguchi *et al.*, 2008; reviewed in Andrew and Strebel, 2010).

1.4 Major Histocompatibility Complex Class II

The ability of the immune system to respond to infections is reliant on the presentation of foreign antigens or peptides to the T cells by the MHC molecules (reviewed in Peters and Sperber, 1999). While MHCI molecules display peptides derived from intracellular microorganisms within the cytoplasm, particularly viruses, to the CD8+ cytotoxic T cells, MHCII molecules present foreign peptides or antigens derived from extracellular microorganisms within the endosomal-lysosomal system including viruses, bacteria, protozoan parasites and cell surface proteins to CD4+ helper T lymphocytes. The CD8+ T cells are known to directly lyse infected cells and the CD4+ T helper cells activate B lymphocytes as well as macrophages, leading to the production of antibodies and the destruction of bacteria, respectively. CD8 and CD4 co-receptors on cytotoxic and –helper T cells, respectively, function to recognize the non-polymorphic regions of MHCI and MHCII, respectively (Ploegh, 1998; Robertson, 1998). The recognition of viral antigens by CD4+ T helper cells that are presented by the MHCII also results in the production of cytokines, which in turn galvanizes the differentiation of CD8+ cytotoxic T lymphocytes (CTLs) that inhibit the replication of the virus through cell lysis, and leads to the spread and differentiation of macrophages and B lymphocytes (Miller and Sedmak, 1999; reviewed in Peters and Sperber, 1999). MHCII molecules are typically only expressed within a specific set of cells that are involved within the immune system such as APCs, B cells, macrophages, dendritic cells, Langerhans cells as well as endothelial cells (Robertson, 1998; reviewed in Peters and Sperber, 1999). Along with CD74, MHCII can also be expressed in response to cytokines (Boss, 1997; Miller and Sedmak, 1999).

The downregulation of MHCI is facilitated mostly by the HIV-1 Nef protein in order to prevent the lysis of infected T cells by CTLs (Specht *et al.*, 2010). Nef functions to remove MHCI molecules directly from the cell surface by the ADP ribosylation factor 6 (ARF6) endocytic pathway using the phosphofurin acidic cluster sorting protein-1 (PACS-1). This endocytosis moves the MHCI to the *trans*-Golgi network (Blagoveshchenskaya *et al.*, 2002). As previously mentioned in section 1.2.4.2, MHCI molecules are also targeted by HIV-1 Vpu. However, this downregulation occurs rather by the interaction of Vpu with immature MHCI molecules within the ER, instead of at the cell surface (Kerkau *et al.*, 1997). Similarly, mature MHCII molecules are downregulated by both Nef and Vpu. Nef upregulates the cell

surface expression of CD74, and is also capable of upregulating immature MHCII molecules at the cell surface, while at the same time decreasing the levels of mature, peptide-loaded MHCII at the cell surface. This interferes with antigen presentation (Stumptner-Cuvelette *et al.*, 2001; reviewed in Kirchhoff, 2010; Ghiglione *et al.*, 2012). Once again, Vpu acts from within the ER, where it binds to CD74 and also prevents formation of the mature MHCII complex (Hussain *et al.*, 2008). In this way, these two accessory proteins of HIV-1 work together to target both antigen presenting complexes to prevent infected cells from being recognized by CD8+ T lymphocytes or CD4+ T helper cells.

MHCI and MHCII differ slightly in terms of structure (Figure 1.3 and Figure 1.4, respectively). Similarities between the two classes include a peptide binding cleft and both are expressed from multiple genes which allows both molecule types to have considerable polymorphism in order to bind and display a large variety of peptides (Robertson, 1998). MHCII has a larger peptide binding cleft in comparison to MHCI, which allows these molecules to bind a more comprehensive assortment of antigens than MHCI (reviewed in Peters and Sperber, 1999).

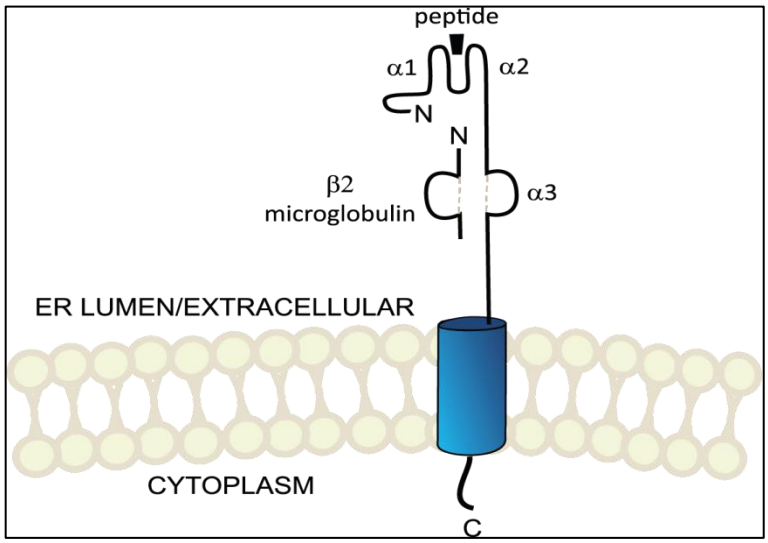


Figure 1.3: Schematic representation of the structure of a major histocompatibility complex class I (MHCI) molecule. These molecules have a cytoplasmic domain, transmembrane domain as well as an extracellular domain that either projects into the lumen of the endoplasmic reticulum (ER) or is displayed on the surface of the cell. MHCI molecules are made up of three α chains that are linked to a β2 microglobulin chain and have a relatively small peptide-binding cleft (adapted from Peters and Sperber, 1999).

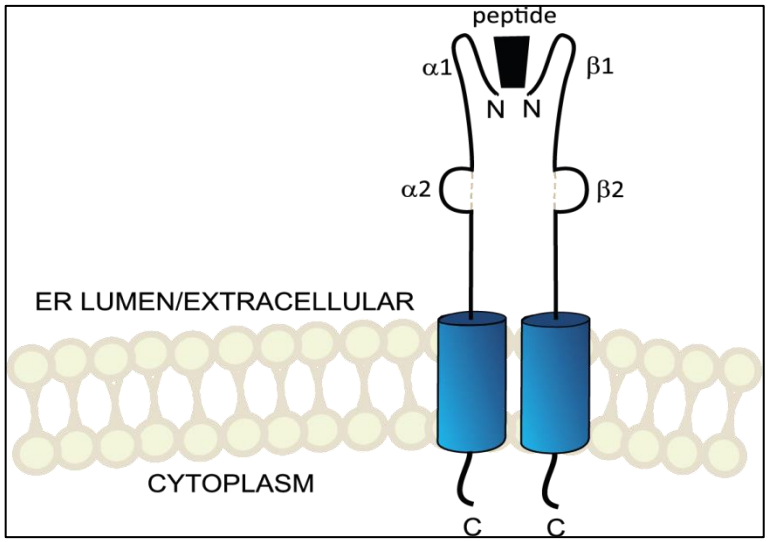


Figure 1.4: Schematic representation of the structure of a major histocompatibility complex class II (MHCII) molecule. As with MHCI molecules, these molecules also have a cytoplasmic domain, transmembrane domain as well as an extracellular domain that either projects into the lumen of the endoplasmic reticulum (ER) or is displayed on the surface of the cell. MHCII molecules are made up of two α chains and two β chains and have a larger peptide-binding cleft in comparison to MHCI (adapted from Peters and Sperber, 1999).

The MHCII molecules are transmembrane glycoproteins (Warmerdam *et al.*, 1996) and are made up of three α and β glycoprotein noncovalently-associated dimers that consist of a cytoplasmic domain, transmembrane domain and extracellular domain. The newly synthesised immature complex of three αβ dimers then associates with a homotrimer of CD74, or invariant chain, within the lumen of the ER. At this stage, the complex is unable to bind any peptides as CD74 is bound to the class II molecules in such a way that it acts to prevent the binding of peptides within the ER compartment (reviewed in Cresswell, 1996). The trafficking of MHCII complexes from the ER to endocytic compartments is determined by two dileucine-based target motifs in the cytoplasmic domain of CD74 (Kang *et al.*, 1998; Miller and Sedmak, 1999; Szaszak *et al.*, 2008). Once within the endocytic compartment, CD74 is proteolytically broken down by cathepsins which leave behind the class-II-associated Ii-chain peptide (CLIP) fragment within the peptide binding cleft. The CLIP fragment of CD74 seems to bind to class II molecules in a manner highly similar to that of a foreign peptide through a labyrinth of hydrogen bonds. It has been proposed that the three class II αβ dimers mainly associate with CD74 by the interaction between the CLIP

fragment of CD74 and the peptide binding cleft of the class II molecules. This interaction may also be stabilized by a small degree of association at the C-terminal region of CD74 (reviewed in Cresswell, 1996). The exchange of CLIP with a foreign peptide is facilitated by the human leukocyte antigen-DM (HLA-DM) within a lysosome-like compartment before the mature complex can move to the cell membrane to present the foreign peptide to the CD4+ T helper cells (Ploegh, 1998; Miller and Sedmak, 1999; reviewed in Peters and Sperber, 1999). It has been found that there is a collection of endocytic compartments for peptide loading of MHCII molecules, and this includes early endosomes, late endosomes or pre-lysosomes as well as multivesicular bodies (Warmerdam *et al.*, 2006).

However, antigen presentation may only be one reason why HIV-1 causes the downregulation of MHCII molecules in infected cells. It has been found that the assembly and budding of HIV-1 may occur either at the plasma membrane or in late endosomes/multivesicular bodies, depending on the cell type. For example, in T lymphocytes and some human cell lines HIV-1 assembles at the plasma membrane, while in macrophages, HIV-1 assembles in the late endosomes/multivesicular bodies (Pelchen-Matthews *et al.*, 2003; Ono and Freed, 2004). Interestingly, it was shown that the cytoplasmic domains of human leukocyte antigen-DR (HLA-DR), which is an important component of the MHCII molecule, affects the assembly and budding of HIV-1 in such a way that it is directed away from the plasma membrane and rather to the late endosomes/multivesicular bodies (Finzi *et al.*, 2006). HLA-DR specifically acts on the relocation of the HIV-1 Gag protein, which is needed for the assembly of virus particles. Although the virions in these intracellular compartments are still infectious, this finding suggests that the MHCII molecules may be able to reduce the release of new viruses from the cell surface (Finzi *et al.*, 2006).

As previously mentioned in section 1.4, HIV-1 Vpu has been found to bind to the cytoplasmic domain of CD74. It is interesting to note that the binding site on Vpu for CD74 may overlap with the immunodominant region which may also be found within the cytoplasmic C-terminal domain of Vpu (Schneider *et al.*, 1990). The interaction between these two proteins may not necessarily only affect antigen presentation; it could possibly also function to prevent the redirection of HIV-1 Gag to late endosome/multivesicular bodies to allow the virus to spread from cell

to cell more efficiently. However, the Vpu/CD74 interaction may have even more widespread downstream consequences than this, as CD74 is a ubiquitous protein and it is involved in many important cellular pathways, as highlighted below.

1.5 CD74/Invariant chain

CD74, the invariant chain of the MHCII, consists of a 30 amino acid N-terminal cytoplasmic domain, a 26 amino acid transmembrane domain and a 160 amino acid sequence that is either displayed on the cell surface or protrudes into the ER lumen, depending on the subcellular location of the protein (Claesson *et al.*, 1983; Strubin *et al.*, 1984; Hussain *et al.*, 2008). The structure of CD74 appears to be extended as it has a large Stokes radius of 72 Å and each of the chains that make up the trimer have limited interaction with each other (reviewed in Cresswell, 1996). A schematic representation of CD74 is given in Figure 1.5.

There are multiple isoforms of CD74, designated p33, p35, p41 and p43. Ii-p33 and Ii-p35 are 33 kDa and 35 kDa, respectively and are involved in MHCII antigen presentation, with the Ii-p33 isoform being the prominent of the two. These isoforms originate in two ways, i.e. by alternative splicing as well as through the use of two different translation initiation sites (Warmerdam *et al.*, 1996). The only difference between these isoforms of CD74 is that Ii-p35 has 16 extra residues at the N-terminus that form part of the cytoplasmic domain. These additional residues differentiate between the routes by which the immature MHCII molecules reach the endocytic compartment for antigen loading. MHCII molecules that are partnered with the Ii-p33 isoform only reach the endosome via the cell membrane, while molecules that are partnered with the Ii-p35 isoform are first trafficked to the Golgi network before moving to the endosome. Finally, MHCII molecules that are associated with a mixture of both CD74 isoforms will be trafficked internally, and not via the cell membrane as the signal motif in the Ii-p35 isoform is stronger than that of the Ii-p33 isoform (Warmerdam *et al.*, 1996). The Ii-p35 isoform is phosphorylated by protein kinase C at serine residues (Ser6 and Ser8) in the cytoplasmic region which are not found in the Ii-p33 isoform. An Ii-p35 phosphorylation mutant inhibits the trafficking of Ii-p35-bound MHCII via intracellular pathways, but does not inhibit exit of these molecules from the ER, indicating that the phosphorylation of this isoform is required for the trafficking of MHCII molecules from the Golgi network to the endosome for antigen loading

and finally presentation (Anderson *et al.*, 1999). As previously mentioned in section 1.4, both Nef and Vpu target CD74 at the plasma membrane and within the ER, respectively. It is possible that the presence of the two isoforms of CD74 that are trafficked along different pathways necessitates the function of both Nef and Vpu to bind to this protein. Nef would therefore target only the Ii-p33 isoform at the cell surface, while Vpu would interact with mainly the Ii-p35 isoform within the ER and Golgi network.

The cytoplasmic tail of CD74 has a dileucine motif which acts as a trafficking signal to move CD74-associated MHCII molecules out of the ER for further processing. These trafficking signals are DQRDLI and EQLPML in the membrane distal and membrane proximal regions of the cytoplasmic domain, respectively, with the first motif lying within a helix and the second motif lying within a turn (Motta *et al.*, 1995; Kang *et al.*, 1998). The DQRDLI motif, in particular, is required for sorting the CD74-bound MHCII molecules from the Golgi network to the endocytic compartment, although both sorting motifs in combination have a greater effect than one motif alone (Kang *et al.*, 1998). Using NMR and aqueous solution at physiological pH, it was determined that there is an α-helix in the cytoplasmic domain of CD74 from residues glutamine to leucine (Gln4 – Leu14) as well as a type I β turn from leucine to leucine (Leu14 – Leu17) and two type II β turns from arginine to alanine and from alanine to serine (Arg20 – Arg23 and Arg23 – Ser26) (Motta *et al.*, 1995). However, the type I β turn can possibly be incorporated into the α-helix without disturbing other residues within the helix. As this helix would then contain proline (Pro15), the resulting helix is a kinked proline α-helix. The proline residue is conserved and removal of this residue prevents internalization of CD74 from the plasma membrane, which then suggests that this residue is highly relevant (Motta *et al.*, 1995).

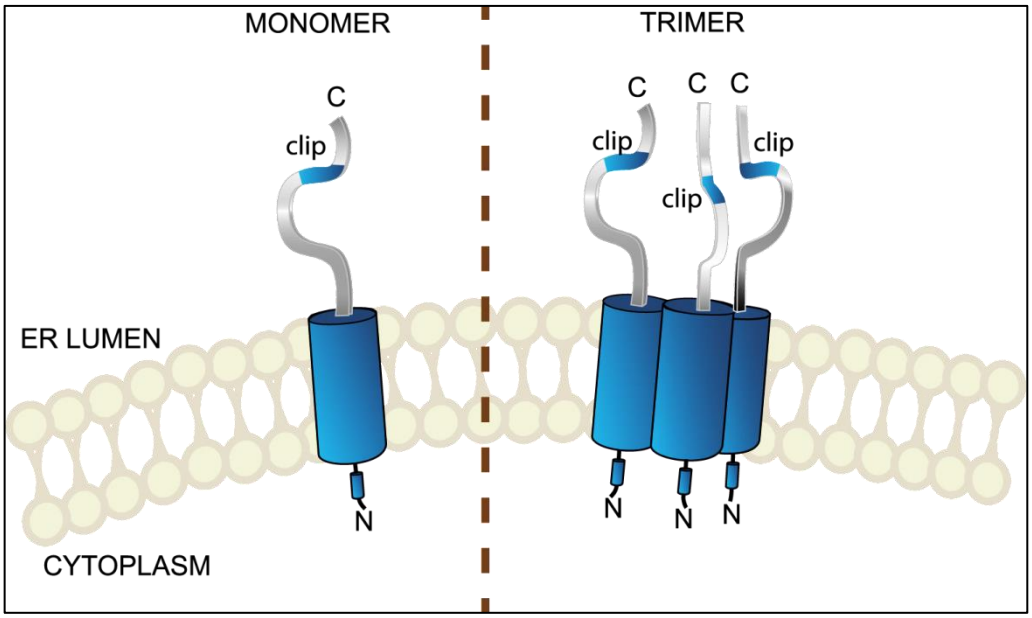


Figure 1.5: Schematic representation of CD74. The N-terminal cytoplasmic domain and the transmembrane domain are relatively small compared to the domain that lies within the lumen of the endoplasmic reticulum (ER) or that is projected extracellularly. The class-II-associated Ii-chain peptide (CLIP) region is indicated in blue and this is the section of CD74 that binds to the peptide-binding site on major histocompatibility complex class II (MHCII) molecules (adapted from Cresswell, 1996).

The N-terminal cytoplasmic tail of the Ii-p35 isoform also contains an arginine-based signal motif that behaves as a retention signal to keep the complex in the ER (Warmerdam *et al.*, 1996; reviewed in Michelsen *et al.*, 2005; Szaszak *et al.*, 2008). It is suggested that there is a general arginine consensus sequence of Φ/Ψ/RRXR, where Φ/Ψ is either an aromatic or a bulky hydrophobic residue and X is any other residue. A protein that contains more than two arginine residues, such as CD74, will have a notably strong retention signal (reviewed in Michelsen *et al.*, 2005). However, association of CD74 with MHCII molecules is thought to mask this retention signal to allow the exit of the complex from the ER. Phosphorylation of Ser6 and Ser8 residues in close proximity to the arginine-based retention motif by protein kinase C may also aid in the trafficking of molecules out of the ER. If this phosphorylation is in any way inhibited, MHCII-associated CD74 is unable to undergo processing within the endosomes, thereby repressing antigen presentation (Anderson *et al.*, 1999; Szaszak *et al.*, 2008).

The expression of CD74 is separate to that of the MHCII molecules and this allows CD74 to have numerous other functions within the cells. CD74 is a regulated intramembrane proteolysis (RIP)-processed protein. RIP proteins are essentially transcription factors that are expressed as dormant membrane-bound regulatory proteins. These proteins are activated by proteolytic cleavage at the plane of the membrane in which they are bound which allows the released cytosolic fragment to migrate to the nucleus in order to modulate transcription. The RIP process takes place within the endocytic compartment and occurs through the action of intramembrane cleaving proteases (I-CLiPs). The peptide bond is hydrolysed in a two-step process (Becker-Herman *et al.*, 2005). A fraction of CD74-ICD migrates to the nucleus where it initiates a signal cascade. This occurs through the activation of phosphatidylinositol 3'-kinase (PI3K), Syk tyrosine kinase and Akt serine/threonine kinase and this then leads to the activation of the NF-κB p65/RelA homodimer as well as its coactivator, TATA box binding protein (TBP)-associated factor $_{II}$105 (TAF$_{II}$105), a subunit of the general transcription factor IID (TFIID) (Matza *et al.*, 2001; Starlets *et al.*, 2006). The ultimate result of the signal cascade is two-fold. First, the cell enters into the synthesis phase (S phase) where DNA synthesis is increased, yielding an increase in cell division and proliferation (Starlets *et al.*, 2006). Second, the expression of the TAp63 protein is upregulated by both CD74-ICD as well as the activated NF-κB p65/RelA homodimer. TAp63 binds to the Bcl-2 promoter and, in doing so, transactivates the *Bcl-2* gene to increase the expression of the antiapoptotic protein, Bcl-2. This enhances the survival of B cells as a result of a decrease in apoptosis (Lantner *et al.*, 2007). Not only is CD74 involved in the proliferation and survival of B cells, it also plays a role in the differentiation of B cells from immature to mature cells within the spleen (Matza *et al.*, 2001; Matza *et al.*, 2002a). An important point to note is that this particular signal cascade is eliminated by the degradation of the active CD74 protein (Lantner *et al.*, 2007; Matza *et al.*, 2002b). This particular function of CD74 is represented schematically in Figure 1.6. Using a similar pathway, CD74-ICD also influences the proinflammatory responses by altering the expression of the monocyte chemoattractant protein-1 (MCP-1), which is involved in the early stages of atherosclerosis (Martin-Ventura *et al.*, 2009). In this case, it was found that CD74 co-localizes with NF-κB, suggesting that these two proteins may interact within atherosclerotic plaques in order to increase the expression of MCP-1, which is

regulated by NF-κB. Overall, an increase in CD74 leads to an increase in inflammation during atherosclerosis (Martin-Ventura *et al.*, 2009). Another way in which CD74 plays a role in inflammation is in the overexpression of CD74 on the surface of gastric epithelial cells due to *Helicobacter pylori* infection. CD74 functions as the receptor for this bacteria and the binding of the bacteria to CD74 not only results in the upregulation of cell surface levels of CD74, but also induces NF-κB pathways that result in the production of proinflammatory cytokines (Beswick *et al.*, 2005; reviewed in Beswick and Reyes, 2009). CD74 has not only been associated with inflammatory disorders, but is also implicated in gastrointestinal cancers, in which an overexpression of CD74 within tumour cells corresponds with a suppression of the immune response to the cancer (Ishigami *et al.*, 2001).

CD74 is also involved in the mediation of signalling on the cell surface in conjunction with the macrophage inhibitory factor (MIF). MIF is a cytokine that mediates many important pathways within the cell such as the production of other cytokines and nitric oxide. MIF has also been shown to bring about the phosphorylation and therefore, activation of the p44/p42 extracellular-signal-regulated kinase family (ERK-1/2). The downstream consequence of this is the activation of effector proteins and transcription factors that are involved in inflammation, such as NF-κB. MIF interacts with the CD74 extracellular domain at the cell surface which allows MIF to bind to the cell and induce the ERK-1/2 cascade. However, it is believed that the signal cascade generated by CD74 requires a second messenger protein and that messenger protein may be CD44 as studies have suggested a complex comprising MIF, CD74 and CD44 may exist (Meyer-Siegler *et al.*, 2004). CD44 is a transmembrane protein that is involved in the activation of tyrosine kinase. Therefore, CD74 functions as a surface binding protein for MIF, and in conjunction with CD44, it regulates MIF's functions in the cell (reviewed in Leng and Bucala, 2006).

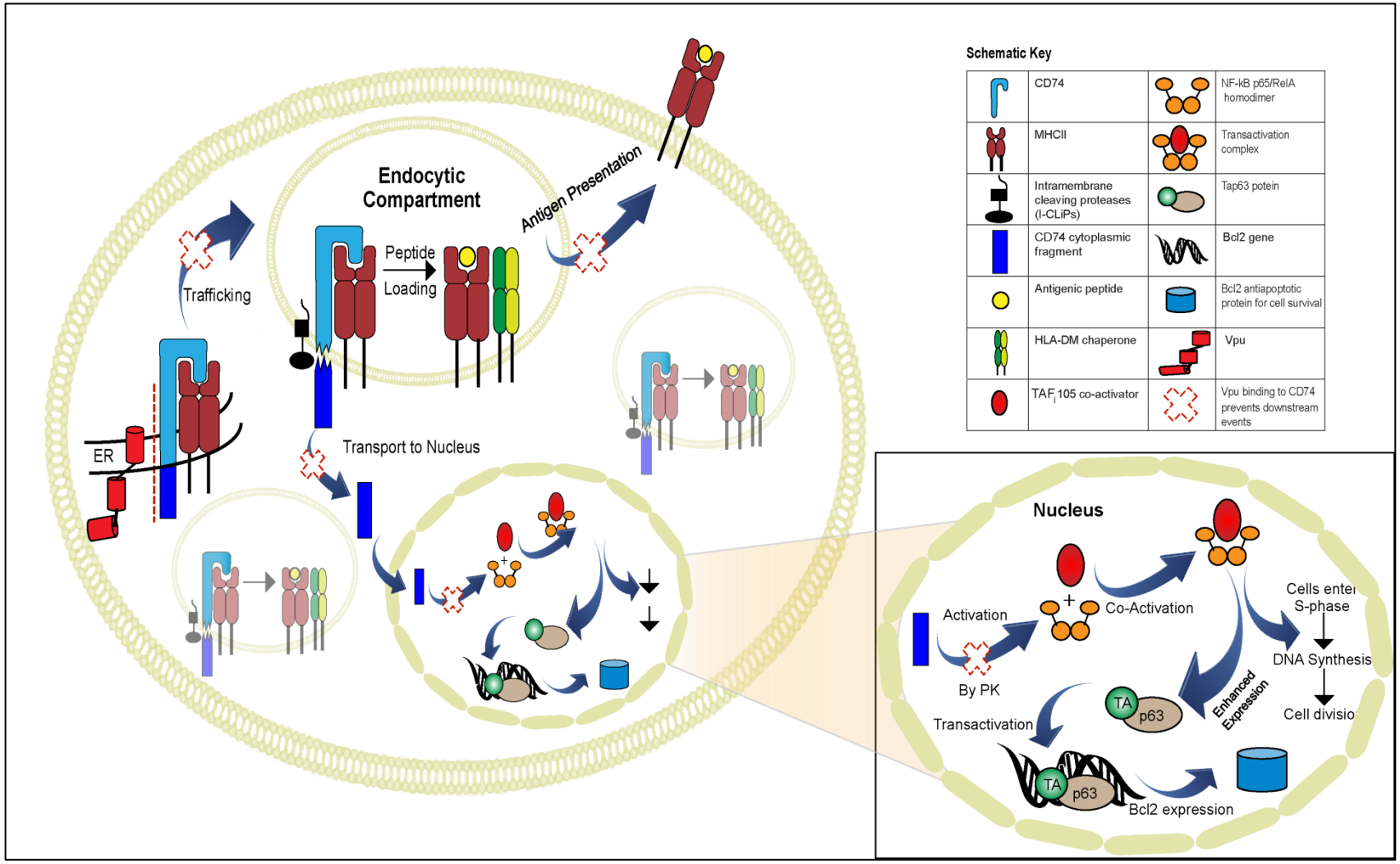

Endocytic Compartment
Antigen Presentation
Trafficking
Peptide Loading
ER
Transport to Nucleus
Schematic Key
CD74
MHCII
Intramembrane cleaving proteases (I-CLiPs)
CD74 cytoplasmic fragment
Antigenic peptide
HLA-DM chaperone
TAF1105 co-activator
NF-kB p65/RelA homodimer
Transactivation complex
Tap63 potein
Bcl2 gene
Bcl2 antiapoptotic protein for cell survival
Vpu
Vpu binding to CD74 prevents downstream events
Nucleus
Activation
By PK
Co-Activation
Transactivation
TA
p63
Enhanced Expression
Cells enter S-phase
DNA Synthesis
Cell division
Bcl2 expression

Figure 1.6: Schematic representation of the signal cascade induced by the CD74 cytoplasmic domain fragment (CD74-ICD) for cell survival. CD74 forms part of the major histocompatibility complex class II (MHCII) in the endoplasmic reticulum (ER). The complex is directed to the endosome, where intramembrane cleaving proteases (I-CLiPs) hydrolyze the peptide bond. The cytoplasmic fragment moves to the nucleus, where a signal cascade is initiated through the activation of protein kinases. This activates the nuclear factor-κB (NF-κB) p65/RelA homodimer and its coactivator, TBP-associated factor $_{II}$105 ($TAF_{II}105$). The cell enters the synthesis (S) phase for increased DNA synthesis, which causes cell division and proliferation. Simultaneously the activated NF-κB p65/RelA homodimer upregulates TAp63 protein expression. TAp63 transactivates the *Bcl-2* gene leading to the expression of the Bcl-2 antiapoptotic protein. This results in enhanced cell survival. Human immunodeficiency virus type-1 (HIV-1) infected cells contain viral protein "u" (Vpu) which binds to the cytoplasmic domain of CD74 in the ER. This not only prevents antigen presentation, but also prevents the translocation of CD74-ICD to the nucleus. Consequently, the signal cascade affecting B cell proliferation and survival cannot be initiated (Le Noury *et al.*, 2015).

CD74 has been implicated as a negative regulator of angiotensin II type 1 receptor (AGTR1), which plays a fundamental role in regulating blood pressure and is therefore involved in hypertension and atherosclerosis. AGTR1 also regulates the hormone angiotensin II (AngII) and in so doing, it influences many other signal pathways that include the activation of G proteins, protein kinase C, tyrosine kinases and mitogen-activated protein kinases (MAPKs). All of these functions are reliant on the C-terminal tail of AGTR1, which is expressed in the ER and was found to bind to CD74 within this compartment. This interaction causes AGTR1 aggregation in the ER and ultimately leads to the proteasomal degradation of AGTR1 (Szaszak *et al.*, 2008). This indicates that CD74 also plays a role in the regulation of these important signal cascades as well as cardiovascular disorders.

The multiple functions of CD74 provide evidence that this protein plays a vital role in many different pathways, not only within a single cell, but also from cell to cell. Vpu binds to the CD74-ICD within the ER (Hussain *et al.*, 2008), yet many downstream consequences of this interaction have not been studied. All of the abovementioned functions of CD74 are likely to be influenced by its interaction with Vpu, as it has already been shown that the interaction between Vpu and CD74 leads to a downregulation in MHCII surface expression, which is naturally

followed by reduced antigen expression and ultimately decreases the activation of T cells. It is not unreasonable to assume that this binding interaction will also impede the role of CD74 in signal transduction. However, it is as yet unclear whether Vpu is able to restrain CD74 simply by binding to it and retaining it within the ER or if Vpu targets CD74 for degradation.

1.6 Similarities between CD4 and CD74

Similarities exist between CD74 and CD4 that may suggest that CD74 is possibly degraded through Vpu binding in a way similar to that of CD4. First, both CD74 and CD4 interact with the cytoplasmic domain of Vpu via their own cytoplasmic domains (Willey *et al.*, 1994; Hussain *et al.*, 2008), which suggests that CD4 and CD74 may bind to the same site on the Vpu cytoplasmic domain. Second, the binding interactions between Vpu and CD4 or CD74 respectively both occur within the same cellular location, which is the ER (Margottin *et al.*, 1998; Belaïdouni *et al.*, 2007). Third, the ion channel activity of Vpu may play a role in influencing intracellular calcium levels and a decrease of calcium within the ER leads to an increase in the proteolysis of many ER proteins (Wileman *et al.*, 1991; Willey *et al.*, 1992a), which may include both CD4 and CD74. Fourth, the ability of Vpu to induce degradation of CD4 requires cytosolic protein polyubiquitination machinery that targets lysine residues in the CD4 cytoplasmic domain (Margottin *et al.*, 1998; Schubert *et al.*, 1998; reviewed in Andrew and Strebel, 2010). It was also shown that serine and threonine residues are ubiquitin sites (Magadan *et al.*, 2010). Although CD74 does not have threonine, both CD4 and CD74 contain lysine and serine residues in their cytoplasmic domains (Schubert *et al.*, 1998; Strubin *et al.*, 1984). The presence of potential ubiquitination sites within the CD74 cytoplasmic domain indicates that this protein may possibly be targeted for ubiquitination. These similarities taken together suggest that the binding sites on Vpu for CD4 and CD74 may be closely related which further suggests that Vpu may mediate the degradation of CD74 via a similar mechanism to that of CD4, i.e. by the ubiquitination of CD74 and subsequent proteasomal degradation.

1.7 Project hypothesis and objectives

The many important functions of CD74 including the chaperoning of antigen presentation and its involvement in cellular signal transduction pathways make this protein an attractive target for downregulation by multiple HIV-1 accessory proteins, including the Vpu accessory protein. To date, it has been shown that

Vpu modulates surface expression of the mature MHCII molecules by interacting with CD74 within the ER. However, it is not yet clear whether Vpu only mediates downregulation of MCHII by retention of the immature complex within the ER or if CD74 itself is downregulated and/or degraded through the binding interaction. As mentioned above, there are numerous reasons that suggest that CD74 may be targeted for proteasomal degradation similar to that of CD4. Additionally, HIV-1 has multiple reasons to downregulate CD74 as this host protein is involved in numerous important functions. Taking this into account, the hypothesis of this study is that the binding of Vpu targets CD74 for proteasomal degradation through the recruitment of β-TrCP in a mechanism similar to that of Vpu-associated CD4 degradation. To this end, the main aim of this study was to elucidate the downstream consequences of the HIV-1 Vpu/CD74 binding interaction, as compared to Vpu/CD4 degradation, more specifically to elucidate whether Vpu mediates the proteasomal degradation of CD74 or if CD74 is merely downregulated. This was achieved through the fulfilment of the following objectives:

- Firstly, to establish the binding interaction of HIV-1 subtype B Vpu with CD4 and CD74 respectively through the use of *in vitro* assays;
- Secondly, to determine the downregulation of both CD4 and CD74 by binding to Vpu in a cell based assay;
- And finally, to investigate the possible mechanism of CD74 downregulation by the interaction with Vpu, as compared to Vpu mediated CD4 proteasomal degradation.

CHAPTER TWO: MATERIALS AND METHODS

2.1 CD4/CD74 homology study

The sequence of the CD74 cytoplasmic domain was obtained from UniProt (www.uniprot.org; accession number P04233; last updated 16 April 2002). The sequence of the CD4 cytoplasmic domain was also obtained from UniProt (accession number P01730; last updated 1 November 1988). The PredictProtein Server was used to calculate the percentage of secondary structure for the CD4 cytoplasmic domain and the CD74 cytoplasmic domain, based on amino acid sequence using the PROFphd method (Rost *et al.*, 2004; Wrzeszczynski and Rost, 2004; Yachdav *et al.*, 2014). The secondary structure was also predicted using Discovery Studio 4 (BIOVIA, USA) and compared to the secondary structure assigned to each protein by the Dictionary of Protein Secondary Structure (DSSP; Kabsch and Sanders, 1983), which is available through the Protein Data Bank (PDB; www.rscb.org). The structure of the transmembrane and cytoplasmic domains of a cysteine-free CD4 mutant in dodecylphosphocholine (DPC) micelles has previously been determined by NMR (Wittlich *et al.*, 2010). The co-ordinates of this protein (PDB 2KLU) were uploaded to Discovery Studio 4 (BIOVIA, USA) in order to obtain a model structure. A representation of the folding of the CD74 cytoplasmic domain was constructed using Discovery Studio 4 (BIOVIA, USA) by building the peptide based on the amino acid sequence, using the right-handed α-helical conformation. The predicted secondary structure was used to determine which sections would be unstructured and the location of the α-helix. Hydrophobicity plots of the CD4 and CD74 cytoplasmic domains were calculated using Discovery Studio 4 (BIOVIA, USA), which makes use of the Kyte and Doolittle hydropathy scale (Kyte and Doolittle, 1982) with a default window size of 5. This scale takes both the hydrophobicity and the hydrophilicity of each of the amino acid side chains into account, in order to determine the average hydropathy within a pre-determined window throughout the primary sequence from the N-terminus to the C-terminus. Residues with hydropathy values greater than zero are considered to be hydrophobic, while those with hydropathy values less than zero are hydrophilic. Although secondary structure and protein folding may also be influenced by steric

effects between side chains, the hydropathy of a peptide or protein gives an estimation of which regions form the interior and which are part of the exterior of the peptide or protein, as well as which regions interact with or traverse a membrane. Additionally, helical wheels were plotted for the α-helices for the cytoplasmic domains of CD4 and CD74 using the program from the RZ Lab (http://rzlab.ucr.edu/scripts/wheel/wheel.cgi). A sequence alignment of the CD4 and CD74 cytoplasmic domains was completed using Discovery Studio 4 (BIOVIA, USA). This was done using the "Align123" multiple sequence alignment method, which is based on the CLUSTAL W program and uses a progressive pairwise alignment algorithm. The alignment was done using the "Fast" pairwise alignment, which makes use of the FASTA format approach. In order to compare these peptides structurally, the primary sequence of the CD74 cytoplasmic domain was modelled onto the 3D structure of the CD4 cytoplasmic domain, using the co-ordinates PDB 2KLU for CD4. This was done using the "Create homology models" tool in Discovery Studio 4 (BIOVIA, USA). Twenty models were predicted in this way and the model with the smallest Root Mean Square Deviation (RMSD) was selected as the most likely model. An energy minimization of the selected model was completed using the CHARMm force field and the Generalized born with molecular volume (GBMV) solvent model. The RMSD, Discrete optimized protein energy (DOPE) score and total probability density function (PDF) energy was calculated after aligning and superimposing the minimized model onto the template (2KLU). A Ramachandran plot was generated in Discovery Studio 4 (BIOVIA, USA) of the energy minimized model (Lovell *et al.*, 2003). A structural alignment of the α-helices of CD4 and CD74 was completed by selecting the regions of Met407-Glu416 of CD4 and Met17-Asn26 of CD74 as tethers and superimposing these regions. The RMSD of this new alignment was recalculated.

2.2 National Institutes of Health Reagents

The reagents listed in Table 2.1 were obtained through the NIH AIDS Research and Reference Reagent Program, Division of AIDS, NIAID, NIH.

Table 2.1: Reagents from the NIH AIDS Research and Reference Reagent Program used within this study. These reagents were used extensively within this study and the NIH AIDS Reagent Program catalogue number, contributors and cited references are listed here.

Catalogue Number	Reagent	Contributors	Reference
969	HIV-1_{NL4-3} Vpu Antiserum	K Strebel	Maldarelli *et al.* (1993)
6444	HIV-1 Consensus Vpu Peptides	DAIDS, NIAID	None
10076	pcDNA-Vphu	S Bour and K Strebel	Nguyen *et al.* (2004)
11942	Anti-Vpu Rabbit Antiserum (Anti-Vpu_C)	MH Kraus and BH Hahn	Kraus *et al.* (2010)

2.3 Culture of U937 and HEK 293T cell lines

The human macrophage U937 suspension cell line (Highveld Biological, RSA) was maintained in Roswell Park Memorial Institute (RPMI) 1640 medium (Gibco, Life Technologies, USA) containing 10% (v/v) foetal calf serum (FCS; Highveld Biological, RSA), 20 µg/ml gentamycin sulphate (Highveld Biological, RSA) and 20 µg/ml penicillin/streptomycin (Highveld Biological, RSA) in a 5% CO_2 environment at 37°C. U937 cells were subsequently used in immunoprecipitation experiments and flow cytometry. HEK 293T (ATCC® CRL-11268^{TM}, USA) adherent cells were maintained in high glucose Dulbecco's Modified Eagle's Medium (DMEM) with L-glutamine and sodium pyruvate (Hyclone, Thermo Scientific, USA) containing 10% (v/v) FCS (Highveld Biological, RSA) and 20 µg/ml gentamycin sulphate (Highveld Biological, RSA) as well as 20 µg/ml penicillin/streptomycin (Highveld Biological, RSA) in a 5% CO_2 environment at 37°C. HEK 293T cells were routinely used for the expression of recombinant Vpu::GFP. Both U937 and HEK 293T cells were grown to confluency before culturing. Cells were centrifuged at 500 *xg* for 5 minutes at 21°C and the cell pellet was resuspended in 1 mL of medium. The cell concentration was determined using a Countess Automated Cell Counter (Life Technologies, USA). Cells were seeded at a density of 1 x 10^5 per ml.

2.4 Construction of Vpu::GFP and Vpu phosphorylation mutants

Bacterial cells (One Shot® TOP10 Chemically Competent *E. coli,* Life Technologies, USA) were transformed with plasmid DNA (adapted from Studier and Moffat, 1986 and Froger and Hall, 2007). Briefly, bacterial cells were incubated with 1 µl of 10 ng/µl pcDNA-Vphu (NIH catalogue number 10076;

Table 2.1) on ice for 30 minutes, followed by heat shock at 42°C for 45 seconds and a further 2 minutes on ice. Following this, 500 µl SOC medium (Luria-Bertani [LB] broth [Conda Pronadisa Molecular Biology, Spain]; 2.5 ml of 1 M KCl [Associated Chemical Enterprises, RSA]; 10 ml of 1 M $MgCl_2$ [Sigma Aldrich, USA]; 20 ml of 1 M glucose [Minema Chemicals, RSA]) was added and the bacteria were incubated at 37°C and shaken at 250 rpm for 1 hour before being spread onto a LB/ampicillin (LB Agar, Lennox, Conda Pronadisa Molecular Biology, Spain; 100 µg/ml ampicillin sodium salt, Melford Laboratories Ltd, UK) plate and left to grow at 37°C for approximately 16 hours. Random colonies were selected and transferred to sterile LB Broth (Conda Pronadisa Molecular Biology, Spain) medium with a final concentration of 100 µg/ml ampicillin (Melford Laboratories Ltd, UK) for growth overnight, at 37ºC and shaking at 250 rpm. Total plasmid DNA was isolated from the bacteria using the Qiagen Plasmid Maxiprep Kit, as per manufacturer's instructions (Qiagen, Netherlands). The Vpu fragment was PCR amplified with *Ex Taq* DNA polymerase (0.5 µl of a stock of 5 units/µl; TaKaRa, Japan) using the following primers (Inqaba Biotechnical Industries, RSA): Vpu FwD, 5' GCCATGGTGCCCATTATTGTCG 3' and Vpu Rev, 5' CAGGTCGTCAATGTCCCAG 3'.

Single and double restriction digests of the plasmid were performed using the *Msc*I and *Acc*65I restriction enzymes (Fermentas Life Sciences, Thermo Scientific, USA). The Vpu fragment was excised from a 1% (w/v) agarose gel after staining with SYBR Gold (Invitrogen Molecular Probes, Life Technologies, USA). This fragment was isolated using the Strataprep DNA Gel Extraction Kit, as per manufacturer's instructions (Stratagene, Agilent Technologies, USA) and ethanol precipitated to concentrate each sample. The amplified fragment was then cloned into the pcDNA^{TM} 6.2/C-EmGFP TOPO adapted vector (Invitrogen Vivid Colours, Life Technologies, USA) as per manufacturer's instructions, and used to transform bacterial cultures as described above. Site-directed mutagenesis was used to remove a stop codon between the Vpu and GFP sequences using the QuikChange Lightning Site-Directed Mutagenesis kit, as per manufacturer's instructions (Agilent Technologies, USA) using the following primers (Inqaba Biotechnical Industries, RSA): Fwd, 5' GGGACATTGACGACCTGTGCTACAGAAAAATTGTGG 3' and Rev, 5' CCACAATTTTTCTGTAGCACAGGTCGTCAATGTCCC 3'. The plasmid,

designated pVpu::GFP, was then sequenced (automated sequencing at Inqaba Biotechnical Industries, RSA) to confirm the correct sequence of the fusion protein.

Site-directed mutagenesis was then used to produce two Vpu::GFP phosphorylation mutants. The first mutant carried a mutation at the Ser52 residue (pVpu-SM) while the second mutant carried mutations at both serine residues, namely Ser52 as well as Ser56 (pVpu-DM). In both mutants, the serine residues were replaced with alanine. These mutations were generated using the QuikChange Lightning Site-Directed Mutagenesis kit, as per manufacturer's instructions (Agilent Technologies, USA) with the following primers (Inqaba Biotechnical Industries, RSA) for pVpu-SM: 5' CGCGCCGAGGAC**GCC**GGCAACGAGAGCGAGGGCGAG 3' and 5' CTCGCCCTCGCTCTCGTTGCC**GGC**GTCCTCGGCGCG 3', and for pVpu-DM: 5' CGCGCCGAGGAC**GCC**GGCAACGAG**GCC**GAGGGCGAG 3' and 5' CTCGCCCTC**GGC**CTCGTTGCC**GGC**GTCCTCGGCGCG 3'. These mutant plasmids were used to transform bacterial cultures as described above and the presence of the mutations were confirmed through sequencing (Inqaba Biotechnical Industries, RSA).

All plasmids with the correct sequences were replicated in bacterial cells in order to increase the plasmid yield. *E. coli* cells were transformed as described above with each plasmid. Random colonies were selected and grown overnight in sterile LB Broth (Conda Pronadisa Molecular Biology, Spain) medium with a final concentration of 100 µg/ml ampicillin (Melford Laboratories Ltd, UK), at 37ºC and shaking at 250 rpm. Total plasmid DNA was isolated from the bacterial cultures using the Qiagen Plasmid Maxiprep Kit (Qiagen, Netherlands) according to the manufacturer's instructions.

2.5 Expression and purification of Vpu::GFP

Optimal mammalian expression and purification conditions of recombinant Vpu::GFP fusion protein were established. HEK 293T cells were plated into 6-well microtiter plates (Becton Dickinson Labware, USA) at a concentration of 0.25 x 10^6 /ml 24 hours prior to being transfected with 5 µg of the pVpu::GFP construct using Lipofectamine LTX with Plus™ reagent, following the manufacturer's

instructions (Life Technologies, USA) for protein expression. Briefly, 5 µg of plasmid was diluted in 100 µl of DMEM with 2.5 µl of the Plus reagent. In a separate tube, 8.75 µl of Lipofectamine was diluted in 100 µl of DMEM. The diluted plasmid and Lipofectamine solutions were added together and incubated for 5 minutes at room temperature before being added to the 70-80% confluent plated cells in a drop-wise manner. Fluorescent images were taken using the Floid® cell imaging station (Life Technologies, USA) and the Olympus CKX41 fluorescent microscope (Wirsam Scientific and Precision Equipment, (Pty) Ltd, RSA).

Transfected cells were lysed 48 hours after transfection using the Mem-PER Eukaryotic Membrane Protein Extraction kit (Pierce, Thermo Scientific, USA) according to the manufacturer's instructions. Briefly, cells were harvested and washed with 1 ml of sterile phosphate buffered saline (PBS; Sigma Aldrich, USA) and then resuspended in 150 µl of Reagent A for 10 minutes at room temperature, with occasional vortexing. Reagent B and C were diluted 1:2 and a total of 450 µl of the diluted reagents was added to the cells and incubated for 30 minutes on ice, vortexing every 5 minutes. The samples were centrifuged at 10 000 *xg* for 3 minutes at 4°C. The pellet fraction was solubilized as previously described (Schubert *et al.*, 1998), i.e. the pellet was dissolved in 2% (w/v) sodium dodecyl sulphate (SDS; Fluka, Sigma Aldrich, USA) with 50 µg/ml DNAse I (Sigma Aldrich, USA) and heated at 95°C for 20 minutes. After solubilisation, the sample was centrifuged at 500 *xg* for 15 minutes to remove the cell debris. The supernatant was decanted and diluted in 50 mM Tris (Melford Laboratories Ltd, UK), 300 mM NaCl (Associated Chemical Enterprises, RSA) and 0.1% (w/v) Triton X-100 (Promega Corporation, USA). The pellet was resuspended in 50 mM Tris (Melford Laboratories Ltd, UK), 300 mM NaCl (Associated Chemical Enterprises, RSA) and 0.1% (w/v) Triton X-100 (Promega Corporation, USA). Both the supernatant and the pellet fractions were separated using SDS polyacrylamide gel electrophoresis (SDS-PAGE) using the Bio-Rad Mini PROTEAN TG-X pre-cast stain-free gels, 4-15%. Gels were visualised using the ChemiDoc™ MP System (Bio-Rad, USA). Proteins were transferred to a polyvinylidene difluoride (PVDF) membrane using mini PVDF transfer stacks (Life Technologies, USA) with the Invitrogen iBlot (Life Technologies, USA) according to the manufacturer's instructions for a standard 7 minute protocol. After blocking

in 1X Tris buffered saline (TBS; 20 mM Tris [Melford Laboratories Ltd, UK], 140 mM NaCl [Associated Chemical Enterprises, RSA], pH 7.6) containing 5% (w/v) casein peptone (Conda Pronadisa Molecular Biology, Spain) for 1 hour at room temperature, the membrane was washed three times with 1X TBS containing 0.1% (w/v) Tween 20 (1X TBST; Sigma Aldrich, USA) and then incubated with 10 000X diluted rabbit anti-Vpu antibody (subtype B; NIH catalogue number 969; Table 2.1) for 1 hour at room temperature. Following this, the membrane was again washed three times with 1X TBST for 10 minutes each before incubation with 20 000X diluted horseradish peroxidase (HRP)-labelled goat anti-rabbit IgG (KPL, USA) for 1 hour at room temperature. After washing again as described, the membrane was incubated with the substrate solution for 5 minutes (SuperSignal West Pico Chemiluminescent Substrate for detection of HRP, Thermo Scientific, USA) and visualised using the ChemiDoc^{TM} MP System and Image Lab^{TM} software (Bio-Rad, USA).

A second western blot was completed with 500X diluted mouse anti-GFP antibody (purified mouse monoclonal IgG, R&D Systems, USA) and 1000X diluted rabbit anti-mouse IgG (peroxidase conjugated affinity purified anti-mouse IgG, gamma chain, Rockland, USA) to confirm the presence of the GFP tag. A third western blot was completed with 1000X diluted mouse anti-phosphoserine antibody (Santa Cruz Biotechnology Inc., USA) and 2000X diluted HRP-labelled goat anti-mouse IgM (Santa Cruz Biotechnology Inc., USA) to indicate the phosphorylation of the serine residues. The NanoDrop spectrophotometer (Thermo Scientific, USA) was used to determine the absorbance to calculate the concentration of recombinant Vpu::GFP. The protein was aliquoted and stored at -80°C until further use.

2.6 In vitro assays for protein-protein interactions

CD74 (MHRRRSRSCREDQKPVMDDQRDLISNNEQL; N-terminal residue positions 1-30), CLIP (MRMATPLLM; residue positions 107-115) and CD4 (RQAERMSQIKRLLSEKKTCQCPHRFQKTC; C-terminal residue positions 427-455) peptides were synthesised by the BIOPEP Peptide Laboratory (Department of Biochemistry, Stellenbosch University, RSA). Enzyme-linked immunosorbent assays (ELISAs) were set up and used to investigate the binding between recombinant Vpu::GFP and CD4, CD74 or CLIP peptides (adapted from Hussain

et al., 2008). The Vpu::GFP fusion protein (400 ng per well) was plated in coating buffer (0.05 M Na_2CO_3 [Sigma Aldrich, USA], 0.05 M $NaHCO_3$ [Saarchem, Merck Chemicals, USA]; 0.1% (w/v) NaN_3 [Sigma Aldrich, USA], pH 9.6), and incubated overnight at 4°C. After washing three times with 1X TBS and blocking with 5% (w/v) casein peptone (Conda Pronadisa Molecular Biology, Spain) for 2 hours at room temperature, plates were washed again with 1X TBS and incubated with CD74, CD4 or CLIP peptides (500 ng per well) and incubated overnight at 4°C. After washing once with 1X TBS, plates were incubated with 1000X diluted rabbit anti-Vpu antibody (subtype B, NIH catalogue number 969; Table 2.1) for 2 hours at room temperature. Plates were then washed three times with 1X TBST and incubated with 2000X diluted goat anti-rabbit IgG peroxidase labelled antibody (KPL, USA) for 90 minutes at room temperature before visualising with the substrate, 3,3',5,5'-tetramethylbenzidine liquid (TMB; Life Technologies, USA). The absorbance was measured 1 hour after the addition of the substrate at 650 nm using the xMark microplate spectrophotometer (Bio-Rad, USA). Controls were included in all plates: wells containing coating buffer only, wells that were only incubated with primary antibody and finally wells that were only incubated with secondary antibody.

The ELISA described above was repeated using 500X diluted mouse anti-GFP (purified mouse monoclonal IgG, R&D Systems, USA) followed by 1000X diluted rabbit anti-mouse IgG (peroxidase-conjugated affinity purified anti-mouse IgG, gamma chain, rabbit, Rockland, USA) or 5000X diluted rabbit anti-CD74 (Abcam, UK) followed by 10 000X diluted goat anti-rabbit IgG peroxidase labelled antibody (KPL, USA), or 5000X diluted rabbit anti-CD4 (Sigma Aldrich, USA) followed by 10 000X diluted goat anti-rabbit IgG peroxidase labelled antibody (KPL, USA).

Once binding had been established, a dose response study was also set up with 100, 250, 500, 1000, 5000 and 10 000 ng of CD74 in order to determine the half maximal inhibitory concentration (IC_{50}). The IC_{50} was calculated using Origin software (OriginLab, USA). To add to this, a competitive inhibition assay was completed in which 400 ng of Vpu::GFP was incubated with different concentrations of CD74 (250, 500, 1000, 5000 and 10 000 ng) before being incubated with the coated CD4 peptide (500 ng) in order to determine if CD4 and CD74 bind to the same/overlapping site on Vpu.

Furthermore, an assay was completed by plating with a set of 19 overlapping Vpu peptides (Table 2.2; NIH catalogue number 6444) at 500 ng each. Initially, these overlapping Vpu peptides were not incubated with any secondary proteins or peptides, i.e. CD74 or CD4 peptides, and were incubated directly with 1000X diluted rabbit anti-Vpu antibody (subtype B, NIH catalogue number 969) with 2000X diluted goat anti-rabbit IgG peroxidase labelled antibody (KPL, USA), or subtype C rabbit anti-Vpu antibody (NIH catalogue number 11942) with 10 000X diluted goat anti-rabbit IgG peroxidase labelled antibody (KPL, USA), or a different source of 1000X diluted rabbit anti-Vpu antibody (Abcam, UK) with 2000X diluted goat anti-rabbit IgG peroxidase labelled antibody (KPL, USA). Following this, the overlapping Vpu peptides were incubated with 500 ng of CD74, CD4 or CLIP after coating, as described above, and incubated with either the subtype B or subtype C rabbit anti-Vpu antibodies, or with 5000X diluted rabbit anti-CD4 (Sigma Aldrich, USA) followed by 10 000X diluted goat anti-rabbit IgG peroxidase labelled antibody (KPL, USA). Wash steps and incubation times were carried out as for all previously described assays.

Table 2.2: Amino acid sequences of the HIV-1 Consensus Vpu Peptides, obtained from the NIH AIDS Research and Reference Reagent Program. The set contains 19 overlapping peptides with the first 6 peptides comprising 9 residues each and the rest comprising 15 residues each, with the exception of the last peptide which comprises 13 residues.

	Cat #	AA Code		Cat #	AA Code
1	6423	MQSLQILAI	**11**	5982	RKIDRLIDRIRERAE
2	6424	QILAIVALV	**12**	5983	RLIDRIRERAEDSGN
3	6425	IVALVVAAI	**13**	5984	RIRERAEDSGNESEG
4	6426	VVAAIIAIV	**14**	5985	RAEDSGNESEGDQEE
5	6427	IIAIVVWTI	**15**	5986	SGNESEGDQEELSAL
6	6428	VVWTIVFIE	**16**	5987	SEGDQEELSALVEMG
7	5978	VVWTIVFIEYRKILR	**17**	5988	QEELSALVEMGHHAP
8	5979	IVFIEYRKILRQRKI	**18**	5989	SALVEMGHHAPWDVD
9	5980	EYRKILRQRKIDRLI	**19**	5990	EMGHHAPWDVDDL
10	5981	ILRQRKIDRLIDRIR			

A set of 10-mer and of 15-mer overlapping CD74 cytoplasmic domain peptides were obtained from the BIOPEP Peptide Laboratory (Department of Biochemistry, Stellenbosch University – Table 2.3). Both sets were used in *in vitro* assays (ELISAs) as described above (500 ng/peptide) and tested in conjunction with both 400 ng of the full-length Vpu::GFP fusion protein as well as 400 ng of each of the 19 overlapping Vpu peptides (NIH catalogue number 6444), following wash steps and incubation times as described above for the subtype B rabbit anti-Vpu antibody (NIH catalogue number 969) and a different source of rabbit anti-Vpu antibody (Abcam, UK).

Finally, the coated Vpu::GFP protein (400 ng) was incubated with consecutive combinations of the 10-mer overlapping CD74 peptide set in the same way as described above, using the subtype B rabbit anti-Vpu antibody (NIH catalogue number 969; Table 2.1). The total concentration of each combination of peptides was equal to that of the single peptides.

Table 2.3: Amino acid sequences of the nine CD74 10-mer and 15-mer overlapping peptides that were produced and used in the ELISA studies. Each of the sets was generated from the CD74 cytoplasmic domain peptide.

10-mer		15-mer	
Name	**Sequence**	**Name**	**Sequence**
CDPep10.1	MHRRRSRSCR	CDPep15.1	MHRRRSRSCREDQKP
CDPep10.2	SRSCREDQKP	CDPep15.2	SRSCREDQKPVMDDQ
CDPep10.3	EDQKPVMDDQ	CDPep15.3	EDQKPVMDDQRDLIS
CDPep10.4	VMDDQRDLIS	CDPep15.4	VMDDQRDLISNNEQL
CDPep10.5	RDLISNNEQL		

In all the ELISAs described above, duplicate samples were included in each plate for each sample type and each plate was repeated three times, making a total of six replicates per sample. The six replicates were used to calculate averages and standard deviations.

2.7 Immunoprecipitations

To validate the ELISA data, the binding of expressed Vpu::GFP to native CD74 in U937 cells was evaluated by immunoprecipitation experiments. U937 cells were cultured as described in section 2.3. Cells were optimally transfected using the Neon Electroporation system (Life Technologies, USA) following the

manufacturer's instructions. Briefly, cells were harvested after treatment and washed with Dulbecco's PBS (Highveld Biological, RSA) and then resuspended in 1 ml of Resuspension buffer R from the 100 µl Neon Electroporation kit (Life Technologies, USA) to a concentration of 2 x 10^7 cells per ml. Samples were prepared containing either 10 µg of a control GFP plasmid, pMax (Lonza, USA), or 10 µg of pVpu::GFP plasmid and 100 µl of the resuspended cells. Untransfected samples did not contain any plasmid. Each sample was electroporated at 1400 volts with a pulse width of 20 ms, three pulses per sample. Each sample was then placed into 2 ml of filter sterilized RPMI medium (Gibco, Life Technologies, USA) containing 10% (v/v) FCS (Highveld Biological, RSA) in a 6-well tissue culture plate and incubated at 37°C with 5% CO_2.

Cells were harvested 24 hours post transfection and washed with Dulbecco's PBS (Highveld Biological, RSA). Following this, cells were resuspended in lysis buffer (150 mM NaCl [Associated Chemical Enterprises, RSA], 50 mM (4-(2-hydroxyethyl)-1-piperazineethanesulfonic acid [HEPES; Sigma Aldrich, USA], 1 mM ethylenediaminetetraacetic acid [EDTA; Sigma Aldrich, USA], 0.5% (w/v) Triton X-100 [Promega Corporation, USA], 0.5% (v/v) Igepal [Sigma Aldrich, USA], 1X protease cocktail inhibitor [Sigma Aldrich, USA], pH 7.4) and sonicated twice using a sonicator probe (Labsonic M, Sartorius, Germany) for 1 minute each on ice at 60% amplitude and a 0.6 cycle. Cell lysates were incubated with 1 µg of mouse anti-CD74 antibody (BD Pharmingen, USA) at 4°C for 1 hour with rotational agitation. Protein G Dynabeads (Life Technologies, USA) were washed with the abovementioned lysis buffer, and 50 µl of beads were added to the lysate-antibody mix and incubated at 4°C for 90 minutes with rotational agitation. Following incubations, the beads were washed 5 times with lysis buffer and resuspended in denaturing SDS sample buffer (Bio-Rad, USA) and boiled for 5 minutes. The beads were removed using the DynaMag magnet (Life Technologies, USA) and the samples were analysed by SDS-PAGE using the Bio-Rad Mini PROTEAN TG-X pre-cast stain-free gels, 4-15%. Gels were visualised using the ChemiDoc™ MP System (Bio-Rad, USA) and a western blot was completed as described in section 2.5 above. The primary antibody used was 1000X diluted mouse anti-CD74 (BD Pharmingen, USA) followed by 2000X diluted HRP-labelled rabbit anti-mouse IgG (Rockland, USA) before substrate was added.

2.8 Flow cytometry

The ability of expressed Vpu::GFP to downregulate CD4, MHCII and CD74 in U937 cells was investigated following the establishment and optimization of a standard flow cytometry protocol for cell treatment, staining and analysis. U937 cells were sub-cultured to a concentration of 5 x 10^5 cells per ml into T75 culture flasks. Three sets of cells were prepared and were either left untreated, treated with 20 ng/ml of phorbol 12-myristate 13-acetate (PMA) or treated with 20 ng/ml of interferon-γ (IFN-γ) for 24 hours at 37°C, 5% CO_2. PMA was used to differentiate the U937 cells to a macrophage-like phenotype which may have an effect on MHCII expression (Tosi *et al.*, 2002; Baek *et al.*, 2009). IFN-γ has been reported to upregulate the expression of the MHCII I-A beta gene (Celada and Maki, 1991) and was used to investigate the effect of this activator on MHCII and CD74 expression. Transfection conditions were optimized and completed using the Neon Electroporation system (Life Technologies, USA) following the manufacturer's instructions as described in section 2.7. However, cells were transfected at a concentration of 1 x 10^7 cells per ml. Samples were prepared containing 10 µg of pVpu::GFP, pVpu-SM or pVpu-DM plasmid and 100 µl of the resuspended cells. Mock-transfected samples did not contain any plasmid. The samples were then electroporated and incubated as described before (section 2.7).

Cells were harvested 24 hour and 48 hours post-transfection and washed with 1 ml PBS containing 1% (w/v) bovine serum albumin (BSA; Highveld Biological, RSA) and 0.1% (w/v) NaN_3 (Sigma Aldrich, USA). Cells were permeabilized in the dark with Cytofix/Cytoperm buffer (BD Pharmingen, USA) for 20 minutes at 4°C and washed twice with 1X diluted Perm/Wash buffer (BD Pharmingen, USA). Following permeabilization, cells were incubated with 5 µg of mouse anti-CD74 (BD Pharmingen, USA), mouse anti-CD4 (Sigma Aldrich, USA) or fluorescein isothiocyanate (FITC)-labelled mouse anti-HLA-DR (Sigma Aldrich, USA) for 30 minutes at room temperature in the dark and then washed twice with 1X diluted Perm/Wash buffer (BD Pharmingen, USA). Cells that were stained for CD4 and CD74 levels were incubated with 1 µg of phycoerythrin (PE)-labelled goat anti-mouse Ig (BD Pharmingen, USA) for 30 minutes at room temperature in the dark. After a final washing step with 1X diluted Perm/Wash buffer (BD Pharmingen, USA), cells were resuspended in 0.5% (w/v) paraformaldehyde (Sigma Aldrich,

USA) before analysis. The stained cells were acquired (5000 events per sample) using a Guava easyCyte™ two laser flow cytometer (Merck Millipore, USA) at a medium flow rate of 0.59 µl per second. Data analysis was completed using the guavaSoft software, version 2.7 (Merck Millipore, USA).

2.9 Statistical analyses

All general statistical analyses such as the calculation of averages and standard deviations were performed using Excel (Microsoft, USA). The calculation of *p* values was done using the Simple Interactive Statistical Analysis (SISA) website, www.quantitativeskills.com/sisa. Six replicates were completed per sample set for each method. For ELISAs, absorbance values were used to calculate averages and standard deviations and for flow cytometry, mean fluorescence was used to calculate averages and standard deviations.

CHAPTER THREE: RESULTS

3.1 Peptide characterization

3.1.1 Predicted structure and peptide properties

In order to compare CD4 and CD74, the PredictProtein Server (www.predictprotein.org/) was used to calculate the percentage of secondary structure for the cytoplasmic domains of CD4 and CD74, based on amino acid sequence (Rost *et al.*, 2004; Wrzeszczynski and Rost, 2004; Yachdav *et al.*, 2014). The cytoplasmic domain of CD74 is mostly unstructured, with 23.33% of α-helix, while the cytoplasmic domain of CD4 has 48.28% of α-helix. The majority of residues in the CD4 and CD74 cytoplasmic domains have more than 16% of their surfaces exposed (89.66% and 93.33%, respectively) and were not found to contain β-sheets. The secondary structure was predicted using Discovery Studio 4 and compared to the secondary structure assigned to each protein by the DSSP (Kabsch and Sanders, 1983), which is available through the PDB (www.rscb.org). However, the only structure available on the PDB was for CD4. The secondary structure of the CD74 cytoplasmic domain was calculated purely on amino acid sequence as this peptide has not been crystallized yet.

Figure 3.1 shows the predicted secondary structure for the transmembrane and cytoplasmic domains of CD4 using the 2KLU co-ordinates; Figure 3.1A was determined using the DSSP (Kabsch and Sanders, 1983) while Figure 3.1B was predicted using Discovery Studio 4. Although the same co-ordinates and sequence of CD4 was used for both the DSSP and Discovery Studio, a discrepancy exists between the results. The DSSP predicts an α-helix that is 7 residues long (Q409-S415) while Discovery Studio predicts an α-helix that is 14 residues long (R401-L414). The co-ordinates for CD4 (2KLU) were uploaded to Discovery Studio to obtain a model of this peptide (Figure 3.1C). The HIV-1 Vpu susceptibility domain (residues 427-455) which is located within the cytoplasmic domain (residues 419-458) is indicated by a black box in Figure 3.1 A, B and C. The cytoplasmic α-helix from Figure 3.1A was used to plot the helical wheel in Figures 3.1D using the program from the RZ Lab (http://rzlab.ucr.edu/scripts/wheel/wheel.cgi), indicating the hydrophobic resides grouped together on the right side of the helix. This program shows charged residues in light blue, with positively charged residues displayed as pentagons

and negatively charged residues displayed as triangles. Hydrophilic residues are shown as red/orange circles, with the deepness of the red colour being proportional to the level of hydrophilicity; hydrophobic residues are shown as green diamonds, again with the intensity of the colour proportional to the level of hydrophobicity.

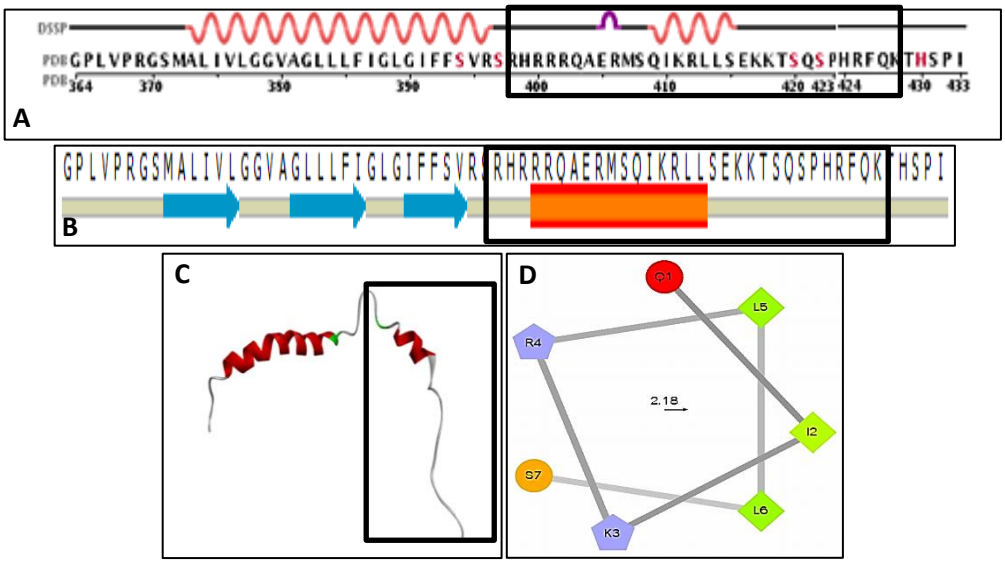


Figure 3.1: Predicted secondary structure of the T-cell surface glycoprotein CD4. The peptide sequence was obtained from the Protein Data Bank, using 2KLU co-ordinates (www.rscb.org). The HIV-1 Vpu susceptibility region (indicated by the black boxes) is located in the cytoplasmic domain and appears to have a short α-helix. The secondary structure is A) assigned from the DSSP and B) predicted by Discovery Studio 4. C) Model of CD4 transmembrane and cytoplasmic domains generated by Discovery Studio 4, using co-ordinates 2KLU. D) Helical wheel of the α-helix in the cytoplasmic domain of CD4 indicating the hydrophobic residues in green clustered on the right side of the helix with the charged and hydrophilic (blue and red/orange, respectively) residues arranged towards the left. This was determined using RZ lab (http://rzlab.ucr.edu/scripts/wheel/wheel.cgi).

The sequence of the CD74 cytoplasmic domain was obtained from UniProt (P04233) and the secondary structure was predicted only using Discovery Studio 4 based on the amino acid sequence as there is no resolved structure on the PDB (Figure 3.2A). This peptide is predicted to contain one α-helix that is 5 residues long (Q20-I24), while the remaining sections are unstructured. A representation or model of the folding of the cytoplasmic domain of CD74 was constructed using Discovery Studio 4 (Figure 3.2B), while the helical wheel of the

predicted α-helix in the cytoplasmic domain of CD74 is shown in Figure 3.2C. This indicates a mix of the hydrophobic and hydrophilic residues on one side, and a collection of charged residues on the opposite side. However, as mentioned above, this helix was predicted on primary sequence alone without taking 3D structure into account.

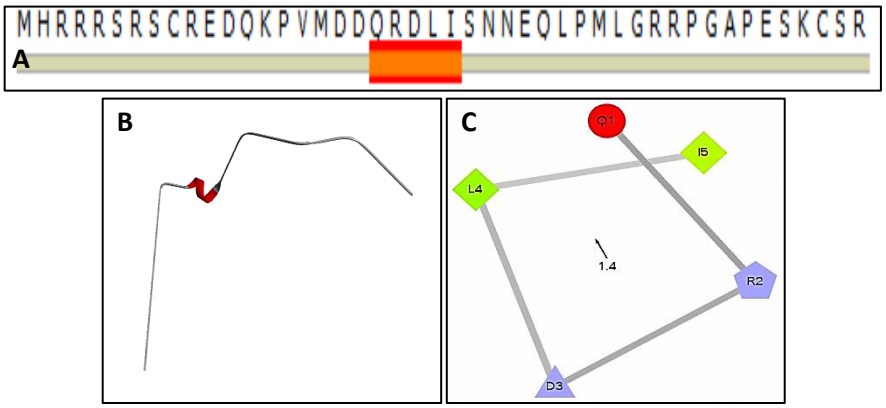


Figure 3.2: The predicted secondary structure of the CD74 cytoplasmic domain. A) The secondary structure was determined using Discovery Studio 4 from the sequence obtained from UniProt, identifier: P04233 (www.uniprot.org). This peptide was predicted to have a small, 5-residue α-helix, with the rest unstructured. B) Model of CD74 cytoplasmic domain predicted using Discovery Studio 4. The secondary structure was predicted based on the amino acid sequence from (A) and this was then used to predict the folding of the peptide. C) Helical wheel of the α-helix in the cytoplasmic domain of CD74 using RZ lab (http://rzlab.ucr.edu/scripts/wheel/wheel.cgi) indicating that the hydrophobic (green) and hydrophilic (red) residues clustered together opposite to the charged residues (blue), possibly due to the aqueous environment this peptide lies in.

The hydrophobicity plots of CD4 and CD74 were calculated with a default window size of 5 using Discovery Studio 4, which makes use of the Kyte and Doolittle hydropathy scale (Kyte and Doolittle, 1982). Figure 3.3 shows the hydrophobicity plots for A) the cytoplasmic domain of CD4 and B) the cytoplasmic domain of CD74. In Figure 3.3A, the CD4 cytoplasmic domain is largely hydrophilic, as expected. The cytoplasmic domain of CD74 (Figure 3.3B) also appears to be mostly hydrophilic, with small hydrophobic regions. It was expected that both of these peptides would be mostly hydrophilic as this domain of CD74 lies within the aqueous cytoplasm.

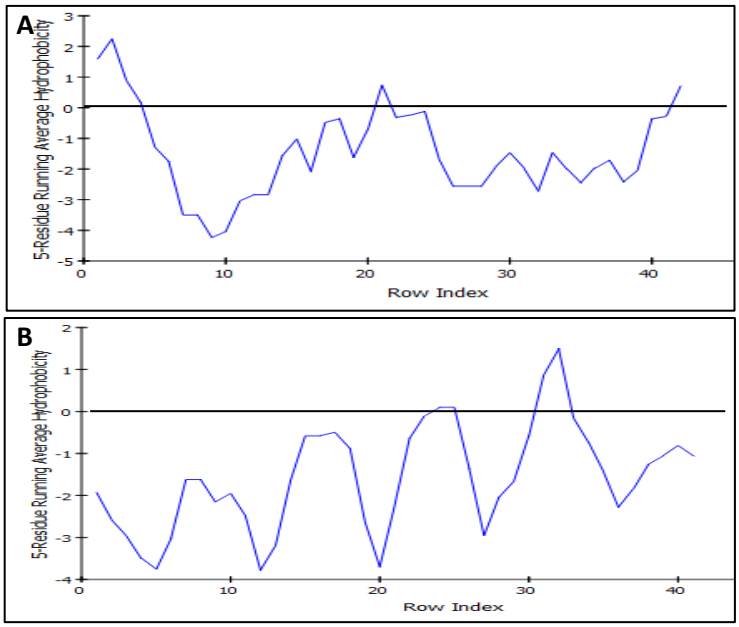


Figure 3.3: Hydrophobicity plots calculated for each of the peptides. A) The cytoplasmic domain of CD4 and B) the CD74 cytoplasmic domain were both found to be largely hydrophilic as indicated by the low hydrophobicity.

3.1.2 Sequence and structural alignment of CD4 and CD74

CD4 and CD74 were compared in terms of primary sequence. This was done by an amino acid sequence alignment of the cytoplasmic domains of CD4 and CD74 in Discovery Studio 4, using the "Align123" multiple sequence alignment method, which is based on the CLUSTAL W program (Figure 3.4). The CLUSTAL W program aligns sequences using a progressive pairwise alignment algorithm. The alignment was done using the "Fast" pairwise alignment, which makes use of the FASTA format approach and is reportedly less accurate than the "Slow" pairwise alignment, which makes use of the dynamic programming approach. However, both programs were used for the alignment and yielded the same result of 25.6% residue identity and 44.2% residue similarity, indicating minimal sequence conservation.

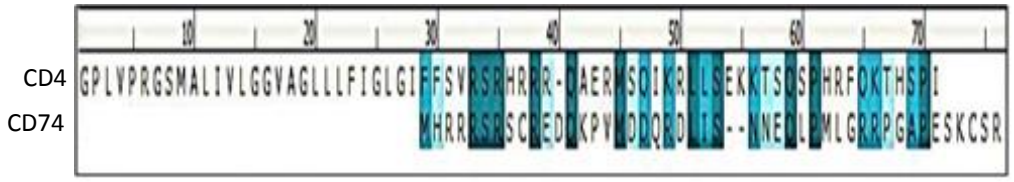


Figure 3.4: Amino acid sequence alignment of the cytoplasmic domains of CD4 and CD74. There is a residue identity of 25.6% and a residue similarity of 44.2% between CD4 and CD74. Colour intensity indicates the level of similarity.

Although there is little similarity between the cytoplasmic domains of CD4 and CD74 in terms of primary structure, this does not necessarily indicate that they will be different in terms of secondary structure. In order to compare these peptides structurally, the primary sequence of CD74 was modelled onto the 3D structure of CD4. This was done using the “Create homology models” tool in Discovery Studio 4. Twenty models were predicted in this way and the model with the smallest RMSD was selected as the most likely model. The RMSD was calculated after aligning and superimposing each of the 20 models onto the template (2KLU) and the model shown in Figure 3.5A has an RMSD of 3.296 Å, a DOPE score of -1278.71 and PDF total energy of 232.684 after energy minimization, showing an overall structural similarity. A Ramachandran plot of the CD74 model was generated using Discovery studio 4 (Figure 3.5B) and indicates no residues with conformational constraints, which verifies the probability of the CD74 model. Owing to the difficulty in comparing unstructured regions of proteins due to the disordered nature of these regions, a further comparison was made of the α-helices only (Figure 3.5C) for Met17 – Asn26 of CD74 and Met407 – Glu416 of CD4. This superimposition yielded a more favourable RMSD value of 1.437 Å, indicating that the α-helices within the cytoplasmic domains of CD4 and CD74 are similar.

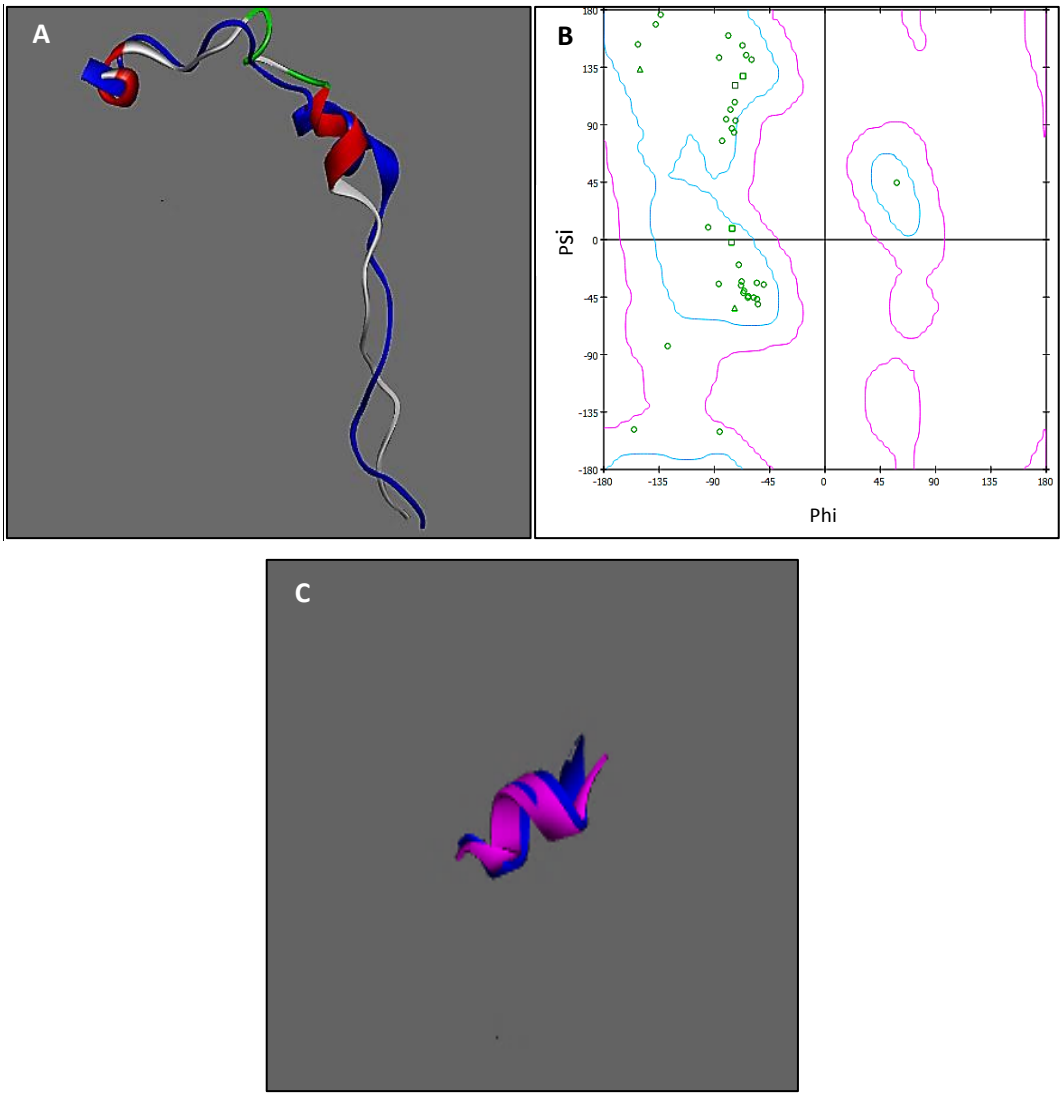


Figure 3.5: Homology model of the CD74 cytoplasmic domain against the CD4 cytoplasmic domain. A) The primary sequence of CD74 (grey and red) was modelled against the cytoplasmic domain of CD4 as a template (blue) yielding an RMSD of 3.296 Å. B) Ramachandran plot of the predicted model indicating that all residues lie within the "core" and "allowed" regions, signified by green points for each residue. C) Superimposition of the α-helices of CD4 and CD74 with an RMSD of 1.437 Å.

3.2 Sequencing and expression of Vpu::GFP in HEK 293T cells

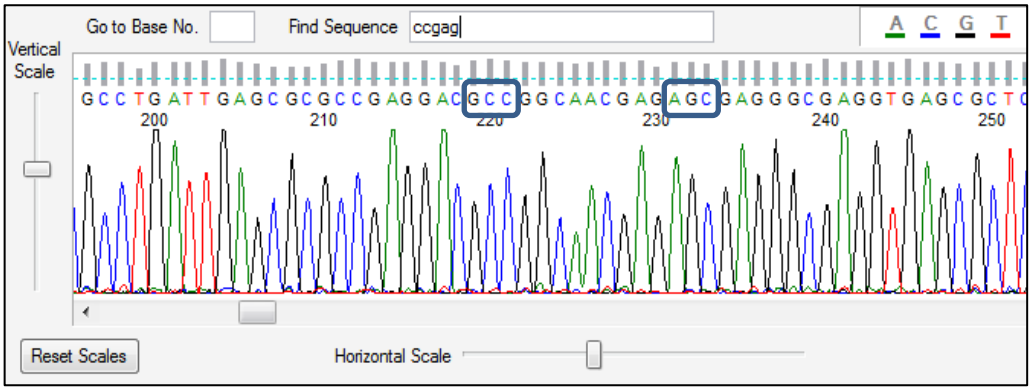
A recombinant pVpu::GFP plasmid was successfully constructed using the pcDNA-Vphu plasmid insert, and subsequently cloning the *vpu* fragment into the pcDNA^{TM} 6.2/C-EmGFP TOPO vector. This recombinant plasmid was amplified, isolated and nucleotide sequence analysis confirmed that the *vpu* fragment had successfully been cloned in frame with the EmGFP (Figure 3.6). This plasmid was subsequently used to generate two Vpu phosphorylation mutants for

subsequent analyses. The first mutant (Vpu-SM) contained the replacement of the first serine residue with alanine at position 52 while the second mutant (Vpu-DM) had both serine residues replaced with alanine at positions 52 and 56, as determined by nucleotide sequence analysis. These residues are underlined and the alanine codons are indicated in pink in Figure 3.6 below.

A.

```
ATGGTGCCCA TTATTGTCGC CATTGTGGCC CTGGTGGTCG CCATTATTAT   50
TGCCATTGTG GTGTGGAGCA TTGTGATTAT TGAGTACCGC AAGATTCTGC  100
GCCAGCGCAA GATTGACCGG TTGATTGACC GCCTGATTGA GCGCGCCGAG  150
    GCC           GCC
GACAGCGGCA ACGAGAGCGA GGGCGAGGTG AGCGCTCTGG TGGAGATGGG  200
CGTGGAGATG GGCCACCACG CCCCCTGGGA CATTGACGAC CTGTGCTACA  250
GAAAAATTGT GGGTCACAGT CTATTATGGA AGGGCGAATT CGACCCAGCT  300
TTCTTGTACA AAGTGGTTGA TGCTGTTAAC ATGGTGAGCA AGGGCGAGGA  350
GCTGTTCACC GGGGTGGTGC CCATCCTGGT CGAGCTGGAC GGCGACGTAA  400
ACGGCCACAA GTTCAGCGTG TCCGGCGAGG GCGAGGGCGA TGCCACCTAC  450
GGCAAGCTGA CCCTGAAGTT CATCTGCACC ACCGGCAAGC TGCCCGTGCC  500
CTGGCCCACC CTCGTGACCA CCTTCACCTA CGGCGTGCAG TGCTTCGCCC  550
GCTACCCCGA CCACATGAAG CAGCACGACT TCTTCAAGTC CGCCATGCCC  600
GAAGGCTACG TCCAGGAGCG CACCATCTTC TTCAAGGACG ACGGCAACTA  650
CAAGACCCGC GCCGAGGTGA AGTTCGAGGG CGACACCCTG GTGAACCGCA  700
TCGAGCTGAA GGGCATCGAC TTCAAGGAGG ACGGCAACAT CCTGGGGCAC  750
AAGCTGGAGT ACAACTACAA CAGCCACAAG GTCTATATCA CCGCCGACAA  800
GCAGAAGAAC GGCATCAAGG TGAACTTCAA GACCCGCCAC AACATCGAGG  850
ACGGCAGCGT GCAGCTCGCC GACCACTACC AGCAGAACAC CCCCATCGGC  900
GACGGCCCCG TGCTGCTGCC CGACAACCAC TACCTGAGCA CCCAGTCCGC  950
CCTGAGCAAA GACCCCAACG AGAAGCGCGA TCACATGGTC CTGCTGGAGT 1000
TCGTGACCGC CGCCGGGATC ACTCTCGGCA TGGACGAGCT GTACAAGTAA 1050
```

B.



C.

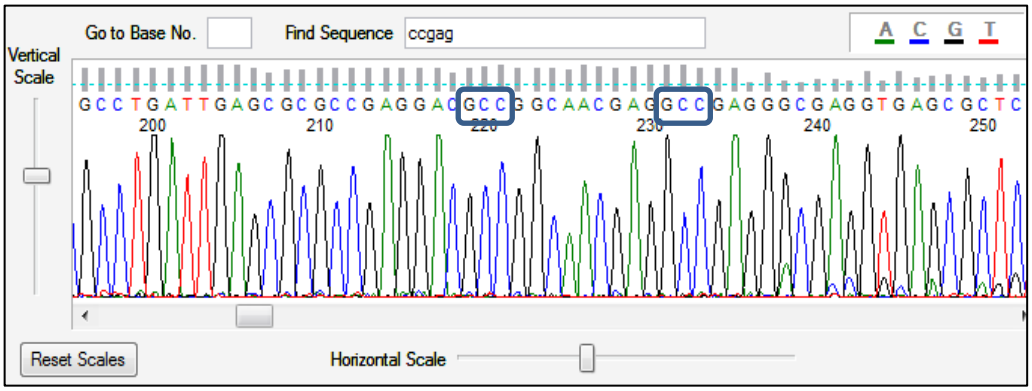


Figure 3.6: Nucleotide sequence analysis of the constructed Vpu::GFP plasmid. A) Nucleotide sequencing confirmed the correct cloning of the Vphu fragment into the pcDNATM 6.2/C-EmGFP TOPO vector in frame with the EmGFP. The *vpu* portion is shown in blue, while GFP is indicated in green. The underlined codons represent the serine residues that were replaced with alanine residues (pink) in both the single and double phosphorylation mutants. B) Nucleotide sequencing chromatogram indicating a single mutation of Ser52 to Ala52 for Vpu-SM. C) Nucleotide sequencing chromatogram indicating a double mutation of both Ser52 and Ser56 to Ala52 and Ala56.

The pVpu::GFP plasmid was used to successfully transfect HEK 293T and U937 cell lines using Lipofectamine and electroporation for protein expression and cell-based assays, respectively, after optimal transfection conditions had been established. Expression of the Vpu::GFP fusion protein was confirmed by the presence of GFP using fluorescence microscopy (Figure 3.7) as well as by SDS-PAGE and Western blotting (Figure 3.8; expected size of approximately 36 kDa). Approximately 1 ml of partially purified protein was obtained at a concentration of 0.979 mg/ml from a 6-well microtiter plate with 0.25 X 10^6 cells /ml in each well, 2 ml per well. The cells from each well were combined before isolation and purification, making a total of 3 X 10^6 HEK 293T cells used to isolate Vpu::GFP and the soluble supernatant fraction was used in subsequent *in vitro* assays. This was calculated using the Beer-Lambert equation and the extinction coefficient of Vpu::GFP (1.042 $g^{-1}.dm^3.cm^{-1}$) after the absorbance had been measured by Nanodrop spectrophotometry (Figure 3.9).

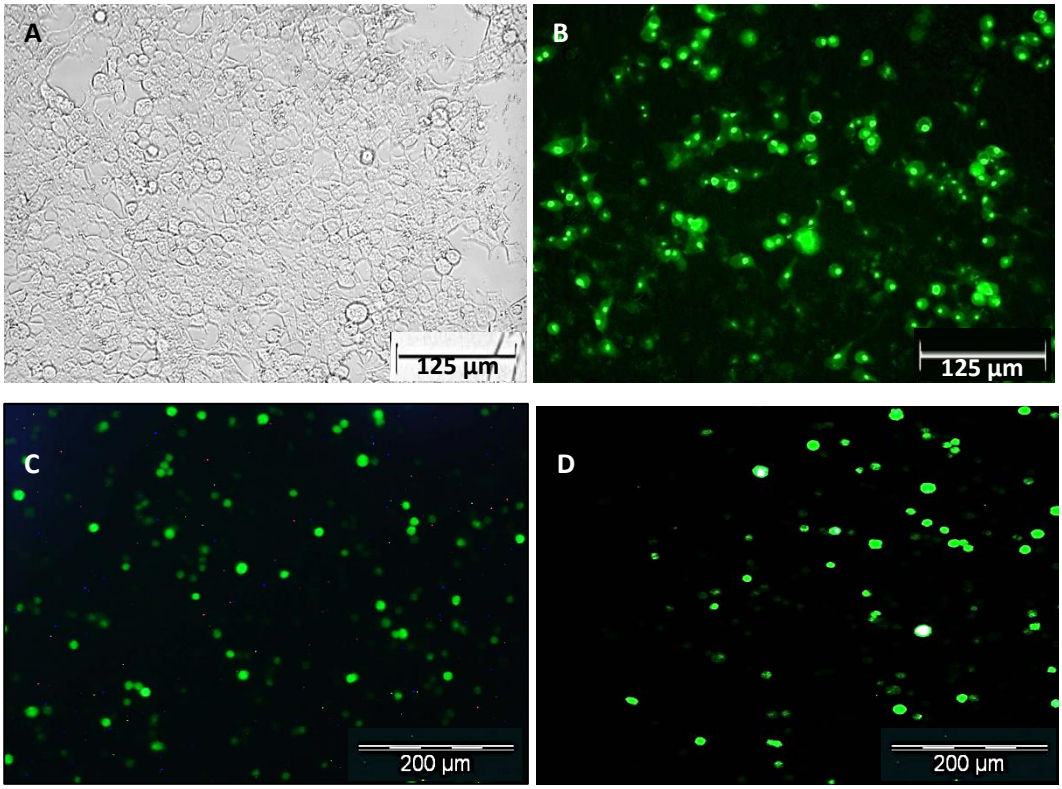


Figure 3.7: Micrographs taken of control and transfected HEK 293T and U937 cells at 48 hours post-transfection. Images were taken of A) control HEK 293T cells and B) Vpu::GFP transfected HEK 293T adherent cells using the Floid fluorescent imager at 20X magnification. An Olympus CKX41 fluorescent microscope was used to take images of C) U937 suspension cells transfected with a control pMax GFP vector and D) Vpu::GFP-transfected U937 cells at 10X magnification.

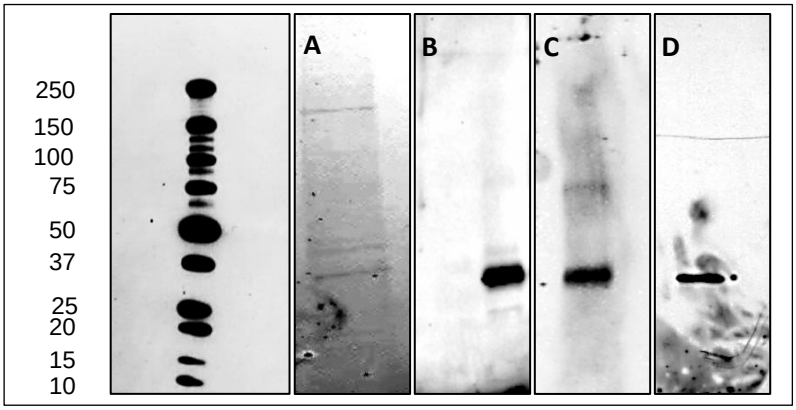


Figure 3.8: Analysis and Western blot showing expression of the Vpu::GFP fusion protein in HEK 293T cells at approximately 36 kDa. The Chemidoc™ MP System was used to obtain images of the A) SDS-PAGE and Western blots and indicated the presence of the Vpu::GFP fusion protein in the solubilized sample (red arrow) using B) anti-Vpu antibodies, C) anti-GFP antibodies and D) the phosphorylation of the fusion protein. Molecular weight (Bio-Rad, USA) in kDa is indicated on the left.

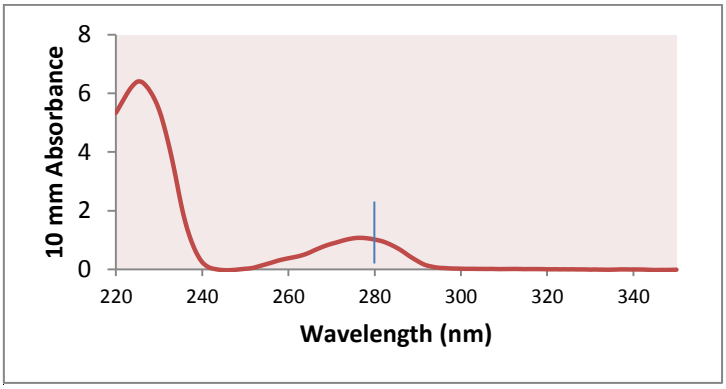


Figure 3.9: The absorbance spectrum of the Vpu::GFP fusion protein. The calculated concentration of the purified recombinant protein in the supernatant fraction was 0.979 mg/ml using Nanodrop spectrophotometry and the extinction coefficient of Vpu::GFP of 1.042 $g^{-1}.dm^{3}.cm^{-1}$.

3.3 Binding interaction of Vpu with CD4 and CD74

The partially purified Vpu::GFP fusion protein was evaluated for its interaction with CD4, CD74 and a control peptide CLIP using *in vitro* assays, as detailed in the subsequent sections. Overlapping peptides for both Vpu and CD74 were also evaluated for binding in the same way. All ELISA results are summarized in Addendum B, Table A.1. Results shown below indicate these detailed data for the binding interactions.

3.3.1 Confirmation of Vpu binding CD4 and CD74

The interaction between recombinant Vpu::GFP and CD4 or CD74 peptides was investigated *in vitro* using ELISAs. The protocol used for this assay was adapted from Hussain et al. (2008) and optimized for this study. Although the binding between Vpu and CD4 had previously been established (Willey *et al.*, 1994; Tiganos *et al.*, 1997), this was investigated through ELISA to confirm the interaction between these two proteins for this study. Using an anti-CD4 antibody that targets the CD4 cytoplasmic domain, it was indirectly observed that Vpu::GFP does indeed bind the CD4 peptide (Figure 3.10). Coating buffer (CB), Vpu::GFP or CD74 alone did not elicit a response. However, when the CD4 peptide was added to the coated Vpu::GFP, the responses obtained were equivalent to that of the CD4 peptide coated and incubated directly with the antibody without the addition of any other peptides. Results also confirm that the recombinant Vpu::GFP used in these assays was of sufficient purity since the background absorbance was low.

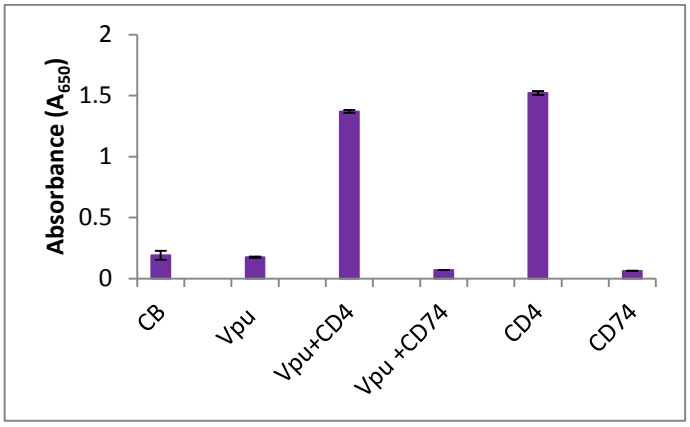


Figure 3.10: Interactions between full length recombinant Vpu::GFP and CD74 or CD4 peptides with anti-CD4 antibody. The interaction between the cytoplasmic domains of CD74 and CD4 peptides (500 ng each) with the full length Vpu::GFP protein (400 ng) using an anti-CD4 antibody directed against the CD4 cytoplasmic region is shown. The responses indicate binding between CD4 and Vpu. Values for each peptide are mean absorbance ± standard deviation. CB – coating buffer.

The binding of an anti-CD74 antibody to the Vpu/CD74 complex was tested in the same manner as that for anti-CD4, in which either Vpu::GFP or CD74 peptide was coated onto an ELISA plate and then incubated with the opposite protein before the addition of anti-CD74 antibody (Figure 3.11). This assay indicated that Vpu and CD74 do bind as previously reported (Hussain *et al.*, 2008), as all wells that contained CD74 resulted in a high signal. This response was specific as the control samples had significantly lower responses ($p < 0.0500$) and CD74 alone yielded similar responses to Vpu incubated with CD74 ($p = 0.9336$).

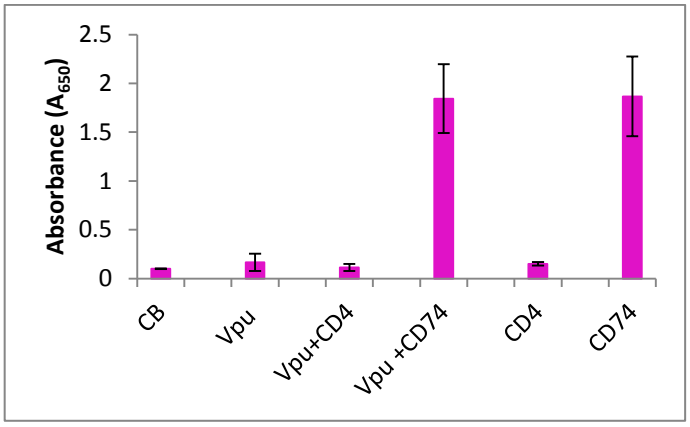


Figure 3.11: Interactions between full length recombinant Vpu::GFP and CD74 or CD4 peptides with anti-CD74 antibody. The interaction between the cytoplasmic domains of CD74 and CD4 peptides (500 ng each) with the full length Vpu::GFP protein (400 ng) using an anti-CD74 antibody directed against the CD74 cytoplasmic region is shown. The responses obtained correlate the binding between CD74 and Vpu. Values for each peptide are mean absorbance ± standard deviation. CB – coating buffer.

3.3.2 CD74 binds to an immunodominant domain on Vpu

The binding interaction between Vpu and CD74 was further investigated using an anti-Vpu antibody as well as an anti-GFP antibody (Figure 3.12), where samples incubated with anti-Vpu are shown in blue and samples incubated with anti-GFP are shown in green. A control peptide, CLIP, is also indicated with no binding to Vpu::GFP. It can be seen that regardless of whether CD74 peptide is coated and incubated with Vpu::GFP, or if CD74 peptide is incubated with the coated Vpu::GFP, the response is significantly lower than that of Vpu::GFP alone using the anti-Vpu antibody ($p = 0.0000$ and 0.0002 for CD74 peptide coating and Vpu::GFP coating respectively). However, when using the anti-GFP antibody, the addition of CD74 peptide to the coated Vpu::GFP does not reduce the response. In addition to this, when CD74 peptide is coated and incubated with Vpu::GFP and followed by anti-GFP, a higher response is obtained, indicating the presence of the Vpu::GFP fusion protein bound to the coated CD74 peptide. This indicates that the CD74 peptide binds to an epitope in the immunodominant domain on Vpu. The use of the anti-GFP antibody eliminated the reduction in response as this antibody would bind to the GFP tag on the Vpu::GFP fusion protein. Therefore, the binding of anti-GFP was not hindered/affected by the presence of the CD74 peptide bound to the immunodominant domain of Vpu.

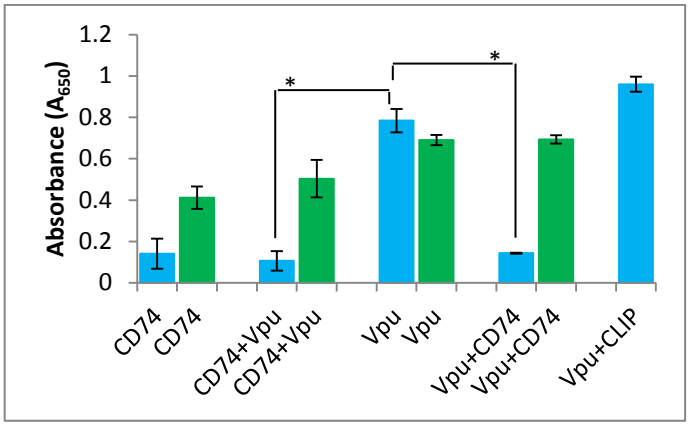


Figure 3.12: Interactions between Vpu::GFP and CD74 or CLIP peptides. The interactions between the full length cytoplasmic domains of CD74 and the CLIP control peptides with the full length Vpu::GFP protein using the subtype B anti-Vpu antibody (blue) and the anti-GFP antibody (green) are indicated respectively. Values for each peptide are mean absorbance ± standard deviation. Asterices are indicative of significant differences in response.

In order to determine the effectiveness of the CD74 peptide in preventing the binding of the anti-Vpu antibody to Vpu::GFP, a dose response assay was conducted in which increasing concentrations of CD74 peptide (100, 250, 500, 1000, 5000 and 10 000 ng) were incubated with 400 ng of coated Vpu::GFP (Figure 3.13). When plotting the response against the log of the CD74 concentration, an IC_{50} of 888.67 ± 130.08 nM was obtained. This indicates that the CD74 peptide competes with anti-Vpu antibody for binding to the immunodominant region on the cytoplasmic domain of Vpu.

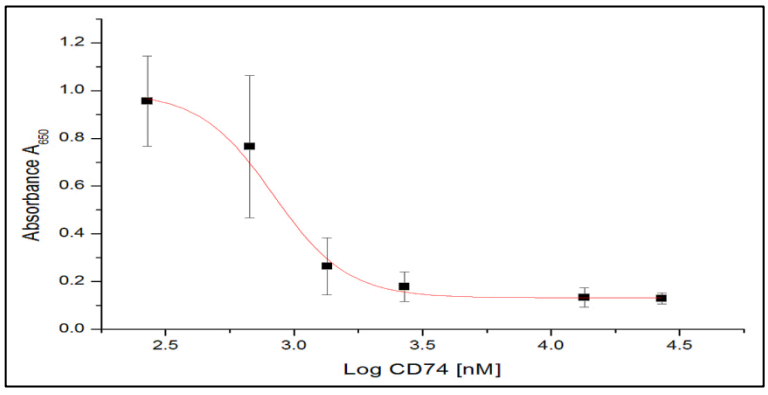


Figure 3.13: Fitted dose response curve for the Vpu/CD74 interaction. Subtype B anti-Vpu antibody was effectively inhibited by the CD74 peptide from binding to Vpu::GFP with an IC_{50} of 888.67 ± 130.08 nM. Values for the CD74 peptide are mean absorbance ± standard deviation.

3.3.3 CD4 and CD74 compete for binding to Vpu

As both CD4 and CD74 interact with Vpu via the cytoplasmic domains, these peptides may compete for binding to Vpu. Results from a competitive binding assay using the 29-mer and 30-mer cytoplasmic peptides of CD4 and CD74, respectively with the full length Vpu::GFP fusion protein are shown in Figure 3.14. The CD4 peptide was coated onto a plate and then incubated with Vpu::GFP that had been pre-incubated with increasing concentrations of the CD74 peptide (0, 250, 500, 1000, 5000 and 10 000 ng). At 0 ng of CD74 peptide, Vpu::GFP was able to bind the CD4 peptide, yielding a high response. However, as the concentration of the CD74 peptide increased, the response decreased, indicating that the ability of Vpu::GFP to bind to CD4 was inhibited. The pre-incubation of Vpu::GFP with the CD74 peptide reduced the binding of Vpu to the CD4 peptide 2-fold at a concentration of 250ng. This data suggests that the tested CD4 and CD74 peptides bind to the cytoplasmic domain of Vpu within closely related regions, and compete for binding to Vpu.

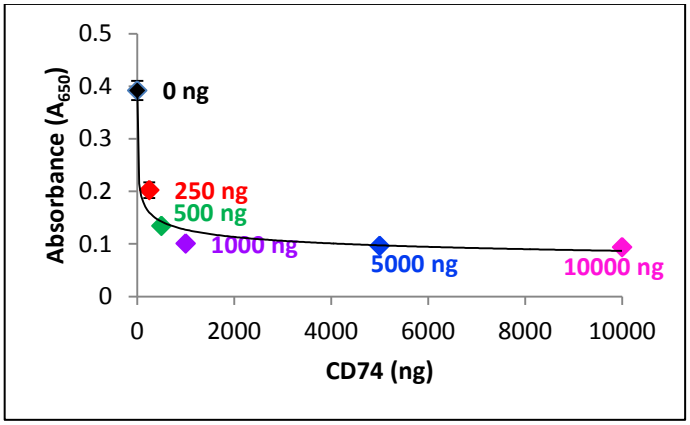
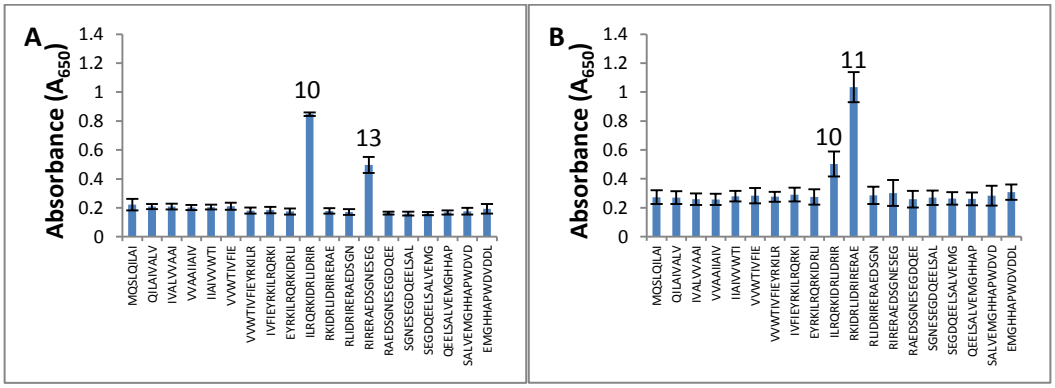


Figure 3.14: Competitive binding study between CD4 and CD74 peptides to Vpu::GFP. The pre-incubation of Vpu::GFP with increasing concentrations of the cytoplasmic CD74 peptide before interaction with the coated CD4 peptide yielded a decrease in response which correlates to a decrease in the binding of Vpu to CD4. This data indicates that CD4 and CD74 bind to Vpu within a closely related region within the cytoplasmic domain.

3.3.4 Binding site delineation

ELISA data presented previously (section 3.3.2) suggested that CD74 binds to the immunodominant region on Vpu and thus prevents the binding of the anti-Vpu antibody. In order to specifically delineate the binding site, the interaction between overlapping peptide sets of both Vpu and CD74 was investigated *in vitro*

using ELISAs. Initially, 400 ng per well of the overlapping Vpu peptides were tested with subtype B (Figure 3.15A) and subtype C (Figure 3.15B) anti-Vpu antiserum, respectively, in order to obtain baseline responses for each of these overlapping peptides with the respective antibodies. For each antibody subtype, two peptides from the overlapping peptide set were recognised and bound, which may indicate the immunodominant regions on the Vpu cytoplasmic domain. For the subtype B antibody, these were peptides 10 and 13 with the amino acid sequences of ILRQRKIDRLIDRIR and RIRERAEDSGNESEG, respectively. When using the subtype C anti-Vpu antibody, the two reactive peptides included numbers 10 and 11 with the amino acid sequence of peptide 11 being RKIDRLIDRIRERAE. Peptide 13 was not recognized and bound by the subtype C antibody, while peptide 11 was not bound by the subtype B antibody. On closer inspection, the subtype B antibody yielded a 1.7 fold higher response for peptide 10 compared to peptide 13 while the subtype C antibody yielded a 2.06 fold higher response for peptide 11 compared to peptide 10.



<u>Figure 3.15:</u> Testing of Vpu overlapping peptides (NIH) with A) a subtype B anti-Vpu antiserum (NIH cat #969) and B) a subtype C anti-Vpu antiserum (NIH cat #11942). In this data set, only two peptides bind the antibodies – numbers 10 and 13 with sequences of ILRQRKIDRLIDRIR and RIRERAEDSGNESEG respectively for subtype B and number 10 and 11 with sequences of ILRQRKIDRLIDRIR and RKIDRLIDRIRERAE respectively for subtype C. Values for each peptide are mean absorbance ± standard deviation.

Following this, the Vpu overlapping peptides were tested against two overlapping peptide sets of the CD74 cytoplasmic domain in which the two responsive Vpu peptides described in Figure 3.15 were coated and then incubated with the CD74 peptide sets (Figure 3.16).

When using the subtype B anti-Vpu antibody (Figure 3.16A), the addition of the CD74 10-mer peptide set to Vpu peptide 10 yielded no significant difference (p > 0.0500) in the response, suggesting that either these CD74 peptides do not bind to the ILRQRKIDRLIDRIR sequence or that the peptides are too small to have any influence over the binding of the antibody. However, when examining the response of Vpu peptide 13, the addition of CD74_10.2 and CD74_10.3 yield a significant response (p = 0.0098 and p = 0.0178, respectively) while the remaining CD74 peptides did not. This suggests that the binding site may be between the Vpu sequence of RIRERAEDSGNESEG and the CD74 overlapping sequences of SRSCREDQKP and EDQKPVMDDQ, both of which contain the residues EDQKP.

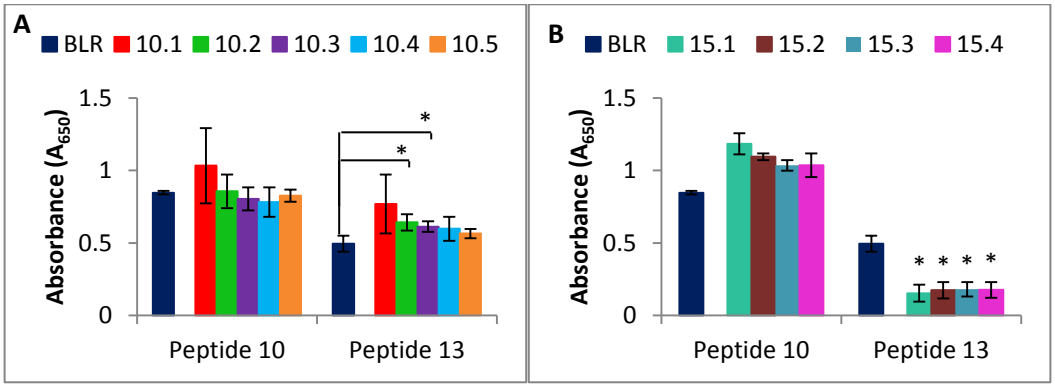


Figure 3.16: Interaction of coated Vpu overlapping peptides 10 and 13 with CD74 overlapping peptides. A) Overlapping 10-mer CD74 peptides and B) overlapping 15-mer CD74 peptides were used followed by the subtype B anti-Vpu antibody. Only data from the two responsive peptides from the Vpu peptide set are shown. Values for each peptide are shown as the mean absorbance ± standard deviation. BLR – baseline response. Asterices are indicative of significant differences in response.

The incubation of the Vpu peptides with a 15-mer overlapping peptide set of the cytoplasmic domain of CD74 yielded a different response to that of the 10-mer CD74 peptide set when using the subtype B anti-Vpu antibody (Figure 3.16B). A significant increase is observed in the responses of Vpu peptide 10 with the different CD74 15-mer peptides (p < 0.0500), as seen in Figure 3.16B in comparison to the baseline responses in Figure 3.15. This indicates a possibility of no binding between the CD74 15-mer peptide and Vpu peptide 10, and this particular increase in response may be due to non-specific binding. On closer inspection of the interaction between the CD74 15-mer peptides and Vpu peptide

13, the response of this Vpu peptide is almost completely abolished in the presence of all four of the 15-mer CD74 peptides ($p < 0.0500$). The reduction in this response may be caused by the blocking of the antibody binding site by the CD74 peptides. The differences in response obtained between the two different CD74 peptide sets suggests that the size of the peptides tested plays a role in this interaction, described in more detail in section 3.3.5 below.

In order to determine if the abovementioned binding site between CD74 and Vpu is specific, a second anti-Vpu antibody was used that recognizes a different immunodominant domain within the Vpu cytoplasmic region. Initially, the overlapping Vpu peptide set was tested using this antibody to determine which peptides were responsive. It was found that the last two peptides, peptides 18 and 19, were the responsive peptides with the sequences of SALVEMGHHAPWDVD and EMGHHAPWDVDDL, respectively. These two responsive peptides were then incubated with the two sets of CD74 overlapping peptides (Figure 3.17) but neither the 10-mer (Figure 3.17A) nor the 15-mer (Figure 3.17B) CD74 peptides were found to bind to these particular Vpu peptides as there was no significant difference in response between the Vpu peptides and those incubated with the CD74 peptides ($p > 0.0500$), which validates the previously mentioned binding site and indicates that the proposed binding site is specific between Vpu and CD74.

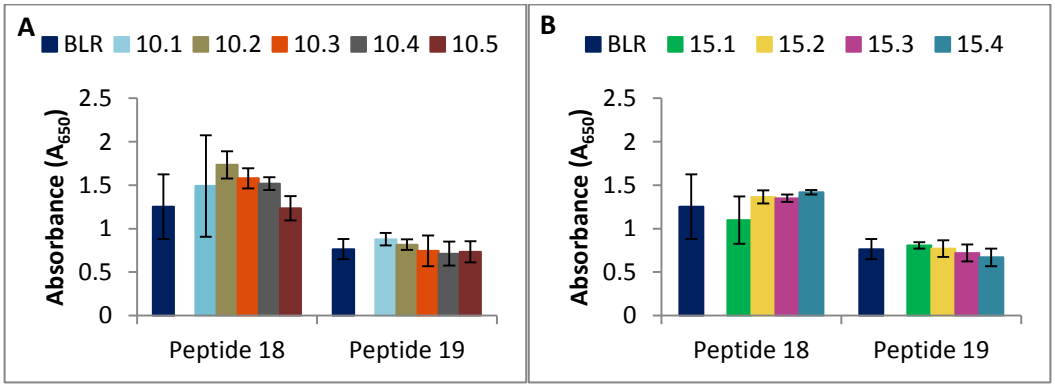


Figure 3.17: Interaction of coated Vpu overlapping peptides 18 and 19 with CD74 overlapping peptides. A) Overlapping 10-mer CD74 peptides were used and B) overlapping 15-mer CD74 peptides were used followed by an anti-Vpu antibody that recognizes a different epitope to that described in Figure 3.16. Values for each peptide are shown as the mean absorbance ± standard deviation. BLR – baseline response.

When this same assay was repeated using the cytoplasmic domain of CD4 (Figure 3.18), it was seen that the addition of CD4 significantly reduced the response of the two Vpu peptides (p = 0.0000 and 0.0006 for peptides 18 and 19, respectively). This concurs with the CD4 binding sites on Vpu found by Schneider *et al.* (1990), Margottin *et al.* (1996) and Tiganos *et al.* (1997). Notably, the decrease in response is more pronounced with peptide 19 than peptide 18, suggesting that these residues may be more important in the binding of CD4 and Vpu.

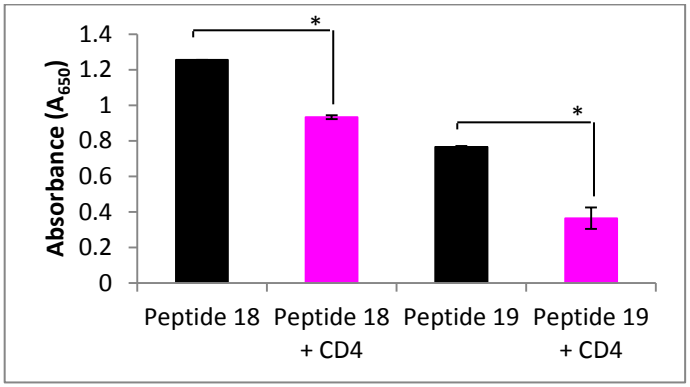


Figure 3.18: Interaction of coated Vpu overlapping peptides 18 and 19 with CD4 cytoplasmic peptide. Responses both with and without the CD4 cytoplasmic domain are indicated after using an anti-Vpu antibody that recognizes a different epitope to that of Figure 3.16. CD4 reduces the responses of peptide 19 by 2.1 fold and peptide 18 by 1.3 fold. Values for each peptide are shown as the mean absorbance ± standard deviation. Asterices are indicative of significant differences in response.

Following this, 400 ng of the responsive Vpu peptides from the overlapping peptide set was then tested for binding against 500 ng of the CLIP control peptide and 500 ng of the cytoplasmic domains of both CD74 and CD4 (Figure 3.19). When using the subtype B antibody (Figure 3.19A), the addition of the CLIP peptide did not reduce the response in comparison to the baseline responses (see Figure 3.15A), while the CD4 cytoplasmic domain peptide enhanced the response of peptides 10 and 13 in comparison to the baseline. This enhanced response was more significant with Vpu peptide 10 than peptide 13 (p = 0.0112 and 0.3722, respectively). In contrast to CD4, the addition of the CD74 cytoplasmic domain peptide resulted in a significant decrease in the response (p = 0.0012 and 0.0112 for peptide 10 and 13, respectively), while there was no significant difference after CLIP incubation (p = 0.2500 and 0.8742,

respectively). When repeating the interaction of the overlapping Vpu peptides with CLIP, CD74 and CD4 using the subtype C antibody (Figure 3.19B), a similar pattern was seen as with the subtype B antibody in which only the CD74 cytoplasmic domain induced a reduction in the response. However in this case, peptides 10 and 11 were tested, as previously mentioned. CD4 once again significantly enhanced the response obtained (p = 0.0008 and 0.0236 for peptides 10 and 11, respectively) while CD74, as with the subtype B antibody, reduced the response obtained significantly in comparison to the baseline response (p = 0.0022 and 0.0000 for peptides 10 and 11, respectively), while there was no significant difference after CLIP incubation (p = 0.2642 and 0.0906 for peptides 10 and 11, respectively).

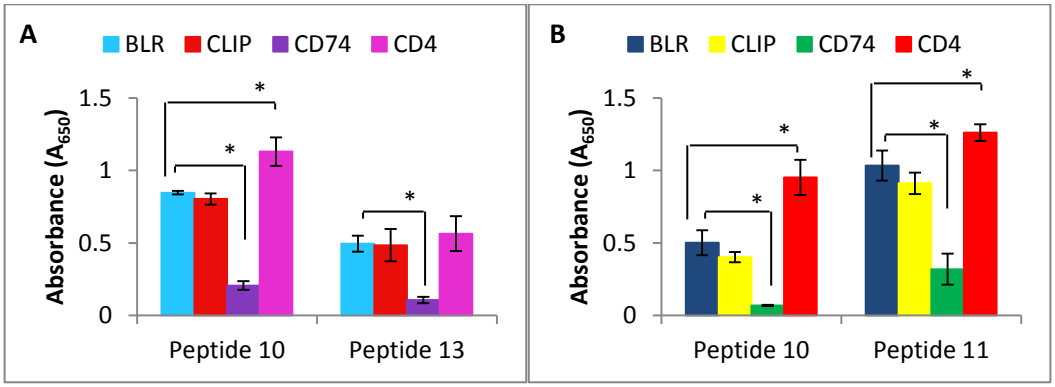


Figure 3.19: CD74 reduces antibody binding to Vpu peptides while CD4 enhances antibody binding. The interaction between the coated Vpu overlapping peptides with the full length cytoplasmic domains of CD74, CD4 and the CLIP peptide using A) the subtype B anti-Vpu antibody and B) the subtype C anti-Vpu antibody. Only the two responsive Vpu peptides (10 and 11) are shown. Values for each peptide are mean absorbance ± standard deviation. BLR – baseline response. Asterices are indicative of significant differences in response.

As an increase in response upon the addition of the CD4 cytoplasmic peptide was unexpected, the presence of CD4 bound to the Vpu peptides was validated by repeating the assay using an antibody that recognizes the C-terminal domain of CD4 (Figure 3.20). The Vpu peptides alone did not yield a response with this antibody, while the addition of the CD4 cytoplasmic peptide generated a significantly increased response (p < 0.0500). This confirmed the presence of CD4, bound to the selected Vpu peptides.

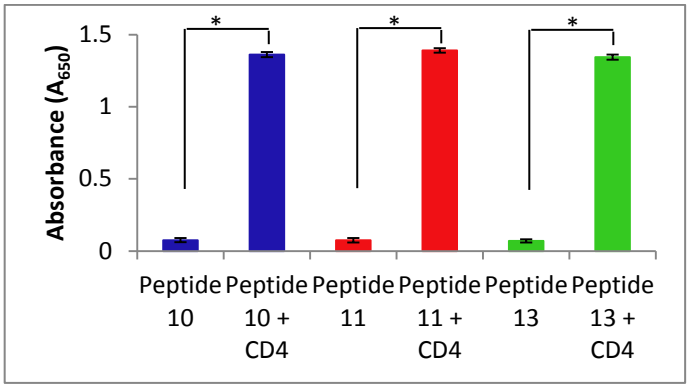


Figure 3.20: CD4 binds to the Vpu responsive peptides. The interaction between the coated Vpu overlapping peptides with the full length cytoplasmic domain of CD4 using an anti-CD4 antibody that recognizes the C-terminus of CD4. Only the responsive Vpu peptides (10 in blue, 11 in red and 13 in green) are shown. Values for each peptide are mean absorbance ± standard deviation. Asterices are indicative of significant differences in response.

3.3.5 Peptide size plays a role in antibody inhibition

Once the interaction between the Vpu and both CD74 overlapping peptide sets had been established, both of the CD74 overlapping peptide sets were tested using the full length purified Vpu::GFP fusion protein (Figure 3.21). With both CD74 peptide sets, the responses obtained were high with the exception of the CD74_15.1 peptide which was slightly lower (not significant) than its counterparts.

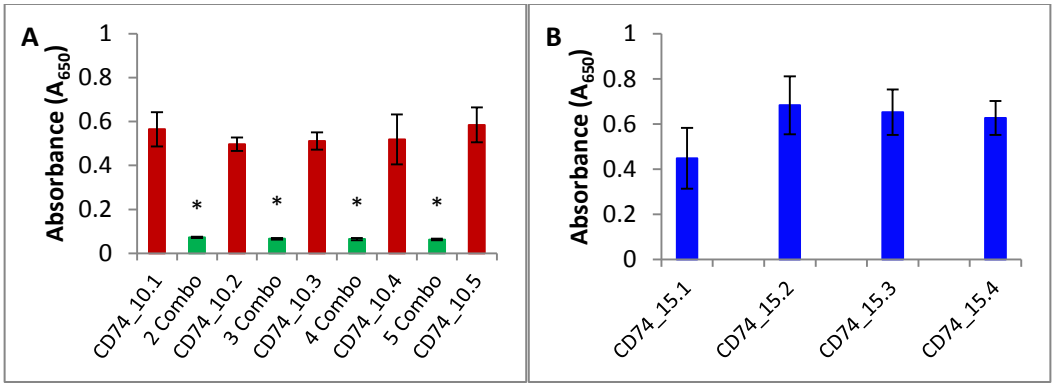


Figure 3.21: Individual peptides are unable to prevent antibody binding. The interaction between the full length Vpu::GFP fusion protein with A) the CD74 10-mer overlapping peptide set both individually (red) and in combinations (green) and B) the CD74 15-mer overlapping peptide set. Values for each peptide are shown as the mean absorbance ± standard deviation. Asterices are indicative of significant differences in response.

As previously mentioned, it was considered that the size of the peptides may be an influencing factor in the ability of CD74 to prevent the binding of the anti-Vpu antibody. In order to explore this concept, combinations of the CD74 10-mer peptides were incubated with the Vpu::GFP fusion protein (Figure 3.21A, green). It was noted that these combinations of the 10-mer CD74 peptides were able to prevent the binding of the anti-Vpu antibody to the Vpu::GFP fusion protein and reduce the response significantly ($p < 0.0500$ for all combinations as compared to all individual peptides) in comparison to individual peptides. While a single, individual CD74 peptide was unable to prevent antibody binding (Figure 3.21A red), a combination of only two of these peptides was enough to reduce the response, indicating that the size of the CD74 overlapping peptides plays a role in preventing the binding of anti-Vpu.

3.4 CD4, CD74 and MHCII are downregulated in the presence of Vpu

The downstream consequence of the Vpu/CD4 interaction is the targeting of CD4 for proteasomal degradation (Fujita *et al.*, 1997; Schubert *et al.*, 1998). Taking into consideration the structural similarities between CD4 and CD74 as indicated in section 3.1, and the competition between these two host proteins for binding to Vpu (Figure 3.14), it is possible that the interaction between CD74 and Vpu will also lead to the downregulation and/or degradation of CD74. Once an optimal protocol for CD74 immunoprecipitation had been established, the transfection of U937 cells with pVpu::GFP resulted in the complete reduction of total cellular CD74 levels (Figure 3.22) seen after immunoprecipitation from whole cell lysate, while both untransfected cells and cells transfected with a control GFP vector (pMax) were still found to have high levels of CD74 after immunoprecipitation.

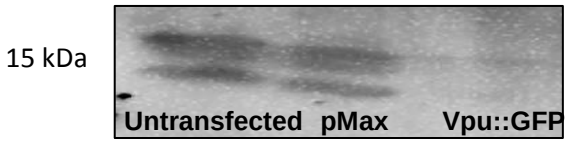


Figure 3.22: Total CD74 levels are downregulated by Vpu::GFP. Western blot probing for CD74 after immunoprecipitation with mouse anti-CD74 antibody from untransfected cells, pMax control transfected cells and Vpu::GFP transfected cells. The presence of CD74 is indicated in both control sets, but a complete absence of CD74 in the presence of Vpu::GFP. CD74 appears as a doublet around 15 kDa. The secondary antibody used was HRP-labelled rabbit anti-mouse IgG.

Next, the downregulation of native CD4, MHCII and CD74 was investigated via flow cytometry. The protocol for cell treatment, staining and analysis was optimized prior to the measurement of samples. The Vpu-mediated downregulation and degradation of CD4 has been previously reported (Fujita *et al.*, 1997; Schubert *et al.*, 1998; Hill *et al.*, 2010; Magadan *et al.*, 2010). This finding was corroborated within this study using flow cytometry in which mock-transfected U937 cells were found to have high/normal levels of CD4 and those cells transfected with pVpu::GFP had significantly lower CD4 levels (p = 0.0000; Figure 3.23). This was investigated at 24 hours only for confirmatory purposes as the downregulation of this protein by HIV-1 Vpu has already been reported, as previously mentioned. Total cellular CD4 levels were measured in U937 cells by permeabilization of the cells prior to staining with an anti-CD4 antibody. Statistical data for six replicates is indicated in Table 3.1.

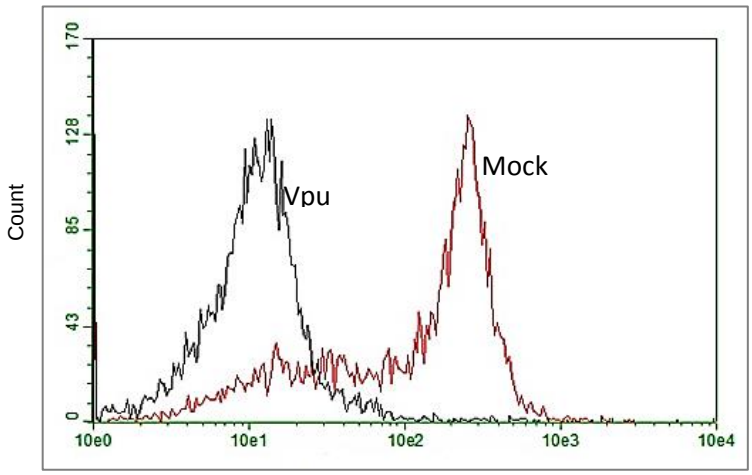
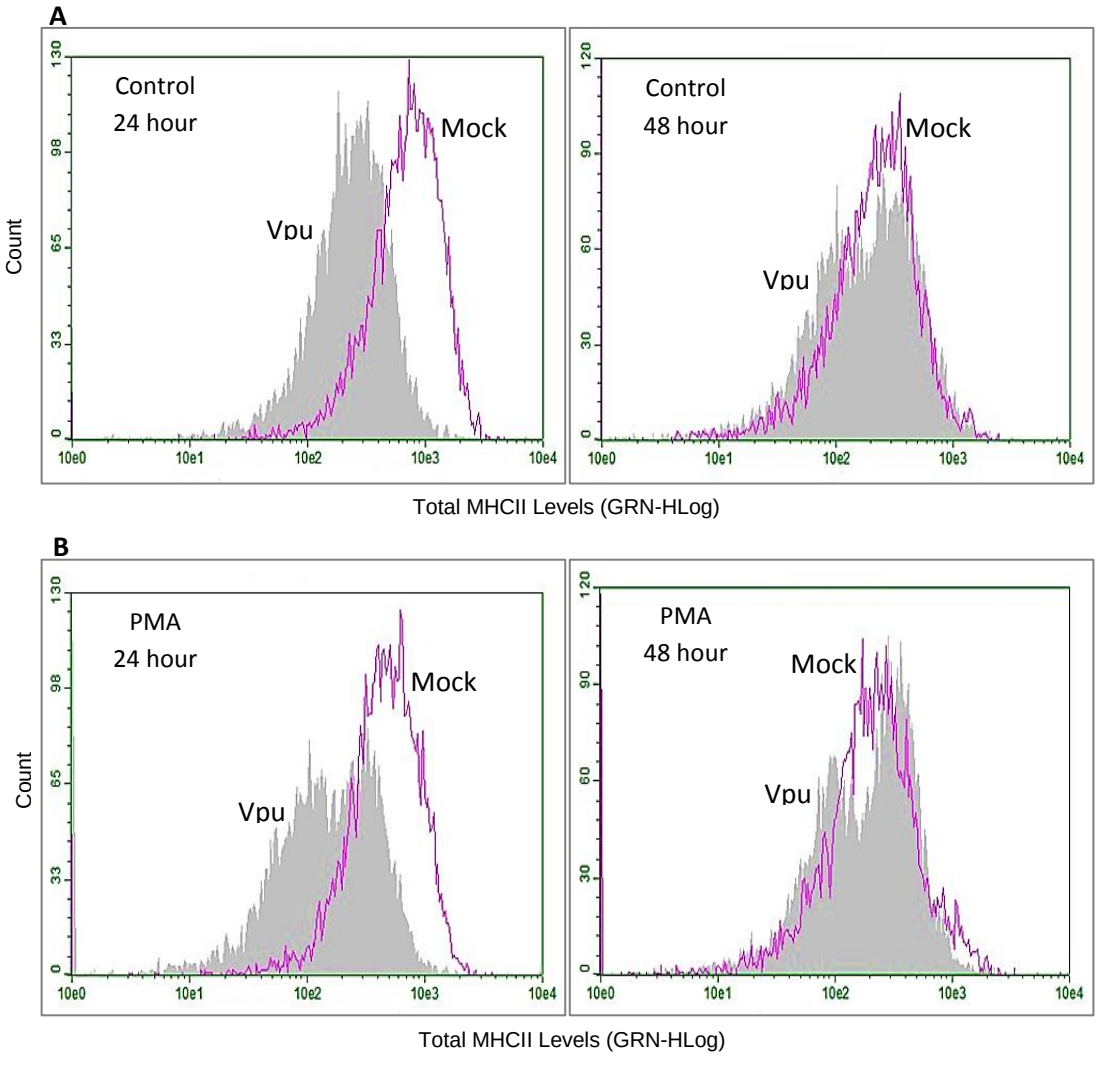


Figure 3.23: CD4 is downregulated by Vpu in U937 cells at 24 hours post-transfection. Yellow fluorescence counts for total CD4 levels of mock-transfected cells (red) and Vpu-transfected cells (black) cells after 24 hours post-transfection and staining with a PE-labelled antibody. The cell count is indicated on the y-axis while CD4 levels are indicated on the x-axis.

Table 3.1: Average fluorescence counts (± SD) for total CD4 levels in U937 cells that were either mock-transfected or Vpu-transfected. Statistically significant differences are indicated by *p* values in bold red.

		Average	Standard Deviation	*p* Value
24 Hours	**Mock-transfected**	155.53	25.42	**0.0000**
	Vpu-transfected	24.44	6.45	

As with CD4 described above, the downmodulation of MHCII in the presence of Vpu in U937 cells has already been reported (Hussain *et al.*, 2008). This downregulation was confirmed within this study via flow cytometry at 24 hours but not at 48 hours post transfection with pVpu::GFP. This trend was seen regardless of the prior treatment of the cells, i.e. no activation or activation with either PMA or IFN-γ. When control cells were left untreated prior to transfection (Figure 3.24A), a significant decrease in total MHCII levels was seen at 24 hours post transfection in the presence of Vpu compared to mock-transfected cells (p = 0.0156), but no significant decrease was seen at 48 hours post transfection (p = 0.4470). This was also indicated with PMA-activation of cells prior to transfection (Figure 3.24B), with a significant decrease again at 24 hours (p = 0.0032) in the presence of Vpu and no significant decrease at 48 hours (p = 0.6184). Finally, IFN-γ-activation of cells prior to transfection (Figure 3.24C) yielded the same significant decrease in total MHCII levels at 24 hours with Vpu (p = 0.0004) and no decrease at 48 hours post transfection (p = 0.6630). At 48 hours post-transfection, Vpu-transfected cells for all three treatment types yielded two populations. These are most likely parent and daughter populations, with the daughter population expressing greater levels of MHCII as these cells were not expressing Vpu. A summary of the statistical data for six replicates of each condition is provided in Table 3.2.


A
Control
24 hour
Mock
Vpu
Control
48 hour
Mock
Vpu
Count
Total MHCII Levels (GRN-HLog)
B
PMA
24 hour
Mock
Vpu
PMA
48 hour
Mock
Vpu
Count
Total MHCII Levels (GRN-HLog)

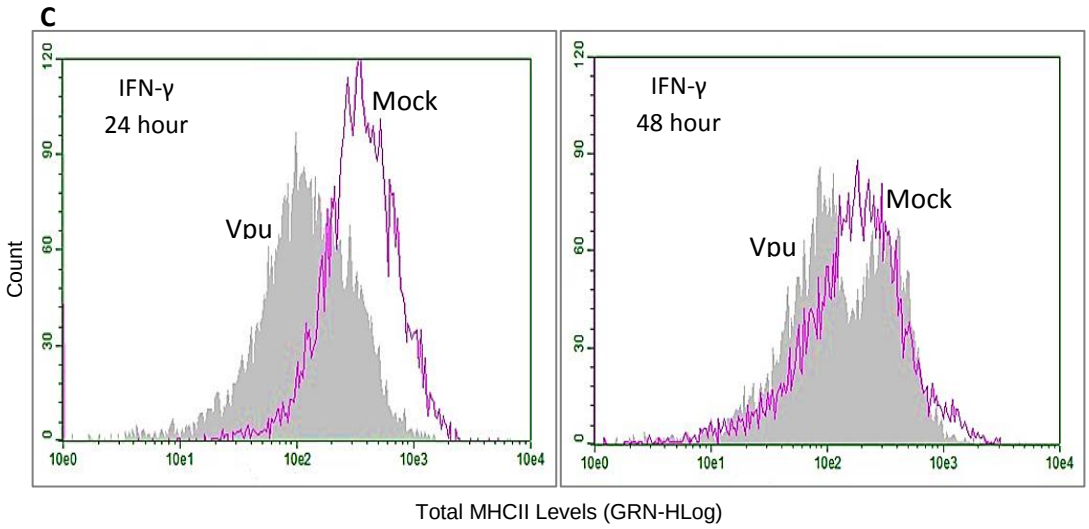
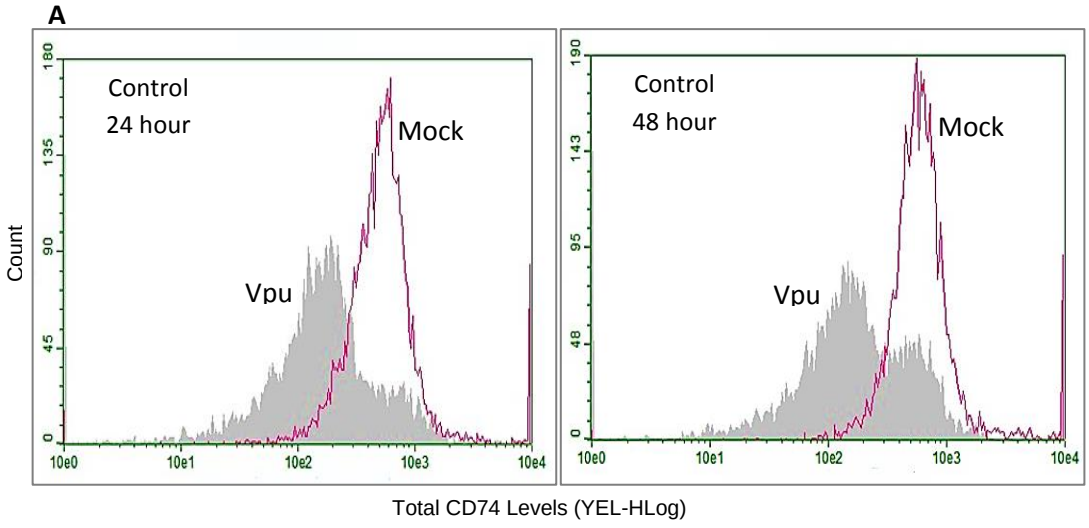


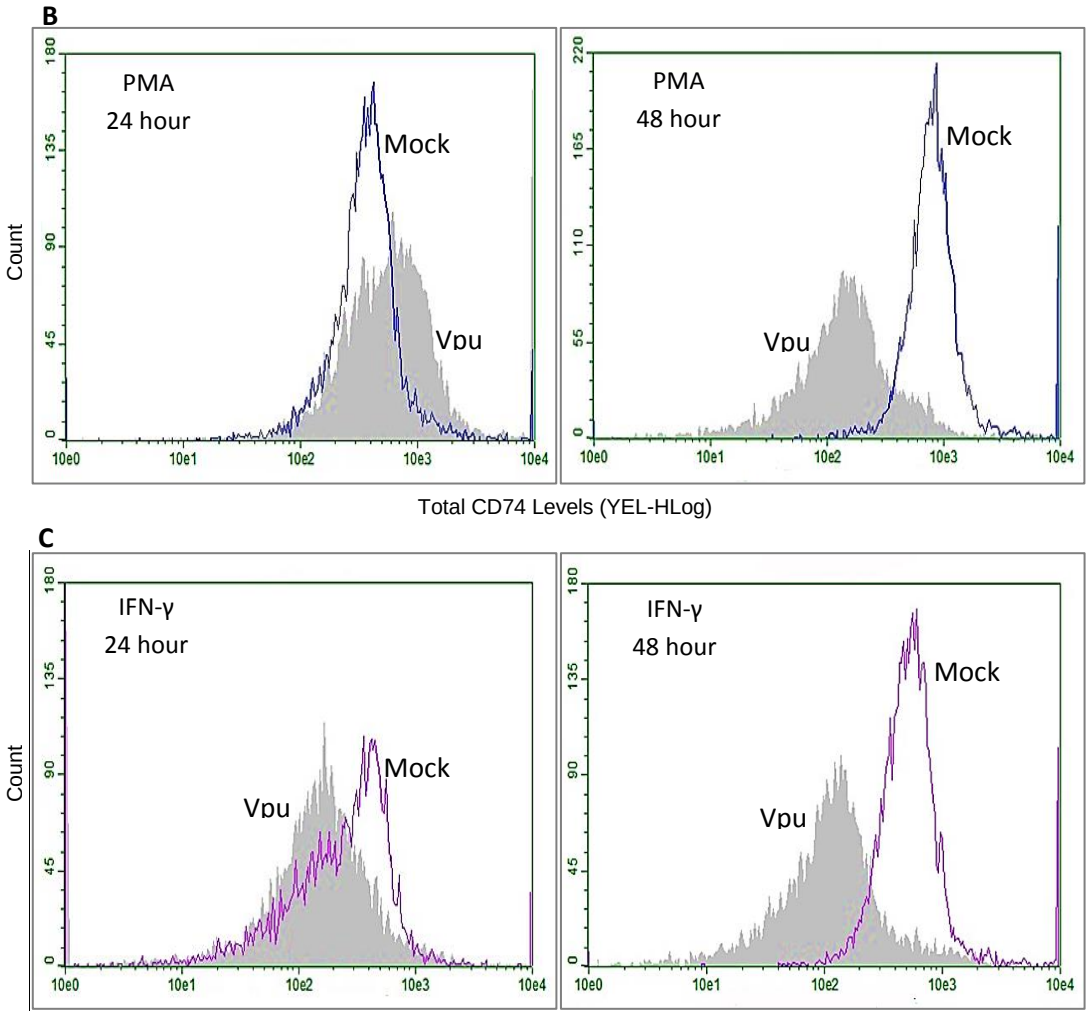
Figure 3.24: Effect of Vpu on MHCII levels in A) control, B) PMA-treated and C) IFN-γ-treated U937 cells at 24 hours but not 48 hours. Green fluorescence counts indicating MHCII levels for control, PMA-treated and IFN-γ-treated, mock-transfected cells (pink) and Vpu-transfected cells (grey) cells after 24 hours and 48 hours post-transfection and staining for GFP. The cell count is indicated on the y-axis while CD4 levels are indicated on the x-axis.

Table 3.2: Average fluorescence counts (± SD) are indicated for total MHCII levels in U937 cells that were either mock-transfected or Vpu-transfected. Statistically significant differences are indicated by *p* values in bold red.

		Average	Standard Deviation	*p* Value
24 hours	**Control Mock**	558.46	166.70	**0.0156**
	Control Vpu	330.65	86.98	
	PMA Mock	528.41	112.02	**0.0032**
	PMA Vpu	304.85	52.02	
	IFN-γ Mock	440.29	40.16	**0.0004**
	IFN-γ Vpu	232.13	77.39	
48 hours	**Control Mock**	371.98	65.68	0.4470
	Control Vpu	431.96	158.10	
	PMA Mock	377.87	52.74	0.6184
	PMA Vpu	355.63	90.67	
	IFN-γ Mock	380.05	72.25	0.6630
	IFN-γ Vpu	351.73	141.75	

The binding of CD74 and Vpu via their cytoplasmic domains as well as the similarities between CD4 and CD74 suggest that this human protein is downregulated and/or degraded in the presence of HIV-1 Vpu. This was indicated previously in Figure 3.22 and subsequently confirmed using flow cytometry. The three different sets of U937 cells - control, PMA-treated and IFN-γ-treated – were either mock-transfected with no plasmid or transfected with 10 µg of pVpu::GFP and analysed for total CD74 levels both at 24 hours and 48 hours post transfection. When cells were left untreated prior to transfection (Figure 3.25A; control), a significant decrease in total CD74 levels was found at 24 hours post transfection in the presence of Vpu compared to mock-transfected cells (p = 0.0270), as well as at 48 hours post transfection (p = 0.0062). However, after PMA-activation of cells prior to transfection (Figure 3.25B) and IFN-γ-activation of cells prior to transfection (Figure 3.25C), no significant decrease in CD74 was seen at 24 hours post transfection (p = 0.1592 and 0.0990, respectively) but 48 hours post transfection yielded a significant decrease in total CD74 levels (p = 0.0236 and 0.0000, respectively). A summary of the statistical data for six replicates of each condition is indicated in Table 3.3 for CD74 levels.



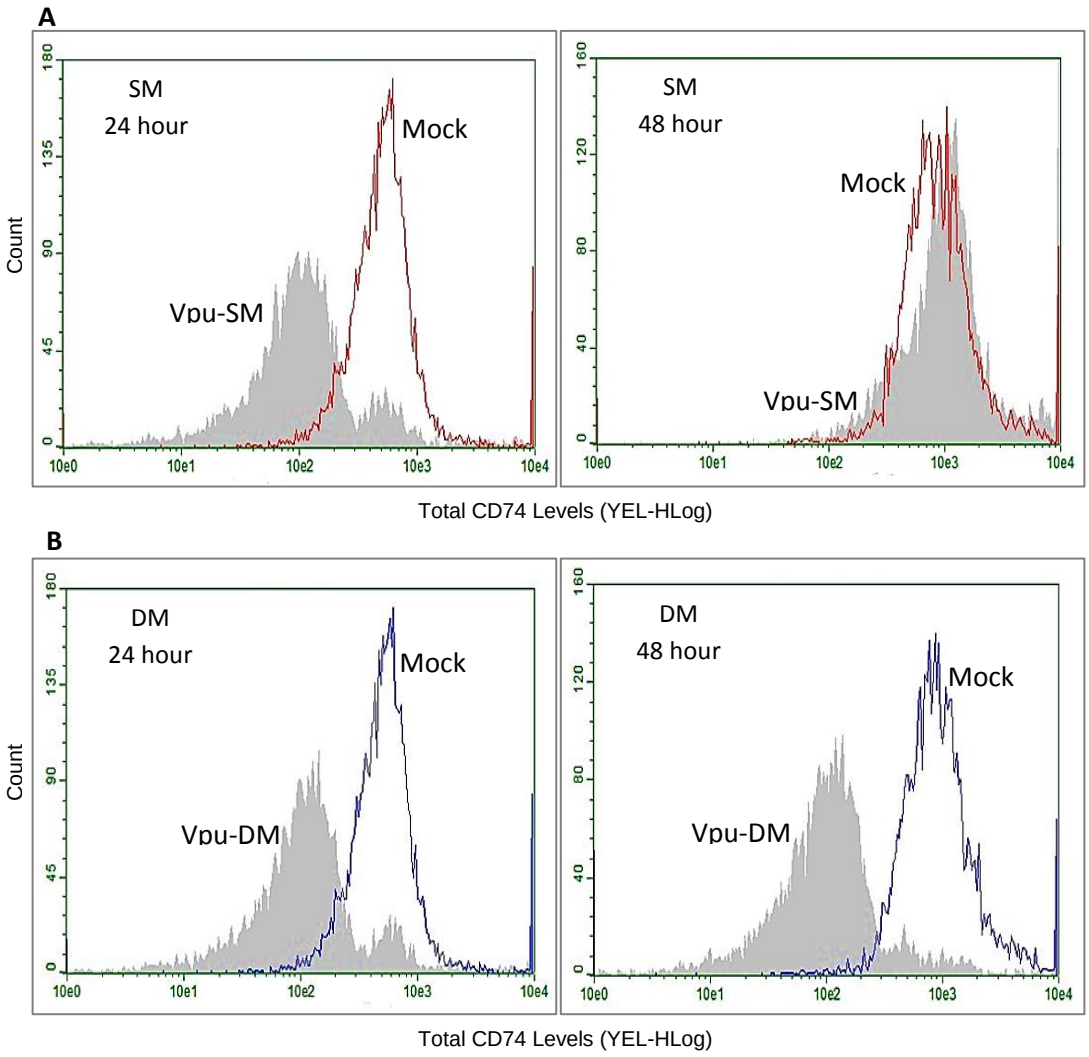


<u>Figure 3.25:</u> Effect of Vpu on CD74 levels in A) control, B) PMA-treated and C) IFN-γ-treated U937 cells. Yellow fluorescence counts indicating CD74 levels for control (pink), PMA-treated (blue) and IFN-γ-treated (purple) mock-transfected cells compared to Vpu-transfected cells (grey) cells after 24 hours and 48 hours post-transfection and staining with a PE-labelled antibody. The cell count is indicated on the y-axis while CD4 levels are indicated on the x-axis.

Table 3.3: Average fluorescence counts (± SD) are indicated for total CD74 levels in U937 cells that were either mock-transfected or Vpu-transfected. Statistically significant differences are indicated by *p* values in bold red.

		Average	Standard Deviation	*p* Value
24 hour	**Control Mock**	765.96	221.72	**0.0270**
	Control Vpu	443.47	210.27	
	PMA Mock	665.81	232.01	0.1592
	PMA Vpu	413.90	328.58	
	IFN-γ Mock	601.85	258.80	0.0990
	IFN-γ Vpu	375.97	147.35	
48 hour	**Control Mock**	1109.68	247.12	**0.0062**
	Control Vpu	684.69	189.46	
	PMA Mock	953.97	245.49	**0.0236**
	PMA Vpu	586.14	233.02	
	IFN-γ Mock	875.17	109.85	**0.0000**
	IFN-γ Vpu	439.83	128.47	

As previously mentioned, Vpu requires two phosphorylated serine residues in order to recruit the E3 ligase complex and target CD4 for proteasomal degradation (Margottin *et al.*, 1998; Nomaguchi *et al.*, 2008; reviewed in Andrew and Strebel, 2010). In order to determine if CD74 may also be degraded via the proteasome, CD74 levels were measured in U937 cells after transfection with two Vpu phosphorylation mutants, pVpu-SM or pVpu-DM and analysed for total CD74 levels both 24 hours and 48 hours post-transfection (Figure 3.26, Table 3.4). A significant decrease in total CD74 levels was seen at 24 hours post-transfection for both Vpu-SM and Vpu-DM compared to mock-transfected cells (p = 0.0088 and 0.0120, respectively). At 48 hours post-transfection, a difference was seen between the Vpu-SM and Vpu-DM mutants. At this time point, Vpu-SM yielded no significant downregulation of CD74 compared to mock-transfected cells (p = 0.3358), while Vpu-DM caused a significant downregulation of CD74 (p = 0.0002).



<u>Figure 3.26:</u> CD74 is downregulated by A) Vpu-SM in U937 cells at 24 hours and is downregulated by B) Vpu-DM at both 24 and 48 hours. Yellow fluorescence counts indicating CD74 levels for mock-transfected cells (Vpu-SM – red; Vpu-DM – blue) and pVpu-SM/DM-transfected cells (grey) cells after 24 hours and 48 hours post-transfection and staining with a PE-labelled antibody. The cell count is indicated on the y-axis while CD4 levels are indicated on the x-axis.

Table 3.4: Average fluorescence counts (± SD) are indicated for total CD74 levels in U937 cells that were either mock-transfected or Vpu-transfected with the Vpu single (SM) and double (DM) phosphorylation mutants. Statistically significant differences are indicated by p values in bold red.

		Average	Standard Deviation	*p* Value
24 hour	**Mock**	765.96	221.72	**0.0088**
	Vpu-SM	400.95	98.12	
	Mock	765.96	221.72	**0.0120**
	Vpu-DM	422.83	131.63	
48 hour	**Mock**	1109.68	247.12	0.3358
	Vpu-SM	1281.75	312.53	
	Mock	1109.68	247.12	**0.0002**
	Vpu-DM	269.56	65.55	

CHAPTER FOUR: DISCUSSION

The HIV-1 Vpu accessory protein is actively involved in the establishment of infective persistence as it is able to connect viral and host cellular proteins to cellular pathways, as well as regulate these pathways through protein-protein interactions in order to promote viral replication (Willey *et al.*, 1992a). As previously mentioned, individuals infected with HIV (or SIV) isolates that do not express a functional Vpu protein exhibit less severe disease outcomes (Leligdowicz and Rowland-Jones, 2008). Within this study, the residues involved in the Vpu/CD74 interaction are described for the first time, and it is demonstrated that Vpu targets intracellular CD74 for downregulation, which occurs at a cellular location where other viral proteins possibly do not, i.e. the ER. Finally, it was found that Vpu does not target CD74 for proteasomal degradation involving the phosphorylated serine residues and the recruitment of β-TrCP.

4.1 CD4 and CD74 are structurally similar

Similarities between CD4 and CD74 highlighted in section 1.6 implied that these proteins have the same fate after interacting with HIV-1 Vpu. The *in silico* comparisons and modelling conducted in this study also indicated structural similarities between the cytoplasmic domains of these two proteins. Both of these proteins have a combination of unstructured regions and α-helices in their cytoplasmic domains, with the hydrophobic residues clustered to one side of the helix (Figures 3.1 and 3.2). Furthermore, the hydropathy was calculated using the Kyte and Doolittle hydropathy scale (Kyte and Doolittle, 1982). As expected, the average hydropathy of the CD4 and CD74 cytoplasmic domains calculated using this scale indicate that these peptides are largely hydrophilic which is indicative of the cytoplasmic environment in which they are found.

The structures of the transmembrane and cytoplasmic domains of a cysteine-free CD4 mutant have been determined by NMR in DPC micelles (Wittlich *et al.*, 2010). Of particular interest to this study is the CD4 cytoplasmic domain which contains a single α-helix consisting of 10 residues (403 to 413), with the remaining sections being mostly unstructured (Wittlich *et al.*, 2010). To date the only structures for CD74 that have been reported and are available on the PDB include the CLIP fragment, the trimeric ectodomain as well as the p41 fragment

(Jasanoff *et al.*, 1998; Guncar *et al.*, 1999; Schlundt *et al.*, 2012). While the structure of the CD74 cytoplasmic domain has been determined in aqueous solution using NMR (Motta *et al.*, 1995), this has not been deposited on the PDB and no crystal structure of the N-terminal cytoplasmic domain has been obtained as yet. Therefore no co-ordinates were available for use within this study. The primary sequence was used to create the CD74 cytoplasmic domain model. The NMR analysis of the CD74 cytoplasmic domain indicated an α-helix from Gln4 to Leu14 (Motta *et al.*, 1995) of the shorter p33 CD74 isoform. However, the longer p35 isoform was used to predict the models as shown in Figures 3.2 and 3.5A. The p35 isoform has additional residues at the N-terminus compared to the p33 isoform (Warmerdam *et al.*, 1996) and this may cause a shift of the position of the α-helix from Gln4-Leu14 to Gln13-Leu23. This largely overlaps with the predicted α-helix as shown in Figures 3.2 and 3.5, which consist of the residues Met17-Asn26. It is also possible that the prediction of the α-helix based on primary sequence alone would introduce some inaccuracies, as the average accuracy of methods that are used to predict protein secondary structure from the primary sequence is reported to be 80 % (King and Sternberg, 1996; Rost, 2001; Li *et al.*, 2014).

Although primary sequence alignment indicated nominal identity and approximately half similarity between the CD4 and CD74 cytoplasmic domains (Figure 3.4), the modelling of the CD74 cytoplasmic domain onto a template of the CD4 cytoplasmic peptide with the exclusion of the transmembrane portion of CD4 (Figure 3.5A) indicated that from a structural standpoint, these regions are similar. A Ramachandran plot indicated that none of the modelled residues were found to be conformationally constrained (Figure 3.5B) suggesting that the Φ and Ψ angles of the residues in this model are indeed possible. It has previously been shown that the region spanning residues 402 to 420 within the CD4 cytoplasmic domain is necessary for the binding to Vpu and the Vpu-mediated degradation of CD4 (Chen *et al.*, 1993; Bour *et al.*, 1995). This region contains an α-helix indicated in Figures 3.1 and 3.5A. In view of this and taking into account that CD74 may also be downregulated and degraded through Vpu binding, the predicted α-helix of the CD74 cytoplasmic domain was aligned to an α-helix of the CD4 cytoplasmic domain. The aligned helices were shown to have a greater degree of similarity than that of the model in which the disordered/unstructured

regions were included in the alignment (Figure 3.5A compared to 3.5C). The disordered/unstructured regions would be more flexible than the structured regions, leading to an increased RMSD and may lead to an inaccuracy in terms of assessing either the similarity or dissimilarity between these proteins. The close similarity in the Vpu-binding site of CD4 (Chen *et al.*, 1993; Tiganos *et al.*, 1997) to an α-helix in CD74 suggests that the CD74 α-helix may also be important for Vpu binding, as the α-helices may provide an interface for the protein-protein interaction. Such structural similarities between CD4 and CD74 lends to the notion that the binding of Vpu to CD74 yields similar downstream consequences to that of CD4, such as the degradation of the host protein.

4.2 CD4 and CD74 bind to different sequences within a closely related region on Vpu

Both CD4 and CD74 are known to interact with Vpu via their cytoplasmic domains. This has been indicated in previous reports (Willey *et al.*, 1994; Tiganos *et al.*, 1997; Hussain *et al.*, 2008) as well as within this study (Figures 3.10 and 3.11). The structural similarity between these two host proteins suggests that they bind to Vpu within a closely related region. Previous reports found that 40 % of a group of individuals in the early stages of HIV infection had antibodies that recognized an 18-residue peptide in the cytoplasmic domain of Vpu, with the sequence VEMGVEMGHHAPWDVDDL. This suggests that this region of Vpu represents an immunodominant domain (Schneider *et al.*, 1990). Following this, Bour *et al.* (1995) were unable to immunoprecipitate Vpu/CD4 complexes with the use of Vpu antisera demonstrating that the binding of CD4 to this particular region of Vpu prevents the binding of the Vpu antibody. It is then possible that this is the specific region associated with CD4 binding. An analogous finding to this is shown in Figure 3.12 in which the binding of the CD74 cytoplasmic peptide to a Vpu::GFP fusion protein significantly reduced the response, and effectively prevented the binding of the anti-Vpu antibody with an IC_{50} of 262.01 nM (Figure 3.13), but was unable to reduce the response when using an anti-GFP antibody. This finding further indicates a similarity between the cytoplasmic domains of CD4 and CD74, as both CD4 and CD74 are able to prevent the binding of anti-Vpu antibodies to Vpu.

In addition to the sequence mentioned above (Schneider *et al.*, 1990), it was found that residues 28-47 (IEYRKILRQRKIDRLIDRIR) and 76-81 (WDVDDL) in

the cytoplasmic domain of Vpu are needed in order to bind CD4 (Margottin *et al.*, 1996). Furthermore, the binding of an antibody directed against a Vpu cytoplasmic peptide with the sequence HAPWDVDDL was masked through the binding of CD4 to Vpu (Tiganos *et al.*, 1997). In addition to these binding sites, two conserved residues, namely Leu63 and Val68 were found to be vital for the Vpu-mediated degradation of CD4 (Hill *et al.*, 2010). These two residues lie within the second α-helix in the Vpu cytoplasmic domain (reviewed in Andrew and Strebel, 2010). Finally, CSP analysis indicated that residues in both Vpu cytoplasmic α-helices are involved in binding CD4 (Singh *et al.*, 2012), which corroborates the finding by Margottin *et al.* (1996).

Analysis of a Vpu overlapping peptide set indicated only two responsive peptides with both subtype B as well as subtype C anti-Vpu antibodies (Figure 3.15 A and B, respectively), suggesting that these peptides contain the immunodominant or antigenic regions for these particular antibodies. The use of an overlapping peptide set of the CD74 cytoplasmic domain in combination with the overlapping Vpu peptide set indicated that the specific CD74 binding site corresponds to the Vpu peptide with the sequence RIRERAEDSGNESEG (Figure 3.16) which is a region that lies between the two abovementioned CD4 binding sites. This binding site contains a 12-residue conserved region within the cytoplasmic domain of Vpu namely, ERAEDSGNESEG (Chen *et al.*, 1993) which forms part of the linker region. This region holds the two conserved phosphorylated serine residues that are required for the binding of β-TrCP and ultimately E3 ligase complex recruitment for proteasomal degradation (Margottin *et al.*, 1998; Nomaguchi *et al.*, 2008; reviewed in Andrew and Strebel, 2010). Further to this, the CD74 cytoplasmic peptide did not bind to the second CD4-binding site at the C-terminus of Vpu (Figure 3.17), while the CD4 cytoplasmic peptide was confirmed to bind to the Vpu C-terminal overlapping peptides (Figure 3.18), corroborating the abovementioned binding site. While it has been confirmed previously that the cytoplasmic domains are involved in the binding interaction between Vpu and CD74 (Hussain *et al.*, 2008), delineation of the novel binding site has not been shown before. However, it must be noted that other potential CD74 binding sites could exist as the antigenic region that is recognized by this particular antibody restricts this particular binding site determination. In other words, the unresponsiveness of the other overlapping Vpu peptides to this particular

antibody prevents the delineation of any other residues that are involved in CD74 binding. Also, it should be considered that the secondary structure of each individual peptide may differ from the overall secondary structure of the native Vpu cytoplasmic domain as a whole and that the solubility of each individual overlapping peptide may also influence the data obtained.

In addition to the differences in specific binding sites mentioned above, the cytoplasmic domains of CD74 and CD4 induced different responses with regard to binding the responsive Vpu peptides with both the subtype B and subtype C antibodies (Figure 3.19). With the subtype B anti-Vpu antibody, peptides 10 and 13 were responsive while with the subtype C anti-Vpu antibody, peptides 10 and 11 were responsive. This shift in responsive peptide may be due to the presence of an additional 2-5 amino acids at the N-terminus of subtype C Vpu compared to subtype B Vpu (Hussain *et al.*, 2007). The addition of the CD74 cytoplasmic peptide yielded lower responses as the presence of this peptide prevented the binding of both antibodies by binding to the same antigenic sites. In contrast, the addition of the CD4 cytoplasmic peptide induced higher responses suggesting that the binding of CD4 to Vpu causes a conformational change in the Vpu peptides, making them more likely to bind the antibody. In agreement with the abovementioned findings that detailed the Vpu cytoplasmic residues that are involved in CD4 binding, there was only a significant difference in response with Vpu peptides 10 (ILRQRKIDRLIDRIR) and 11 (RKIDRLIDRIRERAE), but not with peptide 13 (RIRERAEDSGNESEG) with the addition of the CD4 cytoplasmic peptide. Despite this lack of difference in response with peptide 13, CD4 still does bind to this peptide (Figure 3.20). It is possible that CD4 only induces a difference in response with peptides 10 and 11 as these peptides are more important in the binding interaction between Vpu and CD4, and as already stated, the addition of CD4 may induce conformational changes in the Vpu peptides allowing for better binding of the antibodies. This is because in a natural setting, the conformational state of Vpu may be altered by the interaction with other proteins (Kukol and Arkin, 1999; Lemaitre *et al.*, 2006; Wittlich *et al.*, 2009; reviewed in Andrew and Strebel, 2010). The different responses seen with CD4 and CD74 binding (Figure 3.19) would also suggest that these proteins do not bind to the same sequences within the Vpu cytoplasmic domain. It is interesting to note that although the specific binding sites mentioned above for CD4 and CD74 do indeed differ, both

CD4 and CD74 bind to these same three Vpu peptides. This indicates that, as with CD4, there is more than one binding site for CD74 within the Vpu cytoplasmic domain.

Although the CD4 and CD74 cytoplasmic peptides were shown to compete with each other for binding to Vpu (Figure 3.14), the exact binding site sequences on Vpu for these two proteins do indeed differ (Figures 3.17 to 3.19). When CD74 is bound to Vpu, either the CD4 binding site may be masked or steric hindrance may prevent both host proteins from binding simultaneously. In other words, both CD4 and CD74 are known to interact with Vpu via the cytoplasmic domains of each protein, and while the binding sites for these proteins may overlap, they are distinct from each other in terms of primary Vpu sequence.

Another factor that plays a role in the binding interactions is steric hindrance. While single 10- or 15-mer CD74 peptides were unable to inhibit the antibody from binding the full Vpu protein (Figure 3.21), combinations as few as two peptides were able to abrogate the response indicating that while not all residues are involved in the binding interaction, those residues that are involved may be blocked by larger peptides. This could also explain the steric hindrance between CD4 and CD74 (Figure 3.14) and indicates how these proteins are able to compete for binding to Vpu despite the differences in their binding sites.

Overall, while there may be differences in the exact binding regions between CD4 and CD74, there is enough similarity between these two host proteins and their interaction with HIV-1 Vpu to suggest that the downstream consequences of these protein interactions may be similar.

4.3 Vpu mediates CD74 downregulation

While knowledge of the exact binding site between Vpu and CD74 is beneficial, it is also important to understand the reasons why this interaction takes place. Although Vpu does not work alone, it is possibly one of the principal HIV-1 proteins for immune evasion that has afforded the virus the ability to develop a more severe disease outcome compared to those strains lacking a functional Vpu protein. One of the mechanisms by which Vpu contributes to immune impairment is the downregulation and degradation of CD4, which has been described in

detail (Fujita *et al.*, 1997; Schubert *et al.*, 1998; Hill *et al.*, 2010; Magadan *et al.*, 2010). The Vpu-mediated downregulation of CD4 has been corroborated within this study in untreated U937 cells (Figure 3.23, Table 3.1) – that were selected for these studies as they constitutively express both CD4 (Pelchen-Matthews *et al.*, 1998) and CD74 (Zhou *et al.*, 2011) – as determined by flow cytometry (Figure 3.23). This downregulation occurs within 24 hours post-transfection.

The downregulation of MHCII through the interaction of Vpu with CD74 has also been previously reported (Hussain *et al.*, 2008). Similar to that of CD4, this observation was also corroborated within this study (Figure 3.24). In this study, U937 cells were left untreated or treated with either PMA or IFN-γ 24 hours prior to transfection in order to determine if these factors also influence the levels of MHCII in both the presence and absence of Vpu. Total MHCII levels, including both intracellular and cell surface molecules, were significantly downregulated in the presence of Vpu regardless of the pre-treatment of the cells, and this was seen only at 24 hours post-transfection. This is contrary to what has been reported by another research group. Hussain and co-workers showed that MHCII levels were significantly downregulated in Vpu-transfected U937 cells at 24 hours at the cell surface only, while total MHCII levels that included intracellular molecules remained relatively unchanged by Vpu at this time point (Hussain *et al.*, 2008). The difference between previously reported findings and those presented in this study may be due to the use of different subtypes of Vpu. Although the details of the Vpu plasmid and the method of transfection used are not specified for the flow cytometry analyses, it would seem that Hussain and co-workers made use of subtype C Vpu as this subtype was used for other work within that particular study (Hussain *et al.*, 2008), while subtype B Vpu was used within this study. Subtype B has been reported to localize mostly at intracellular membranes while subtype C is more commonly found at the plasma membrane (Bell, 2009; reviewed in Dubé *et al.*, 2010a). It is possible that the different localization of these two subtypes may influence MHCII molecules within different compartments at different times during the infection cycle. Another possibility is that MHCII in U937 cells could be more concentrated at the cell surface and the inclusion of intracellular MHCII levels in the analysis may have had an insignificant effect. MHCII levels at 48 hours post-transfection were statistically similar between mock-transfected and Vpu-transfected cells (Table 3.2). It is

possible that the transient expression of Vpu in these cells may be reduced while normal protein expression would continue thus accounting for a natural increase in MHCII levels.

The differential pre-treatment of cells yielded little to no variation in results on closer inspection of the mock-transfected cells, both at 24 and at 48 hours post-transfection. The effects of both PMA and IFN-γ on U937 cells have been reported before (Celada and Maki, 1991; De Lerma Barbaro *et al.*, 2005; Tosi *et al.*, 2002). However these reports indicate conflicting data regarding the effect of PMA on the expression of MHCII levels within U937 cells. Celada and Maki reported that the MHCII I-A beta gene was not stimulated in macrophages by the treatment of PMA but was upregulated by IFN-γ (Celada and Maki, 1991), while Tosi *et al.* (2002) found that the PMA-treatment of U937 cells resulted in the differentiation of these cells to a macrophage-like phenotype and led to an increase in the levels and phosphorylation of the class II transactivator (CIITA). This ultimately causes an increase in the expression of MHCII molecules as CIITA is responsible for the regulation of MHCII expression (Tosi *et al.*, 2002). Contrary to this, in a later study it was shown that CIITA and MHCII expression, in particular the HLA-DR molecule, is decreased in U937 cells after treatment with PMA, while IFN-γ did not have any effect on the levels of MHCII (De Lerma Barbaro *et al.*, 2005). The difference between these two studies may be due to the different time points at which the levels of CIITA and MHCII were measured, as well as the different concentrations of PMA used. Within this thesis, U937 cells were treated with either PMA or IFN-γ for 24 hours before transfection and the activators were washed off. This may explain why no difference was seen in MHCII levels between untreated, PMA-treated and IFN-γ-treated cells (Table 3.2). Perhaps, if cells had been treated for longer periods, differences in the MHCII levels may have been detected. Hussain *et al.* showed a decrease in MHCII in the presence of Vpu after the activation of U937 cells with 10 ng/µl of PMA (Hussain *et al.*, 2008) and within this study, the cells were treated with double that concentration. However, it is possible that neither of these particular concentrations were sufficient to mediate an effect on MHCII expression. Future work may evaluate this more thoroughly.

The downregulation of MHCII occurs through the binding of Vpu to CD74 before the mature MHCII complex can reach the cell surface. It is possible that this occurs through the downregulation of CD74 itself, as this would prevent the maturation and peptide loading of MHCII. Within this study, we confirm the novel finding that CD74 is indeed downregulated through its interaction with HIV-1 Vpu and this occurs within a 24 hour time frame. This downregulation was indicated both via immunoprecipitation (Figure 3.22) as well as flow cytometry (Figure 3.25; Table 3.3). Statistical replicates indicated that CD74 levels were significantly reduced after Vpu transfection in untreated U937 cells only, but not in cells that were pre-treated with PMA or IFN-γ. The effect of PMA on MHC has been discussed above and while PMA was unable to induce the expression of CD74 mRNA in keratinocytes (Freeman *et al.*, 1998), it is not clear if PMA would have any effect on CD74 expression in U937 cells. Perhaps by halting MHCII expression through PMA treatment, total CD74 levels may increase rapidly as this protein would then not be incorporated into newly formed mature MHCII complexes, thereby overcoming downregulation via Vpu. However, there did not appear to be any notable difference in CD74 levels between untreated cells, PMA-treated cells and IFN-γ-treated cells in the mock-transfected samples (Table 3.3). Despite this, it is possible that both PMA and IFN-γ have some effect on CD74 expression at 24 hours post-transfection. These treated cells were able to maintain CD74 levels consistent with those in mock-transfected cells, indicating that CD74 expression was high enough to overcome Vpu-mediated downregulation. At 48 hours post-transfection, all three sample types displayed a significant decrease in total CD74 levels. Possibly, at this time point the effect of the activators has been overcome and progeny cells may be expressing normal levels of CD74, which is then decreased in the presence of Vpu.

While this specific data does not indicate CD74 degradation, it does indicate that total CD74 levels were downregulated in the presence of Vpu as whole cell lysate was used for immunoprecipitation, and cells were permeabilized prior to staining for flow cytometry, allowing for the measurement of total CD74 protein regardless of cellular location. Contrary to this, Hussain and co-workers indicated no significant decrease in cell surface CD74 levels in Vpu-EGFP-transfected U937 cells 24 hours post-transfection (Hussain *et al.*, 2008) and this has been attributed to the retention of CD74 within intracellular compartments (Patel *et al.*,

2014). Within this work, total CD74 levels including surface and intracellular fractions were measured. It is possible that if the total levels of CD74 had been measured after transfection, as opposed to the cell surface levels only, within the Hussain study (Hussain *et al.*, 2008), a difference in CD74 levels may have been seen. By investigating surface CD74 only, it is possible that Hussain and co-workers were only analysing one or two of the CD74 isoforms. The p35 isoform has an ER retention signal within the cytoplasmic tail (Warmerdam *et al.*, 1996; reviewed in Michelsen *et al.*, 2005). Therefore this CD74 isoform may not have been included in the analysis. Another contemplation is that there may be a difference in the concentration of Vpu used to transfect the cells between the two studies. More efficient expression, or a greater concentration of Vpu present in the cells would lead to a more pronounced effect on the CD74 host protein. Finally, as with MHCII above, the difference in the reported results may be due to the use of different subtypes of Vpu.

Analysis of total CD74 levels in cells expressing either of two Vpu phosphorylation mutants (Vpu-SM and Vpu-DM, respectively) resulted in CD74 downregulation at 24 hours (Figure 3.26; Table 3.4). This suggests that Vpu does not mediate the proteasomal degradation of CD74 via the recruitment of β-TrCP, as both phosphorylated serines have been reported to be needed for the binding of β-TrCP in order to recruit the E3 ligase complex (Bour *et al.*, 1995; Paul and Jabbar, 1997). However, it is still possible that Vpu mediates CD74 degradation through the ERAD pathway, as this viral protein has been reported to target both CD4 (Magadan *et al.*, 2010) and tetherin (Mangeat *et al.*, 2009) via ERAD in addition to β-TrCP-dependent degradation. A further consideration is that Vpu may be capable of downregulating CD74 through altering CD74 gene expression. Vpu has recently been observed to impede NF-κB-related antiviral gene expression (Sauter et al., 2015). Vpu mutants lacking both the phosphorylated serines at position 52 and 56 were equally capable of downregulating antiviral gene expression (Sauter et al., 2015), indicating that the phosphorylated serines are not required for this function. At 48 hours post-transfection, CD74 levels are downregulated significantly by the double phosphorylation mutant (Vpu-DM), but not by the single mutant (Vpu-SM), in which total CD74 levels were statistically equivalent to the mock-transfected cells (Table 3.4). This difference in CD74 levels between the 24 hour and 48 hour Vpu-SM-transfected samples may be

due to the degradation of the Vpu-SM protein at 48 hours post-transfection. As mentioned previously, Vpu itself undergoes proteasomal degradation due to the phosphorylation of the serine residue at position 61 (Estrabaud *et al.*, 2007). Vpu proteins that have a mutation at both Ser52 and Ser56 are not degraded in this way, indicating that these two conserved residues are required for Vpu ubiquitination and degradation, along with the phosphorylated Ser61 residue (Belaïdouni *et al.*, 2007; Estrabaud *et al.*, 2007). However, Vpu proteins containing a mutation of only one of the phosphorylated serines were not analysed for degradation during these studies (Belaïdouni *et al.*, 2007; Estrabaud *et al.*, 2007) and it is possible that the presence of a phosphorylated serine at position 56 and at 61 in combination allows for the recognition of Vpu as a target protein for degradation. The single mutant (Vpu-SM) used in this study only had Ser52 replaced with alanine, but still contained Ser56. It is possible that this mutant became phosphorylated at Ser61 and had been degraded by the 48 hour time point. This would allow for normal CD74 expression to resume.

Although Hussain and co-workers also demonstrated reduced levels of MHCII and no reduction in CD74 levels in virus-infected cells (Hussain *et al.*, 2008), this data is incomparable to the work presented here as there are additional HIV-1 viral proteins that are involved in the downregulation of MHCII and that are reported to interact with CD74. These include the Nef accessory protein and the gp41 protein. HIV-1 Nef interferes with both CD74 and MHCII as it downmodulates MHCII by increasing CD74 at the cell surface, and by upregulating cell surface expression of immature MHCII. Nef is also capable of decreasing the surface levels of mature, peptide-loaded MHCII (Stumptner-Cuvelette *et al.*, 2001; reviewed in Kirchhoff, 2010; Ghiglione *et al.*, 2012). HIV-1 gp41 has also been shown to interact with cell surface CD74 early in infection, causing the modulation of the ERK/MAPK pathway in order to enhance viral infections (Zhou *et al.*, 2011). The interaction of these other viral proteins with CD74 and the effect that this would have on MHCII production may have influenced the data obtained from virus-infected cells.

4.4 Further considerations

While the present study gives insight not only to the specific binding interaction between Vpu and CD74, but also to the downstream consequences of this

interaction, there are further aspects that could be considered in future studies. This study could be repeated in a different cell line to determine if the same data would be generated. An NMR structure for CD74 has previously been described (Motta *et al.*, 1995) but no three dimensional crystal structures have as yet been uploaded on the PDB for the cytoplasmic domain in particular. A three dimensional structure of the CD74 cytoplasmic domain with co-ordinates uploaded to the PDB would greatly aid in the investigation of the specific binding site between CD74 and Vpu. This would allow for the "hot spot" residues in the interaction to be identified using *in silico* modelling. In conjunction with this, the specific binding site between Vpu and CD74 could be confirmed using a different technique such as CSP, as previously described for the interaction between Vpu and CD4 (Singh *et al.*, 2012). This would most likely result in a clearer indication of the residues involved in the interaction as this technique also allows for the secondary structure of each protein to be taken into consideration, and this may also influence the binding sites. This particular technique would also allow for the investigation of which residues are involved in binding while using full-length proteins that are correctly folded. Further to this, *in vitro* assays that mimic a membrane environment might also be considered. For example, the inclusion of DPC micelles within the assay would also allow for the correct folding of each peptide. This may be used with the overlapping peptide sets (described in Chapter 2) to overcome the difficulty of possible differences in folding for each small peptide in an aqueous buffer system.

In addition, studies investigating the existence of a Vpu/CD74/β-TrCP ternary complex would complement the work presented here. The discovery of this complex, should it exist, would lend to the description of Vpu-mediated CD74 degradation and would indicate the type of degradation. This is because β-TrCP is involved in the recruitment of the E3 ubiquitin ligase complex through interaction with the Skp1p factor (Margottin *et al.*, 1998). Therefore the existence of the Vpu/CD74/β-TrCP ternary complex would suggest that by binding with Vpu, CD74 becomes ubiquitinated after the recruitment of β-TrCP and the E3 ligase complex. Once ubiquitinated, CD74 would then be degraded via the 26 S proteasome (Tu *et al.*, 2012). This investigation could be taken one step further by the discovery of an ubiquitinated form of CD74 after either infection of cells by HIV-1 or transfection with Vpu. Furthermore, the effects of a proteasome inhibitor,

such as MG132, on the degradation of CD74 could also be investigated. This would serve as a confirmatory assay.

Following the confirmation of the specific binding sites and further delineation of the downregulation or possible degradation of CD74, the inhibition of this interaction should be considered. The information regarding the specific binding site detailed within this study will contribute to the design of drug molecules targeting this interaction. Furthermore, structural details of the binding sites would allow for the design of compounds as potential inhibitors using *in silico* modelling. This would be aided by the knowledge of the three dimensional structure of the CD74 cytoplasmic domain. Once synthesized, these compounds could then be screened using a functional inhibition assay. There is already evidence to support Vpu as a suitable drug target. This is indicated by the BIT225 candidate drug, which was found to block the ion channel activity of Vpu specifically. BIT225 also has been found to have anti-HIV-1 activity within macrophages and has been reported to have very low cell toxicity (Khoury *et al.*, 2010). This candidate drug was discovered through the exploration of amiloride analogues that were capable of inhibiting the flow of ions through the Vpu ion channel (Ewart *et al.*, 2002). BIT225 was shown to be ineffective against HIV-2 which lacks a functional Vpu protein, indicating that the drug target is specific to HIV-1 Vpu (Khoury *et al.*, 2010) and affects the viroporin activity of HIV-1 Vpu without mediating an effect on the Vpu/tetherin interaction (Kuhl *et al.*, 2011). This same approach could be followed for the design and analysis of potential inhibitors of the Vpu/CD74 interaction. Alternatively, inhibitors of the Vpu immunodominant domain indicated within this study could be designed as CD74 binds to this region. Any compound or molecule that prevents the binding of the anti-Vpu antibody would then most likely bind to the same region as CD74.

Finally, once HIT compounds have been found and developed, they could be tested in an animal model in order to investigate the efficacy of these possible drug compounds to determine the modulation, if any, of this disease.

4.5 Concluding remarks

This study undertook the description of the Vpu/CD74 interaction and details the downstream consequences following the binding of these two proteins. Using *in vitro* assays, it was confirmed that CD4 and CD74 compete for binding to Vpu,

despite inducing different responses. This work provides novel information on the definitive protein-protein binding site between HIV-1 Vpu and the host protein CD74. Furthermore, the deleterious effect of HIV-1 Vpu on host cell immunity has been indicated within this study through the novel finding of the Vpu-mediated downregulation of CD74 in U937 cells. However, CD74 is not targeted for degradation in a mechanism similar to that of CD4 through binding HIV-1 Vpu.

CD74 was able to prevent the binding of an anti-Vpu antibody, most likely by binding to an immunodominant domain on Vpu. The binding site between these proteins was identified and the specific residues involved were RIRERAEDSGNESEG and EDQKP within the Vpu and CD74 cytoplasmic domains, respectively. In addition to this, it was shown that steric hindrance may be a determining factor in the binding interaction between these two proteins. Moreover, total CD74 levels in U937 cells were downregulated both at 24 and 48 hours post-transfection with Vpu under normal conditions. Finally, two Vpu phosphorylation mutants were also found to cause downregulation of total CD74 levels at 24 hours under normal conditions, suggesting that Vpu does not mediate the degradation of CD74 through traditional recruitment of the E3 ligase complex.

Considering the wide variety of roles that CD74 plays within a cell, both in cell signalling and in the functioning of the immune system, it is important for this host protein to be able to continue to function. Therefore CD74 is an attractive host target for HIV-1 and inhibition of the interaction between Vpu and CD74 may be disadvantageous for viral persistence. In view of this, the targeting of this particular HIV-1 accessory protein would greatly aid in the modulation of this disease.

REFERENCES

Akari H, Bour S, Kao S, Adachi A and Strebel K. “The human immunodeficiency virus type 1 accessory protein Vpu induces apoptosis by suppressing the nuclear factor κB-dependent expression of antiapoptotic factors.” *Journal of Experimental Medicine* 194 (2001): 1299-1311.

Anderson HA, Bergstralh DT, Kawamura T, Blauvelt A and Roche PA. “Phosphorylation of the invariant chain by protein kinase C regulates MHC class II trafficking to antigen-processing compartments.” *Journal of Immunology* 163 (1999): 5435-5443.

Andrew A and Strebel K. “HIV-1 Vpu targets cell surface markers CD4 and BST-2 through distinct mechanisms.” *Molecular Aspects of Medicine* 31 (2010): 407-417.

Baek YS, Haas S, Hackstein H, Bein G, Hernandez-Santana M, Lehrach H, Sauer S and Seitz H. “Identification of novel transcriptional regulaters involved in macrophage differentiation and activation in U937 cells.” *BMC Immunology* 10 (2009): 18-32.

Banning C, Votteler J, Hoffmann D, Koppensteiner H, Warmer M, Reimer R, Kirchhoff F, Schubert U, Hauber J and Schindler M. “A flow cytometry-based FRET assay to identify and analyse protein-protein interactions in living cells.” *PLoS ONE* 5 (2010): e9344-e9353.

Becker-Herman S, Arie G, Medvedovsky H, Kerem A and Shachar I. “CD74 is a member of the Regulated Intramembrane Proteolysis-processed protein family.” *Molecular Biology of the Cell* 16 (2005): 5061-5069.

Belaidouni N, Marchal C, Benarous R and Besnard-Guerin C. “Involvement of the βTrCP in the ubiquitination and stability of the HIV-1 Vpu protein.” *Biochemical and Biophysical Research Communications* 357 (2007): 688-693.

Bell CM. “Differential timing of translocation of HIV-1 subtype B and C Vpu to the ER/Golgi and plasma membrane compartments.” *MSc Dissertation* Faculty of Health Sciences (2009): University of the Witwatersrand.

Beswick E and Reyes VE. “CD74 in antigen presentation, inflammation, and cancers of the gastrointestinal tract.” *World Journal of Gastroenterology* 15 (2009): 2855-2861.

Beswick EJ, Das S, Pinchuk IV, Adegoboyega P, Suarez G, Yamaoka Y and Reyes VE. “Helicobacter pylori-induced IL-8 production by gastric epithelial cells upregulates CD74 expression.” *Journal of Immunology* 175 (2005): 171-176.

Binette J, Dube M, Mercier J, Halawani D, Latterich M and Cohen EA. “Requirements for the selective degradation of CD4 receptor molecules by the human immunodeficiency virus type I Vpu protein in the endoplasmic reticulum.” *Retrovirology* 4 (2007): 75-89.

Blagoveshchenskaya AD, Thomas L, Feliciangeli SF, Hung CH and Thomas G. “HIV-1 Nef downregulates MHC-I by a PACS-1- and PI3K-regulated ARF6 endocytic pathway.” *Cell* 111 (2002): 853-866.

Boss JM. “Regulation of transcription of MHC class II genes.” *Current Opinions in Immunology* 9 (1997): 107-113.

Bour S, Perrin C, Akari H and Strebel K. “The human immunodeficiency virus type 1 Vpu protein inhibits NF-κB activation by interfering with βTrCP-mediated degradation of IκB.” *Journal of Biological Chemistry* 276 (2001): 15920-15928.

Bour S, Schubert U and Strebel K. “The human immunodeficiency virus type 1 Vpu protein specifically binds to the cytoplasmic domain of CD4: implications for the mechanism of degradation.” *Journal of Virology* 69 (1995): 1510-1520.

Celada A and Maki RA. “IFN-gamma induces the expression of the genes for MHC class II I-A beta and tumor necrosis factor through a protein kinase C-independent pathway.” *Journal of Immunology* 146 (1991): 114-120.

Chen MY, Maldarelli F, Karczewski MK, Willey RL and Strebel K. “Human immunodeficiency virus type 1 Vpu protein induces degradation of CD4 in vitro: the cytoplasmic domain of CD4 contributes to Vpu sensitivity.” *Journal of Virology* 67 (1993): 3877-3884.

Chun TW and Fauci AS. “Latent reservoirs of HIV: obstacles to the eradication of virus.” *Proceedings of the National Academy of Sciences USA* 96 (1999): 10958-10961.

Claesson L, Larhammar D, Rask L and Peterson PA. “cDNA clone for the human invariant γ chain of class II histocompatibility antigens and its implications for the protein structure.” *Proceedings of the National Academy of Sciences USA* 80 (1983): 7395-7399.

Cresswell P. “Invariant chain structure and MHC class II function.” *Cell* 84 (1996): 505-507.

De Lerma Barbaro A, Procopio FA, Mortara L, Tosi G and Accolla RS. “The MHC class II transactivator (CIITA) mRNA stability is critical for the HLA class II gene expression in myelomonocytic cells.” *European Journal of Immunology - Molecular Immunology* 35 (2005): 603-611.

Dube M, Bego MG, Paquay C and Cohen EA. “Modulation of HIV-1-host interaction: role of the Vpu accessory protein.” *Retrovirology* 7 (2010a): 114-132.

Dube M, Roy BB, Guiot-Guillain P, Binette J, Mercier J, Chiasson A and Cohen EA. “Antagonism of tetherin restriction of HIV-1 release by Vpu involves binding and sequestration of the restriction factor in a perinuclear compartment.” *PLoS Pathogens* 6 (2010b): e1000856-e1000874.

Estrabaud E, Le Rouzic E, Lopez-Verges S, Morel M, Belaidouni N, Benarous R, Transy C, Berlioz-Torrent C and Margottin-Goguet F. “Regulated degradation of the HIV-1 Vpu protein through a β-TrCP-independent pathway limits the release of viral particles.” *PLoS Pathogens* 3 (2007): e104-e113.

Ewart GD, Mills K, Cox GB and Gage PW. “Amiloride derivatives block ion channel activity and enhancement of virus-like particle budding caused by HIV-1 protein Vpu.” *European Biophysics Journal* 31 (2002): 26-35.

Finzi A, Brunet A, Xiao Y, Thibodeau J and Cohen EA. “Major histocompatibility complex class II molecules promote human immunodeficiency virus type 1 assembly and budding to late endosomal/multivesicular body compartments.” *Journal of Virology* 80 (2006): 9789-9797.

Freeman GJ, Cardoso AA, Boussiotis VA, Anumanthan A, Groves RW, Kupper TS, Clark EA and Nadler LM. “The BB1 monoclonal antibody recognizes both cell surface CD74 (MHC class II-associated invariant chain) as well as B7-1 (CD80), resolving the question regarding a third CD28/CTLA-4 counterreceptor.” *Journal of Immunology* 161 (1998): 2709-2715.

Froger A and Hall JE. “Transformation of plasmid DNA into E. coli using the heat shock method.” *Journal of Visualised Experiments* 6 (2007): e253.

Fujita K, Omura S and Silver J. “Rapid degradation of CD4 in cells expressing human immunodeficiency virus type 1 Env and Vpu is blocked by proteasome inhibitors.” *Journal of General Virology* 78 (1997): 619-625.

Ghiglione Y, Rodriguez AM, De Candia C, Carobene M, Benaroch P, Schindler M, Salomon H and Turk G. “HIV-mediated up-regulation of invariant chain (CD74) correlates with generalized immune activation in HIV+ subjects.” *Virus Research* 163 (2012): 380-384.

Guncar G, Pungercic G, Klemencic I, Turk V and Turk D. “Crystal structure of MHC class II-associated p41 Ii fragment bound to cathepsin L reveals the structural basis for differentiation between cathepsins L and S.” *EMBO Journal* 18 (1999): 793-803.

Hill MS, Ruiz A, Schmitt K and Stephens EB. “Identification of amino acids within the second alpha helical domain of the human immunodeficiency virus type 1 Vpu that are critical for preventing CD4 cell surface expression.” *Virology* 397 (2010): 104-112.

Hussain A, Das SR, Tanwar C and Jameel S. “Oligomerization of the human immunodeficiency virus type 1 (HIV-1) Vpu protein - a genetic, biochemical and biophysical analysis.” *Virology Journal* 4 (2007): 81-91.

Hussain A, Wesley C, Khalid M, Chaudhry A and Jameel S. “Human immunodeficiency virus type 1 Vpu protein interacts with CD74 and modulates major histocompatibility complex class II presentation.” *Journal of Virology* 82 (2008): 893-902.

Ishigami S, Natsugoe S, Tokuda K, Nakajo A, Iwashige H, Aridome K, Hokita S and Aikou T. “Invariant chain expression in gastric cancer.” *Cancer letters* 168 (2001): 87-91.

Jasanoff A, Wagner G and Wiley DC. “Structure of a trimeric domain of the MHCII-associated chaperonin and targeting protein Ii.” *EMBO Journal* 17 (1998): 6812-6818.

Kabsch W and Sander C. “Dictionary of protein secondary structure: pattern recognition of hydrogen-bonded and geometrical features.” *Biopolymers* 22 (1983): 2577-2637.

Kang S, Liang L, Parker CD and Collawn JF. “Structural requirements for major histocompatibility complex class II invariant chain endocytosis and lysosomal targeting.” *Journal of Biological Chemistry* 273 (1998): 20644-20652.

Kerkau T, Bacik I, Bennink JR, Yewdell JW, Hunig T, Schimpl A and Schubert U. “The human immunodeficiency virus type 1 (HIV-1) Vpu protein interferes with an early step in the biosynthesis of major histocompatibility complex (MHC) class I molecules.” *Journal of Experimental Medicine* 185 (1997): 1295-1305.

Khoury G, Ewart G, Luscombe C, Miller M and Wilkinson J. “Antiviral efficacy of the novel compound BIT225 against HIV-1 release from human macrophages.” *Antimicrobial Agents and Chemotherapy* 54 (2010): 835-845.

Killar L, MacDonald G, West J, Woods A and Bottomly K. “Cloned, Ia-restricted T cells that do not produce interleukin 4 (IL 4)/B stimulatory factor (BSF-1)

fail to help antigen-specific B cells." *Journal of Immunology* 138 (1987): 1674-1679.

King RD and Sternberg MJE. "Identification and application of the concepts important for accurate and reliable protein secondary structure prediction." *Protein Science* 5 (1996): 2298-2310.

Kirchhoff F. "Immune evasion and counteraction of restriction factors by HIV-1 and other primate lentiviruses." *Cell Host and Microbe* 8 (2010): 55-67.

Komoto S, Tsuji S, Ibrahim MS, Li YG, Warachit J, Taniguchi K and Ikuta K. "The Vpu protein of human immunodeficiency virus type 1 plays a protective role against virus-induced apoptosis in primary CD4+ T lymphocytes." *Journal of Virology* 77 (2003): 10304-10313.

Kraus MH, Parrish NF, Shaw KS, Decker JM, Keele BF, Salazar-Gonzalez JF, Grayson T, McPherson DT, Ping LH, Anderson JA, Swanstrom R, Williamson C, Shaw GM and Hahn BH. "A rev1-vpu polymorphism unique to HIV-1 subtype A and C strains impairs envelope glycoprotein expression from rev-vpu-env cassettes and reduces virion infectivity in pseudotyping assays." *Virology* 397 (2010): 346-357.

Kuhl BD, Cheng V, Donahue DA, Sloan RD, Liang C, Wilkinson J and Wainberg MA. "The HIV-1 Vpu viroporin inhibitor BIT225 does not affect Vpu-mediated tetherin antagonsim." *PLos ONE* 6 (2011): e27660-e27667.

Kukol A and Arkin IT. "Vpu transmembrane peptide structure obtained by site-specific fourier transform infrared dichroism and global molecular dynamics searching." *Biophysical Journal* 77 (1999): 1594-1601.

Kyte J and Doolittle RF. "A simple method for displaying the hydrophobic character of a protein." *Journal of Molecular Biology* 157 (1982): 105-132.

Lantner F, Starlets D, Gore Y, Flaishon L, Yamit-Hezi A, Dikstein R, Leng L, Bucala R, Machluf Y, Oren M and Shachar I. "CD74 induces TAp63 expression leading to B-cell survival." *Blood* 110 (2007): 4303-4311.

Le Noury DA, Mosebi S, Papathanasopoulos MA and Hewer R. “Functional roles of HIV-1 Vpu and CD74: details and implications of the Vpu-CD74 interaction.” *Cellular Immunology*, 2015: Published Ahead of Print.

Leligdowicz A and Rowland-Jones S. “Tenets of protection from progression to AIDS: lessons from the immune responses to HIV-2 infection.” *Expert Review of Vaccines* 7 (2008): 319-331.

Lemaitre V, Willbold D, Watts A and Fischer WB. “Full length Vpu from HIV-1: combining molecular dynamics simulations with NMR spectroscopy.” *Journal of Biomolecular Structure and Dynamics* 23 (2006): 485-496.

Leng L and Bucala R. “Insight into the biology of Macrophage Migration Inhibitory Factor (MIF) revealed by the cloning of its cell surface receptor.” *Cell Research* 16 (2006): 162-168.

Li Q, Dahl DB, Vannicci M, Joo H and Tsai JW. “Bayesian model of protein primary sequence for secondary structure prediction.” *PLos ONE* 9 (2014): e109832-e109843.

Lovell SC, Davis IW, Arendall III WB, de Bakker PIW, Word M, Prisant MG, Richardson JS and Richardson DC. “Structure validation by Cα geometry: Φ, Ψ and Cβ deviation.” *Proteins: Structure, Function and Genetics* 50 (2003): 437-450.

Ma C, Marassi FM, Jones DH, Straus SK, Bour S, Strebel K, Schubert U, Oblatt-Montal M, Montal M and Opella SJ. “Expression, purification and activities of full-length and truncated versions of the integral membrane protein Vpu from HIV-1.” *Protein Science* 11 (2002): 546-557.

Magadan JG, Perez-Victoria FJ, Sougrat R, Ye Y, Strebel K and Bonifacino JS. “Multilayered mechanism of CD4 downregulation by HIV-1 Vpu involving distinct ER retention and ERAD targeting steps.” *PLoS Pathogens* 6 (2010): e1000869-e1000886.

Maldarelli F, Chen M-Y, Willey RL and Strebel K. “Human immunodeficiency virus type 1 Vpu protein is an oligomeric type 1 integral membrane protein.” *Journal of Virology* 67 (1993): 5056-5061.

Mangeat B, Gers-Huber G, Lehmann M, Zufferey M, Luban J and Piguet V. “HIV-1 Vpu neutralizes the antiviral factor Tetherin/BST-2 by binding it and directing its beta-TrCP2-dependent degradation.” *PLoS Pathogens* 5 (2009): e1000574-e1000585.

Marassi FM, Ma C, Gratkowski H, Straus SK, Strebel K, Oblatt-Montal M, Montal M and Opella SJ. “Correlation of the structural and functional domains in the membrane protein Vpu from HIV-1.” *Proceedings of the National Academy of Sciences USA* 96 (1999): 14336-14341.

Margottin F, Benichou S, Durand H, Richard V, Liu LX, Gomas E and Benarous R. “Interaction between the cytoplasmic domains of HIV-1 Vpu and CD4: role of Vpu residues involved in CD4 interaction and in vitro CD4 degradation.” *Virology* 223 (1996): 381-386.

Margottin F, Bour SP, Durand H, Selig L, Benichou S, Richard V, Thomas D, Strebel K and Benarous R. “A novel human WD protein h-βTrCP, that interacts with HIV-1 Vpu connects CD4 to the ER degradation pathway through an F-box motif.” *Molecular Cell* 1 (1998): 565-574.

Martin-Ventura JL, Madrigal-Matute J, Munoz-Garcia B, Blanco-Colio LM, Van Oostrom M, Zalba G, Fortuno A, Gomez-Guerrero C, Ortega L, Ortiz A, Diez J and Egido J. “Increased CD74 expression in human atherosclerotic plaques: contribution to inflammatory responses in vascular cells.” *Cardiovascular Research* 83 (2009): 586-594.

Matza D, Kerem A, Medvedovsky H, Lantner F and Shachar I. “Invariant chain-induced B cell differentiation requires intramembrane proteolytic release of the cytosolic domain.” *Immunity* 17 (2002b): 549-560.

Matza D, Lantner F, Bogoch Y, Flaishon L, Heshkoviz R and Shachar I. “Invariant chain induces B cell maturation in a process that is independent of its chaperone activity.” *Proceeding of the National Academy of Science USA* 99 (2002a): 3018-3023.

Matza D, Wolstein O, Dikstein R and Shachar I. “Invariant chain induces B cell maturation by activating a $TAF_{II}105$-NF-κB-dependent transcription program.” *Journal of Biological Chemistry* 276 (2001): 27203-27206.

Meyer-Siegler KL, Leifheit EC and Vera PL. “Inhibition of macrophage migration inhibitory factor decreases proliferation and cytokine expression in bladder cancer cells.” *BMC Cancer* 4 (2004): 34-45.

Michelsen K, Yuan H and Schwappach B. “Hide and run. Arginine-based endoplasmic-reticulum-sorting motifs in the assembly of heteromultimeric membrane proteins.” *EMBO Reports* 6 (2005): 717-722.

Miller DM and Sedmak DD. “Viral effects on antigen processing.” *Current Opinion in Immunology* 11 (1999): 94-99.

Moll M, Andersson SK, Smed-Sorensen A and Sandberg JK. “Inhibition of lipid antigen presentation in dendritic cells by HIV-1 Vpu interference with CD1d recycling from endosomal compartments.” *Blood* 116 (2010): 1876-1884.

Mosman TR and Coffman RL. “TH1 and TH2 cells: different patterns of lymphokine secretion lead to different functional properties.” *Annual Review of Immunology* 7 (1989): 145-173.

Motta A, Bremnes B, Castiglione Morelli MA, Frank RQ, Saviano G and Bakke O. “Structure-activity relationship of the leucine-based sorting motifs in the cytosolic tail of the major histocompatibility complex-associated invariant chain.” *Journal of Biological Chemistry* 270 (1995): 27165-27171.

Neil SJD, Zang T and Bieniasz PD. “Tetherin inhibits retrovirus release and is antagonized by HIV-1 Vpu.” *Nature* 451 (2008): 425-430.

Nguyen KL, Llano M, Akari H, Miyagi E, Poeschla EM, Strebel K and Bour S. “Codon optimization of the HIV-1 vpu and vif genes stabilizes their mRNA and allows for highly efficient Rev-independent expression.” *Virology* 319 (2004): 163-175.

Nomaguchi M, Fujita M and Adachi A. “Role of HIV-1 Vpu protein for virus spread and pathogenesis.” *Microbes and Infection* 10 (2008): 960-967.

Ono A and Freed EO. “Cell-type-dependent targeting of human immunodeficiency virus type 1 assembly to the plasma membrane and the multivesicular body.” *Journal of Virology* 78 (2004): 1552-1563.

Pacyniak E, Gomez ML, Gomez LM, Mulcahy ER, Jackson M, Hout DR, Wisdom BR and Stephens EB. “Identification of a region within the cytoplasmic domain of the subtype B Vpu protein of human immunodeficiency virus type I (HIV-I) that is responsible for retention in the Golgi complex and its absence in the Vpu protein from a subtype C HIV-I.” *AIDS Research and Human Retroviruses* 21 (2005): 379-394.

Park SH, Mrse AA, Nevzorov AA, Mesleh MF, Oblatt-Montal M, Montal M and Opella SJ. “Three-dimensional structure of the channel-forming transmembrane domain of virus protein "u" (Vpu) from HIV-1.” *Journal of Molecular Biology* 333 (2003): 409-424.

Patel P, Khan N, Rani M, Gupta D and Jameel S. “The expression of HIV-1 Vpu in monocytes causes increased secretion of TGF-B that activates profibrogenic genes in hepatic stellate cells.” *PLos ONE* 9 (2014): e88934-e88943.

Paul M and Jabbar MA. “Phosphorylation of both phosphoacceptor sites in the HIV-1 Vpu cytoplasmic domain is essential for Vpu-mediated ER degradation of CD4.” *Virology* 232 (1997): 207-216.

Paul WE and Seder RA. “Lymphocyte responses and cytokines.” *Cell* 76 (1994): 241-251.

Pelchen-Matthews A, da Silva RP, Bijlmakers MJ, Signoret N, Gordon S and Marsh M. “Lack of p561ck expression correlates with CD4 endocytosis in primary lymphoid and myeloid cells.” *European Journal of Immunology* 28 (1998): 3639-3647.

Pelchen-Matthews A, Kramer B and Marsh M. “Infectious HIV-1 assembles in late endosomes in primary macrophages.” *Journal of Cell Biology* 162 (2003): 443-455.

Peters VB and Sperber KE. “The effect of viruses on the ability to present antigens via the major histocompatibility complex.” *Microbes and Infection* 1 (1999): 335-345.

Ploegh HL. “Viral strategies of immune evasion.” *Science* 280 (1998): 248-253.

Ref. Dassault Systemes BIOVIA. “Discovery Studio Modeling Environment, Release 4, San Diego: Dassault Systemes.” 2013.

Richard J and Cohen EA. “HIV-1 Vpu disarms natural killer cells.” *Cell Host and Microbe* 8 (2010): 389-391.

Robertson M. “Antigen Presentation.” *Current Biology Primer Magazine* 8 (1998): R829-R831.

Rost B. “Review: protein secondary structure prediction continues to rise.” *Journal of Structural Biology* 134 (2001): 204-218.

Rost B, Yachdav G and Liu J. “The PredictProtein server.” *Nucleic Acids Research* 32 (2004): W321-W326.

Sauter D, Hotter D, Van Driessche B, Sturzel CM, Kluge SF, Wildum S, Yu H, Baumann B, Wirth T, Plantier JC, Leoz M, Hahn BH, Van Lint C and Kirchhoff F. “Differential regulation of NF-κB-mediated proviral and antiviral host gene expression by primate lentiviral Nef and Vpu proteins.” *Cell Reports* 10 (2015): 586-599.

Schlundt A, Gunther S, Sticht J, Wieczorek M, Roske Y, Heinemann U and Freund C. “Peptide linkage to the a-subunit of MHCII creates a stably inverted antigen presentation complex.” *Journal of Molecular Biology* 423 (2012): 294-302.

Schneider T, Hildebrandt P, Ronspeck W, Weigelt W and Pauli G. “The antibody response to the HIV-1 specific "out" (vpu) protein: identification of an immunodominant epitope and correlation of antibody detectability to clinical stages.” *AIDS Research and Human Retroviruses* 6 (1990): 943-950.

Schubert U and Strebel K. “Differential activities of the human immunodeficiency virus type 1-encoded Vpu protein are regulated by phosphorylation and occur in different cellular compartments.” *Journal of Virology* 68 (1994): 2260-2271.

Schubert U, Anton LC, Bacik I, Cox JH, Bour S, Bennink JR, Orlowski M, Strebel K and Yewdell JW. “CD4 glycoprotein degradation induced by human

immunodeficiency virus type 1 Vpu protein requires the function of proteasomes and the ubiquitin-conjugating pathway." *Journal of Virology* 72 (1998): 2280-2288.

Schubert U, Bour S, Ferrer-Montiel AV, Montal M, Maldarelli F and Strebel K. "The two biological activities of human immunodeficiency virus type 1 Vpu protein involve two separable structural domains." *Journal of Virology* 70 (1996): 809-819.

Shah AH, Sowrirajan B, Davis ZB, Ward JP, Campbell EM, Planelles V and Barker E. "Degranulation of natural killer cells following interaction with HIV-1-infected cells is hindered by downmodulation of NTB-A by Vpu." *Cell Host and Microbe* 8 (2010): 397-409.

Singh SK, Mockel L, Thiagarajan-Rosenkranz P, Wittlich M, Willbold D and Koenig BW. "Mapping the interaction between the cytoplasmic domains of HIV-1 viral protein U and human CD4 with NMR spectroscopy." *FEBS Journal* 279 (2012): 1-10.

Skasko M, Tokavre A, Chen CC, Fischer WB, Pillai SK and Guatelli J. "BST-2 is rapidly down-regulated from the cell surface by the HIV-1 protein Vpu: evidence for a post-ER mechanism of Vpu-action." *Virology* 411 (2011): 65-77.

Specht A, Telenti A, Martinez R, Fellay J, Bailes E, Evans DT, Carrington M, Hahn BH, Goldstein DB and Kirchhoff F. "Counteraction of HLA-C-mediated immune control of HIV-1 by Nef." *Journal of Virology* 84 (2010): 7300-7311.

Starlets D, Gore Y, BinskyI, Haran M, Harpaz N, Shvidel L, Becker-Herman S, Berrebi A and Shachar I. "Cell-surface CD74 initiates a signaling cascade leading to cell proliferation and survival." *Blood* 107 (2006): 4807-4816.

Strebel K. "Structure and function of HIV-1 Vpu." In *Human retroviruses and AIDS 1996: A compilation and analysis of nucleic acid and amino acid sequences*, by Korber BT, Foley BT, Jeang KT, Mellors JW and Wain-Hobson S Myers G, 11119-11127. Los Alamos: Theoretical Biology and Biophysics Group, 1996.

Strubin M, Mach B and Long EO. “The complete sequence of the mRNA for the HLA-DR-associated invariant chain reveals a polypeptide with an unusual transmembrane polarity.” *EMBO Journal* 3 (1984): 869-872.

Studier FW and Moffatt BA. “Use of bacteriophage T7 RNA polymerase to direct selective high-level expression of cloned gene.” *Journal of Molecular Biology* 189 (1986): 113-130.

Stumptner-Cuvelette P, Morchoisne S, Dugast M, Le Gall S, Raposo G, Schwartz O and Benaroch P. “HIV-1 Nef impairs MHC class II antigen presentation and surface expression.” *Proceedings of the National Academy of Sciences USA* 98 (2001): 12144-12149.

Szaszak M, Chen HD, Chen HC, Baukal A, Hunyady L and Catt KJ. “Identification of the invariant chain (CD74) as an angiotensin AGTR1-interacting protein.” *Journal of Endocrinology* 199 (2008): 165-176.

Tiganos E, Friborg J, Allain B, Daniel NG, Yao XJ and Cohen EA. “Structural and functional analysis of the membrane-spanning doman of the Human Immunodeficiency Virus Type 1 Vpu protein.” *Virology* 251 (1998): 96-107.

Tiganos E, Yao XJ, Friborg J, Daniel N and Cohen EA. “Putative alpha-helical structures in the human immunodeficiency virus type 1 Vpu protein and CD4 are involved in binding and degradation of the CD4 molecule.” *Journal of Virology* 71 (1997): 4452-4460.

Tosi G, Jabrane-Ferrat N and Peterlin BM. “Phosphorylation of CIITA directs its oligomerization, accumulation and increased activity on MHCII promoters.” *The EMBO Journal* 21 (2002): 5467-5476.

Tu Y, Chen C, Pan J, Xu J, Zhou ZG and Wang CY. “The ubiquitin proteasome pathway (UPP) in the regulation of cell cycle control and DNA damage repair and its implication in tumorigenesis.” *International Journal of Clinical and Experimental Pathology* 5 (2012): 726-738.

Van Damme N, Goff D, Katsura C, Jorgenson RL, Mitchell R, Johnson MC, Stephens EB and Guatelli J. “The interferon-induced protein BST-2

restricts HIV-1 release and is downregulated from the cell surface by the viral Vpu protein." *Cell Host and Microbe* 3 (2008): 245-252.

Warmerdam PAM, Long EO and Roche PA. "Isoforms of the invariant chain regulate transport of MHC class II molecules to antigen processing compartments." *Journal of Cell Biology* 133 (1996): 281-291.

Weaver CT, Harrington LE, Mangan PR, Gavrieli M and Murphy KM. "Th17: an effector of CD4 T cell lineage with regulatory T cell ties." *Immunity* 24 (2006): 677-688.

Wileman T, Kane LP, Carson GR and Terhorst C. "Depletion of cellular calcium accelerates protein degradation in the endoplasmic reticulum." *Journal of Biological Chemistry* 266 (1991): 4500-4507.

Willey RL, Buckler-White A and Strebel K. "Sequences present in the cytoplasmic domain of CD4 are necessary and sufficient to confer sensitivity to the human immunodeficiency virus type 1 Vpu protein." *Journal of Virology* 68 (1994): 1207-1212.

Willey RL, Maldarelli F, Martin MA and Strebel K. "Human immunodeficiency virus type 1 Vpu protein induces rapid degradation of CD4." *Journal of Virology* 66 (1992a): 7193-7200.

Willey RL, Maldarelli F, Martin MA and Strebel K. "Human immunodeficiency virus type 1 Vpu protein regulates the formation of intracellular gp160-CD4 complexes." *Journal of Virology* 66 (1992b): 226-234.

Wittlich M, Koenig BW, Stoldt M, Schmidt H and Willbold D. "NMR structural characterization of HIV-1 virus protein U cytoplasmic domain in the presence of dodecylphosphatidylcholine micelles." *FEBS Journal* 276 (2009): 6560-6575.

Wittlich M, Thiagarajan P, Koenig BW, Harmann R and Willbold D. "NMR structure of the transmembrane and cytoplasmic domains of human CD4 in micelles." *Biochimica et Biophysica Acta* 1798 (2010): 122-127.

Wonderlich ER, Leonard JA and Collins KL. “HIV immune evasion: disruption of antigen presentation by the HIV Nef protein.” *Advances in Virus Research* 80 (2011): 103-127.

Wrzeszczynski KO and Rost B. “Cataloguing proteins in cell cycle control.” *Methods in Molecular Biology* 241 (2004): 219-233.

Yachdav G, Kloppmann E, Kajan L, Hecht M, Goldberg T, Hamp T, Honigschmid P, Schafferhans A, Roos M, Bernhofer M and others. “PredictProtein---an open resource for online prediction of protein structural and functional features.” *Nucleic Acids Research*, 2014: gku366.

Zhou C, Lu L, Tan S, Jiang S and Chen YH. “HIV-1 glycoprotein 41 ectodomain induces activation of the CD74 protein-mediated extracellular signal-regulated kinase/mitogen-activated protein kinase pathway to enhance viral infection.” *Journal of Biological Chemistry* 286 (2011): 44869-44877.

Zhu J and Paul WE. “CD4 T cells: fates, functions, and faults.” *Blood* 112 (2008): 1557-1569.

APPENDICES

Appendix A

R14/49 Ms Denise Downer

HUMAN RESEARCH ETHICS COMMITTEE (MEDICAL)

CLEARANCE CERTIFICATE NO. M130387

NAME: (Principal Investigator)	Ms Denise Downer
DEPARTMENT:	Molecular Medicine & Haematology Medical School
PROJECT TITLE:	Comparison of the HIV-1 Vpu Interactions with CD4 and CD74
DATE CONSIDERED:	Ad hoc
DECISION:	Approved unconditionally
CONDITIONS:	
SUPERVISOR:	Prof M Papathanasopoulos
APPROVED BY:	Professor PE Cleaton-Jones, Chairperson, HREC (Medical)

DATE OF APPROVAL: 08/04/2013

This clearance certificate is valid for 5 years from date of approval. Extension may be applied for.

DECLARATION OF INVESTIGATORS

To be completed in duplicate and **ONE COPY** returned to the Secretary in Room 10004, 10th floor, Senate House, University.

I/we fully understand the conditions under which I am/we are authorized to carry out the above-mentioned research and I/we undertake to ensure compliance with these conditions. Should any departure be contemplated, from the research protocol as approved, I/we undertake to resubmit the application to the Committee. **I agree to submit a yearly progress report**.

Principal Investigator Signature Date

PLEASE QUOTE THE PROTOCOL NUMBER IN ALL ENQUIRIES

Appendix B

Table A.1: Absorbance (A_{650}) values for all ELISA data recorded in the Results chapter, indicating which peptides were coated/plated and which were incubated with the plated peptides. For Vpu, only Vpu::GFP (full length protein) and the responsive, numbered Vpu peptides are indicated. Key: black – anti-Vpu, subtype B (NIH); blue – anti-Vpu, subtype C (NIH); red – anti-Vpu (Abcam); green – anti-GFP; purple – anti-CD4; pink – anti-CD74. Orange bars indicate intensity of response. NA – not applicable.

		Plated									
	60min	Vpu #10 (B)	Vpu #13 (B)	Vpu #10 (C)	Vpu #11 (C)	Vpu #18	Vpu #19	Vpu::GFP	Vpu::GFP	Vpu::GFP	Vpu::GFP
Incubated	Antibodies only	0.848	0.496	0.503	1.034	1.254	0.764	0.784	0.691	0.176	0.168
	CD4 (FLP)	1.131	0.564	0.952	1.263	NA	NA	0.507	NA	1.370	NA
	CD74 (FLP)	0.207	0.106	0.069	0.319	NA	NA	0.144	0.693	NA	1.844
	CLIP	0.804	0.485	0.402	0.912	NA	NA	0.959	NA	NA	NA
	CD74_10mer1	1.034	0.769	NA	NA	1.490	0.878	0.564	NA	NA	NA
	CD74_10mer2	0.857	0.642	NA	NA	1.733	0.815	0.497	NA	NA	NA
	CD74_10mer3	0.804	0.613	NA	NA	1.579	0.744	0.512	NA	NA	NA
	CD74_10mer4	0.783	0.599	NA	NA	1.517	0.713	0.518	NA	NA	NA
	CD74_10mer5	0.826	0.566	NA	NA	1.234	0.734	0.585	NA	NA	NA
	CD74_15mer1	1.185	0.154	NA	NA	1.098	0.808	0.449	NA	NA	NA
	CD74_15mer2	1.096	0.174	NA	NA	1.364	0.769	0.683	NA	NA	NA
	CD74_15mer3	1.036	0.181	NA	NA	1.350	0.719	0.652	NA	NA	NA
	CD74_15mer4	1.037	0.176	NA	NA	1.419	0.669	0.627	NA	NA	NA
	Combo 2	NA	NA	NA	NA	NA	NA	0.073	NA	NA	NA
	Combo 3	NA	NA	NA	NA	NA	NA	0.067	NA	NA	NA
	Combo 4	NA	NA	NA	NA	NA	NA	0.065	NA	NA	NA
	Combo 5	NA	NA	NA	NA	NA	NA	0.063	NA	NA	NA
	Antibody only	0.075	0.071	NA	0.075	NA	NA	NA	NA	NA	NA
	CD4 (FLP)	1.362	1.344	NA	1.390	NA	NA	NA	NA	NA	NA